BULLETIN DE L'ASSOCIATION MINÉRALOGIQUE DU CANADA

THE CANADIAN MINERALOGIST

JOURNAL OF THE MINERALOGICAL ASSOCIATION OF CANADA

Volume 44 December 2006 Part 6

The Canadian Mineralogist
Vol. 44, pp. 1273-1330 (2006)

FROM STRUCTURE TOPOLOGY TO CHEMICAL COMPOSITION. I. STRUCTURAL HIERARCHY AND STEREOCHEMISTRY IN TITANIUM DISILICATE MINERALS

ELENA SOKOLOVA

Department of Geological Sciences, University of Manitoba, Winnipeg, Manitoba R3T 2N2, Canada

ABSTRACT

The structural hierarchy and stereochemistry have been considered for 24 titanium disilicate minerals that contain the TS (Titanium Silicate) block, a central trioctahedral (O) sheet, and two adjacent (H) sheets of [5]- and [6]-coordinated polyhedra and (Si_2O_7) groups. The TS block is characterized by a planar cell based on translation vectors $\mathbf{t_1}$ and $\mathbf{t_2}$, with $t_1 \approx 5.5$ and $t_2 \approx 7$ Å, and $\mathbf{t_1} \wedge \mathbf{t_2}$ close to 90°. The general formula of the TS block is $A^P_2\ B^P_2\ M^H_2\ M^O_4\ (Si_2O_7)_2\ X_{4+n}$, where M^H_2 and M^O_4 are cations of the H and O sheets; M^H represents Ti (= Ti + Nb), Zr, Mn^{2+}, Ca; M^O represents Ti, Zr, Mn^{2+}, Ca, Na; A^P and B^P represent cations at the peripheral (*P*) sites, *i.e.*, Na, Ca, Ba; X represents the anions O, OH, F and H_2O; n = 0, 2, 4. Cations in each sheet of the TS block form a close-packed layer, and the three layers are cubic close-packed. There are three topologically distinct TS blocks, depending on the type of linkage of two H sheets and the central O sheet. The H sheets of one TS block are invariably identical and attach to the O sheet in the same way. All structures consist of a TS block and an **I** (intermediate) block that comprises atoms between two TS blocks. Usually, the **I** block consists of alkali and alkaline-earth cations, (H_2O) groups and oxyanions $(PO_4)^{3-}$, $(SO_4)^{2-}$ and $(CO_3)^{2-}$. These structures naturally fall into four groups, based on differences in topology and stereochemistry of the TS block. In Group I, Ti = 1 *apfu*, Ti occurs in the O sheet, and (Si_2O_7) groups link to a Na polyhedron of the O sheet (linkage 1). In Group II, Ti = 2 *apfu*, Ti occurs in the H sheet, and (Si_2O_7) groups link to two M^{2+} octahedra of the O sheet adjacent along $\mathbf{t_2}$ (linkage 2). In Group III, Ti = 3 *apfu*, Ti occurs in the O and H sheets, and (Si_2O_7) groups link to the Ti octahedron of the O sheet (linkage 1). In Group IV, Ti = 4 *apfu* (the maximum possible content of Ti in the TS block), Ti occurs in the O and H sheets, and (Si_2O_7) groups link to two Ti octahedra of the O sheet adjacent along $\mathbf{t_1}$ (linkage 3). The stability of the TS block is due to an extremely wide range in Ti(Nb)–O bond lengths, 1.68–2.30 Å, which allows the chemical composition of the TS block to vary widely. In a specific structure, only one type of TS block and only one type of **I** block occur. The TS block propagates close-packing of cations into the **I** block. General structural principles have been developed for these 24 titanium disilicates, and the relation between structure topology and chemical composition has been established for minerals based on the TS block.

Keywords: titanium disilicate mineral, TS block, structure topology, stereochemistry, chemical composition, end-member formula, structural hierarchy.

SOMMAIRE

La hiérarchie structurale et les relations stéréochimiques ont été évaluées pour 24 minéraux disilicatés de titane contenant le bloc TS (silicate de titanium), un feuillet central trioctaédrique (O), et deux feuillets adjacents (H) contenant des polyèdres à coordinence [5] et [6] et des groupes (Si_2O_7). Le bloc TS contient une maille planaire fondée sur les vecteurs de translation $\mathbf{t_1}$ et $\mathbf{t_2}$, avec $t_1 \approx 5.5$ et $t_2 \approx 7$ Å, et $\mathbf{t_1} \wedge \mathbf{t_2}$ près de 90°. La formule générale du bloc TS est $A^P_2\ B^P_2\ M^H_2\ M^O_4\ (Si_2O_7)_2\ X_{4+n}$, dans

E-mail address: elena_sokolova@umanitoba.ca

laquelle M^H_2 et M^O_4 sont des cations des feuillets H et O; M^H représente Ti (= Ti + Nb), Zr, Mn^{2+}, Ca; M^O représente Ti, Zr, Mn^{2+}, Ca, Na; A^P et B^P représentent les cations aux sites périphériques (*P*), *i.e.*, Na, Ca, Ba; X représente les anions O, OH, F et H_2O; n = 0, 2, 4. Les cations de chaque feuillet d'un bloc TS définissent un agencement à empilement compact, et les trois niveaux ont un empilement compact cubique. Il existe trois blocs TS topologiquement distincts, dependant du type d'agencement des deux feuillets H et du feuillet central O. Les feuillets H d'un bloc TS sont dans tous les cas identiques, et se rattachent au feuillet O de la même façon. Toutes les structures contiennent un bloc TS et un bloc **I** (intermédiaire) contenant des atomes entre deux blocs TS. En général, le bloc **I** contient des cations alcalins et alcalino-terreux, des groupes (H_2O), et des oxyanions $(PO_4)^{3-}$, $(SO_4)^{2-}$ et $(CO_3)^{2-}$. Ces structures se regroupent naturellement en quatre catégories qui se distinguent par des différences en topologie et en stéréochimie du bloc TS. Dans le groupe I, Ti = 1 *apfu*, le Ti se trouve dans le feuillet O, et des groupes (Si_2O_7) sont liés à un polyèedre de Na faisant partie du feuillet O (agencement 1). Dans le groupe II, Ti = 2 *apfu*, le Ti se trouve dans le feuillet H, et les groupes (Si_2O_7) sont liés à deux octaèdres M^{2+} du feuillet O adjacent le long de $\mathbf{t_2}$ (agencement 2). Dans le groupe III, Ti = 3 *apfu*, le Ti se trouve dans les feuillets O et H, et les groupes (Si_2O_7) sont liés à l'octaèdre Ti du feuillet O (agencement 1). Dans le groupe IV, Ti = 4 *apfu* (le contenu maximum en Ti dans le bloc TS), le Ti est présent dans les feuillets O et H, groupes (Si_2O_7) sont liés à deux octaèdres Ti du feuillet O adjacent le long de $\mathbf{t_1}$ (agencement 3). La stabilité du bloc TS serait due à la grande variabilité de la distance Ti(Nb)–O, 1.68–2.30 Å, ce qui permet à la composition chimique du bloc TS de varier largement. Dans une structure donnée, il y a une seule sorte de bloc TS et une seule sorte de bloc **I**. Le bloc TS propage le motif d'empilement compact des cations parmi les cations du bloc **I**. Les principes structuraux généralisés ont été développés pour ces 24 disilicates de titane, et la relation entre la topologie de la structure et la composition chimique a été établie pour les minéraux fondés sur le bloc TS.

(Traduit par la Rédaction)

Mots-clés: minéraux disilicate de titane, bloc TS, topologie de la structure, stéréochimie, composition chimique, formule des pôles, hiérarchie structurale.

Introduction

In a group of minerals whose structure has a fixed topology, the relation between structure and chemical composition is straightforward: the sum of the sites in the structure gives the stoichiometry of all minerals in that group. However, in a group of minerals of reasonable complexity in which the structure topology is related but not identical, the general relation between structure topology and chemical composition is not known. This problem is of major significance in terms of the relation between structure and chemical composition. It is simple to go from structure topology to chemical composition. However, what one wants to do is to go in the reverse direction: from chemical composition to structure topology. Here, I consider first the relation between structure topology and chemical composition for a group of structurally related but topologically distinct titanium disilicate minerals with the view of developing a general relation between structure topology and chemical composition. Once this is established, I will consider the inverse problem: to establish a distinct structure-topology for a specific chemical composition.

In this paper, I consider the structure topology and stereochemistry of 24 titanium disilicate minerals with the TS (titanium silicate) block, which has a three-layered structure: the central part is a sheet of octahedra (*i.e.*, trioctahedral sheet that is common in micas), and there are two adjacent sheets containing different polyhedra, including (Si_2O_7) groups. The TS block is a major structural unit in the crystal structures of 24 minerals. In a structure, the TS block can alternate with another block, which I call an intermediate (**I**) block, as it is intercalated between two TS blocks. The TS block can have different topologies, and its chemical composition changes, but the Si–O radical is always the same, the [Si_2O_7] group. In minerals, Ti^{4+} is generally [6]-coordinated, and less commonly [5]-coordinated. In many Ti-silicate minerals, Ti ⇌ Nb substitution is common (r $[^{[6]}Ti^{4+}]$ = 0.605, r $[^{[6]}Nb^{5+}]$ = 0.64 Å; Shannon 1976). Hence, where I refer to (TiO_6) octahedra, I include ({Ti,Nb}O_6) and ({Nb,Ti}O_6) octahedra.

I consider only minerals of known structure. I do not take into account minerals for which data on the crystal structure are not available. The structure data and references for 24 minerals are summarized in Table 1. I will establish a structure hierarchy, consider the stereochemistry of these structures, and develop the general structural principles characteristic for titanium disilicate minerals. I will use these principles to (1) test whether or not all aspects of the structure and chemical formula of a mineral are correct, and (2) eliminate any contradictions between structure and chemical composition for specific minerals.

Preliminary Considerations

Inspection of the formulae of the alkali titanium disilicate minerals (Table 1) shows that the ratio of Si to other cations is unusually low, about 1 : 2. Furthermore, inspection of the localities in which these minerals occur shows them to be very deficient in Si relative to most igneous rocks; alkali and alkaline-earth phosphates and alkali fluorides are common minerals in these parageneses. Thus crystallization of disilicate minerals proceeds with the minimum of Si available for incorporation into the crystallizing mineral. The octahedral (O) sheet of

the TS block forms from what common octahedrally coordinated cations are available, primarily Na, Ca and Ti^{4+}. Following this mica analogy, the adjacent sheet will form from silicate tetrahedra. However, there is a paucity of Si in this environment, and there is also no Al to form aluminosilicate polymerizations. This problem is overcome by incorporation of [5]- or [6]-coordinated cations to form a heteropolyhedral (H) sheet. This being the case, a sheet must be formed from octahedra and tetrahedra with the minimum amount of Si in the sheet, reflecting the low activity of Si in this environment. If I write the formula of the sheet as $M^{[N]}(Si_xO_y)$, where M is an [5]- or [6]-coordinated cation, the coordination number of the *M* polyhedron in the plane of the H sheet is [4], and the coordination number of the (Si_xO_y) unit in the plane of the H sheet is [N]. The simplest solution for complete linkage in this sheet is N = 4. So, one is looking for a silicate cluster with four free vertices in the plane of the H sheet; this is the case for both $(Si_2O_7)^{6-}$ and $(Si_4O_{12})^{8-}$. However, one is also looking for the arrangement with the minimum amount of Si: $(Si_2O_7)^{6-}$. Hence the H sheet in these minerals will have the stoichiometry $M(Si_2O_7)$.

The titanium disilicate minerals have very interesting structures with complicated chemical compositions. Besides (Si_2O_7) groups, three other complex anions, (PO_4), (SO_4) and (CO_3), occur outside the TS block in the crystal structure of these minerals. The alternation of chemically different blocks in a significant number of these structures was originally described by Egorov-

TABLE 1. STRUCTURAL FORMULAE* AND UNIT-CELL PARAMETERS FOR MINERALS WITH THE TS BLOCK

Mineral	Formula	*a* (Å)	*b* (Å)	*c* (Å)	α(°)	β(°)	γ(°)	Sp. gr.	*Z*	Ref.
Group I										
götzenite	$Ca_2(Ca,Na)_2Ca_2NaTi(Si_2O_7)_2F_2F_2$	9.6192	5.7249	7.3307	89.981	101.132	100.639	$P\bar{1}$	1	(1)
hainite	$(Ca,Zr,Y)_2(Na,Ca)_2Ca_2NaTi(Si_2O_7)_2F_2F_2$	9.6079	5.7135	7.3198	89.916	101.077	100.828	$P\bar{1}$	1	(2)
seidozerite	$Zr_4Na_2Mn_2Na_4Na_2Ti_2(Si_2O_7)_4F_4O_4$	5.5558	7.0752	18.406		102.713		$P2_1/c$	1	(3)
grenmarite	$(Zr,Mn)_2(Zr,Ti)(Mn,Na)(Na,Ca)_4(Si_2O_7)_2(O,F)_4$	5.608	7.139	18.575		102.60		$P2_1/c$	1	(4)
rinkite	$\{TiF(O,F)[Si_2O_7]_2\}\{Na(Na,Ca)_2F(O,F)\}\{(Ca,TR)_4\}$	5.679	7.412	18.835		101.23		$P2_1$	2	(5)
kochite	$Zr_2(Mn,Zr)_2(Na,Ca)_4Ca_4Na_2Ti_2(Si_2O_7)_4F_4O_4$	10.032	11.333	7.202	90.192	100.334	111.551	$P\bar{1}$	1	(6)
rosenbuschite	$Zr_2Ca_2(Na,Ca)_4Ca_4Na_2ZrTi(Si_2O_7)_4F_4O_4$	10.137	11.398	7.2717	90.216	100.308	111.868	$P\bar{1}$	1	(7)
Group II										
perraultite**	$(Na,Ca)_2(Ba,K)_2(Mn,Fe)_8[(Ti,Nb)_4O_4(OH)_2[Si_2O_7]_4(OH,F)_4$	10.731	13.841	24.272		121.19		$C2$	4	(8)
surkhobite	$\{[Ba_{1.65}K_{0.35}][Ca_{1.2}Na_{0.8}]\}\{[Fe_4][Mn_{3.7}Na_{0.3}]\}$ $\{[Ti_{3.2}(Zr,Nb)_{0.8}O_4F\{OH,O)][Si_2O_7]_4\}\{[F_3OH]\}$	10.723	13.826	20.791		95.00		$C2$	4	(9)
bafertisite	$BaFe_2TiO[Si_2O_7](OH)_2$	10.6	13.64	12.47		119.5		Cm	8	(10)
hejtmanite-P	$BaMn_2TiO[Si_2O_7](OH)_2$	5.361	6.906	12.556		119.8		$P2_1/m$	2	(11)
hejtmanite-C	$BaMn_2TiO[Si_2O_7](OH)_2$	10.7232	13.812	12.563		119.9		Cm	8	(11)
yoshimuraite	$Ba_2Mn_2TiO[Si_2O_7](PO_4)(OH)$	5.386	6.999	14.748	89.98	93.62	95.50	$P\bar{1}$	2	(12)
bussenite	$Na_2Ba_2Fe^{2+}Ti(Si_2O_7)(CO_3)O(OH)(H_2O)F$	5.399	7.016	16.254	102.44	93.18	90.10	$P1$	2	(13)
Group III										
lamprophyllite-2*M*	$(Sr_{1.18}Na_{0.65}Ca_{0.12})Na(Na_{1.3}Mn_{0.36}Fe_{0.22}Mg_{0.12})$ $Ti_3O_2(Si_2O_7)_2(OH)_2$	19.215	7.061	5.3719		96.797		$C2/m$	2	(14)
lamprophyllite-2*O*	$(Sr_{1.18}Na_{0.65}Ca_{0.12})Na(Na_{1.3}Mn_{0.36}Fe_{0.22}Mg_{0.12})$ $Ti_3O_2(Si_2O_7)_2(OH)_2$	19.128	7.0799	5.3824				$Pnmn$	2	(14)
barytolamprophyllite	$KBa\{Na[Na_{1.2}(Fe^{2+},Mn^{2+})_{0.8}][Ti(O,OH)_2]\}$ $\{[Si_2O_7]_2Ti_2O_2\}$	20.086	7.099	5.411		96.65		$C2/m$	2	(15)
nabalamprophyllite	$Ba(Na,Ba)\{Na_3Ti[Ti_2O_2Si_4O_{14}](OH,F)_2\}$***	19.741	7.105	5.408		96.67		$P2/m$	2	(16)
innelite	$Na_2Ba_4CaTi_3O_4(Si_2O_7)_2(SO_4)_2$	14.76	7.14	5.38	90.00	95.00	99.00	$P1$	1	(17)
epistolite	$Na_4Nb_2TiO_2(Si_2O_7)_2(OH)_2(H_2O)_4$	5.460	7.170	12.041	103.63	96.01	89.98	$P\bar{1}$	1	(18)
vuonnemite	$Na_{11}TiNb_2(Si_2O_7)_2(PO_4)_2O_3(F,OH)$	5.4984	7.161	14.450	92.60	95.30	90.60	$P\bar{1}$	1	(19)
Group IV										
murmanite	$Na_4Ti_4O_4(Si_2O_7)_2(H_2O)_4$	5.383	7.053	12.170	93.16	107.82	90.06	$P1$	1	(20)
lomonosovite	$Na_5Ti_2(Si_2O_7)(PO_4)O_2$	5.49	7.11	14.50	101	96	90	$P\bar{1}$	2	(21)
quadruphite	$Na_{14}Ca_2Ti_4(Si_2O_7)_2(PO_4)_4O_4F_2$	5.4206	7.0846	20.3641	86.89	94.42	89.94	$P1$	1	(22)
sobolevite	$Na_{12}Ca(NaCaMn)Ti_2(TiMn)(Si_2O_7)_2(PO_4)_4O_3F_3$	7.0755	5.4106	40.623		93.156		Pc	2	(23)
polyphite	$Na_5(Na_4Ca_2)Ti_2O_2(Si_2O_7)(PO_4)_3O_2F_2$	5.3933	7.0553	26.451	95.216	93.490	90.101	$P\bar{1}$	2	(24)

* The structural formulae are as presented in the original article about the structure, and hence they are not consistent in format.

** There is some confusion about this cell (see discussion in the text).

*** This formula is from the description of a new mineral (Chukanov *et al.* 2004) rather than the structure work of Rastsvetaeva & Chukanov (1999).

References (the latest reference on the structure is the first entry in the numbered list of references): (1) Christiansen *et al.* (2003a), Cannillo *et al.* (1972); (2) Christiansen *et al.* (2003a), Rastsvetaeva *et al.* (1995b); (3) Christiansen *et al.* (2003a), Simonov & Belov (1960), Skszat & Simonov (1966), Puscharovskii *et al.* (2002); (4) Bellezza *et al.* (2004); (5) Rastsvetaeva *et al.* (1991a), Galli & Alberti (1971): (6) Christiansen *et al.* (2003b); (7) Christiansen *et al.* (2003a), Shibaeva *et al.* (1964); (8) Yamnova *et al.* (1998); (9) Rozenberg *et al.* (2003); (10) Guan *et al.* (1963); (11) Rastsvetaeva *et al.* (1991b); (12) McDonald *et al.* (2000), Takéuchi *et al.* (1997); (13) Zhou *et al.* (2002); (14) Krivovichev *et al.* (2003); Rastsvetaeva & Dorfman (1995); Rastsvetaeva *et al.* (1990), Saf'yanov *et al.* (1983), Woodrow (1964); (15) Rastsvetaeva *et al.* (1995a), Peng *et al.* (1984); (16) Rastsvetaeva & Chukanov (1999); (17) Chernov *et al.* (1971); (18) Sokolova & Hawthorne (2004); (19) Ercit *et al.* (1998), Drozdov *et al.* (1974); (20) Khalilov (1989), Khalilov *et al.* (1965a), Rastsvetaeva & Andrianov (1986); (21) Belov *et al.* (1977), Rastsvetaeva *et al.* (1971); (22) Sokolova & Hawthorne (2001), Sokolova *et al.* (1987a); (23) Sokolova *et al.* (2005), Sokolova *et al.* (1988); (24) Sokolova *et al.* (2005), Sokolova *et al.* (1987b).

Tismenko & Sokolova (1987, 1990); they considered 15 minerals: seidozerite, rinkite, götzenite, rosenbuschite, lamprophyllite, murmanite, epistolite, bafertisite, hejtmanite, innelite, lomonosovite, vuonnemite, quadruphite, polyphite and sobolevite, as a unique series of structures based on the TS block, and they emphasized the importance of the TS block as a basic structural unit. Later, this particular series was considered in numerous publications; it was enlarged by the addition of structurally related mineral species, but the TS block is the basis for considering these minerals as a coherent series. Related work, which includes description of new minerals, structure solution and refinement, and descriptive crystal chemistry of various types, is summarized in Appendix A: Previous work. Related minerals that do not contain the TS block as it is defined in the Introduction are listed in Appendix B.

The TS block has been always considered as a stable unit, but it has been assigned different types of formula by different authors. The **I** block is always considered of variable chemical composition and topology. When a general formula of the mineral is written as a sum of the formulae of two types of blocks, it is usually long and contains a large number of commas and brackets. These formulae can be very complicated, and it is very difficult to understand the chemical composition of each mineral and its relation to other minerals where there is such a degree of ambiguity in the formulae of most of these minerals. Indeed, this ambiguity is the reason, in spite of all the work done on this series of minerals, that a *quantitative* understanding of the structures and chemical compositions of these minerals has remained elusive.

The Topology of the TS (Titanium Silicate) Block. I. General Features

The structures of all minerals considered in this paper have one common fundamental building block or structure unit, a Ti silicate (TS) block. For a description of its components, I will use the (HOH) notation of Ferraris *et al.* (1997).

The O sheet

The O sheet is commonly an array of close-packed octahedra with the formula $M^{O}X^{O}_{2}$, where M^{O} and X^{O} are cations and anions of the O sheet (Fig. 1a). In all minerals with the TS block, all cation sites of the O sheet are fully occupied, *i.e.*, the O sheet is a trioctahedral sheet analogous to that in micas. Delindeite, $Ba_2\{(Na,K,\square)_3(Ti,Fe)[Ti_2(O,OH)_4Si_4O_{14}](H_2O,OH)_2\}$, is the only known mineral where all Na sites of the O sheet are statistically occupied by Na (Ferraris *et al.* 2001b, Appleman *et al.* 1987). Thus delindeite does not have a trioctahedral O sheet, and I do not consider its structure in this paper.

The H sheet

The H sheet consists of various polyhedra: silicate tetrahedra joined into (Si_2O_7) groups and [6]- or [5]-coordinated M^{H} polyhedra in the ratio 1:1. Each (Si_2O_7) group links to four M^{H} polyhedra, and each M^{H} polyhedron links to four (Si_2O_7) groups (Fig. 1b). The topology of the H sheet dictates two translation vectors, $\mathbf{t_1}$ and $\mathbf{t_2}$, with lengths of these vectors being $t_1 \approx 5.5$ and $t_2 \approx 7$ Å, and $\mathbf{t_1} \wedge \mathbf{t_2}$ close to 90°. In the H sheet in all structures, (Si_2O_7) groups are invariably oriented with their Si–Si distance parallel to $\mathbf{t_2}$.

The TS block

The TS block has a three-layered structure consisting of a central sheet of octahedra (O sheet) and two adjacent heteropolyhedral sheets (H sheets). The O and H sheets link together through common vertices of constituent polyhedra (Figs. 2a, b). As the topology of

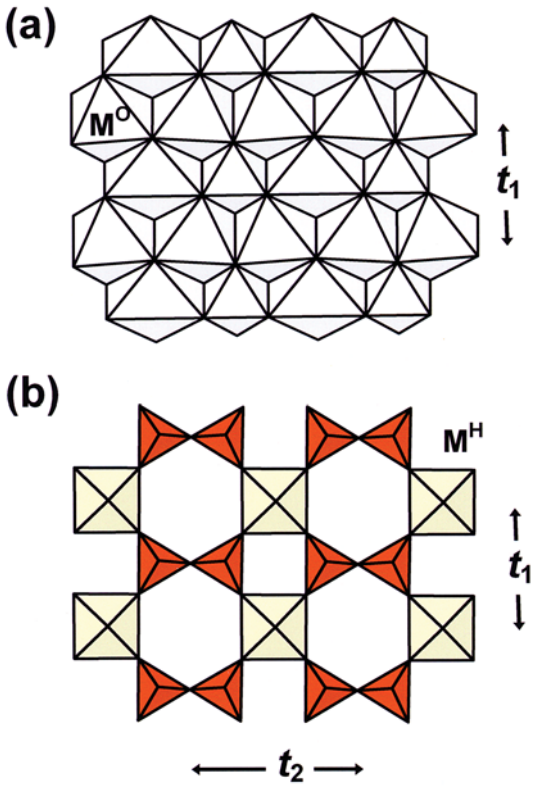

FIG. 1. Titanium silicate (TS) block; general view of (a) the sheet of octahedra (O sheet), and (b) the heteropolyhedral sheet (H sheet). The M^{O} and M^{H} octahedra are white and yellow, (SiO_4) tetrahedra are orange, $t_1 \approx 5.5$ Å and $t_2 \approx 7$ Å.

the H sheet dictates two translation vectors, $\mathbf{t_1}$ and $\mathbf{t_2}$, then the O sheet has the same periodicity, and thus the TS block is invariably characterized by two minimal lengths of translation vectors, as was noted by Egorov-Tismenko & Sokolova (1987). The t_1 and t_2 lengths of these translation vectors for each mineral are given in Table 2, as well as several geometrical characteristics of the (Si_2O_7) group, including <∠Si–O–Si> and mean O–O distances along $\mathbf{t_2}$ in the O and H sheets.

The peripheral (P) cation sites

Linkage of O and H sheets results in two types of voids, which host the A^P and B^P sites (Fig. 3a). In the plane of the H sheet, the A^P void is formed by two (Si_2O_7) groups and two M^H polyhedra and is hexagonal in outline, whereas the B^P void is formed by two (SiO_4) tetrahedra and two M^H polyhedra and is tetragonal in outline. The A^P site can occur in the plane of the H sheet where its constituent cation is bonded to an anion of the O sheet (X^O_A). In this case, two bonds, A^P–X^P_A and A^P–X^O_A, are oriented perpendicular to the plane of the H sheet (Fig. 3b); the number of bonds in the plane of the H sheet varies from 6 to 3 (Fig. 3c), resulting most commonly in coordination numbers from [8] to [5]. In one structure (rinkite), there are two A^P–X^P_A bonds, and the A^P site is [7]-coordinated. The B^P site is too small to accommodate any cation in the plane of the H sheet. The cations occupying the *P* site can move into the intermediate space (out of the H sheet), and their coordination numbers become [9] to [12]. In this case, I consider them as part of the **I** block. In Table 2, I report A^P–X^O_A bond lengths in all structures.

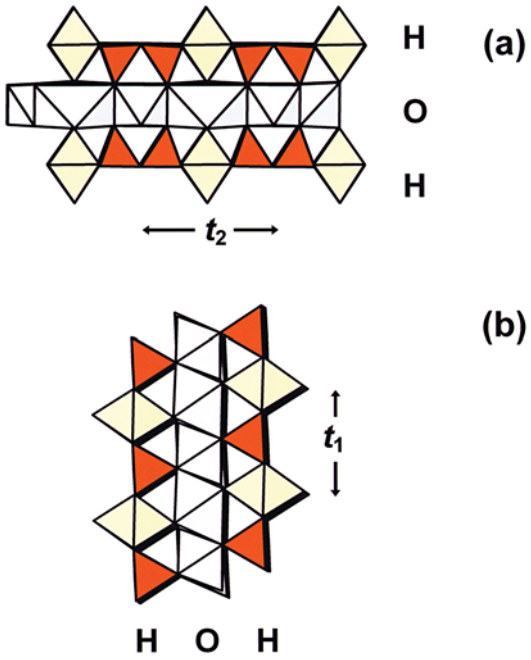

FIG. 2. The TS block. Linkage of O and H sheets viewed (a) down the t_1 translation, and (b) down the t_2 translation. Legend as in Figure 1.

TABLE 2. SELECTED STRUCTURE PARAMETERS FOR MINERALS WITH THE TS BLOCK

Mineral	t_1 (Å)	t_2 (Å)	(Si_2O_7) <Si–O–Si> (°)	<O–O> along t_2 (Å) O sheet $(O–O)^O$	H sheet $(O–O)^H$	<A^P–X^O_A> (Å)
Group I						
götzenite	5.72	7.33	205.9	4.52	3.87	2.34
	b	*c*				
hainite	5.71	7.32	205.9	4.52	3.87	2.34
	b	*c*				
seidozerite	5.56	7.08	186.8	4.27	4.14	2.22
	a	*b*				
grenmarite	5.61	7.14	186.2	4.23	4.17	2.23
	a	*b*				
rinkite	5.68	7.41	206.8	4.56	3.78	2.39
	a	*b*				
kochite	5.67	7.20	198.9	4.37	3.82	2.24
	b/2	*c*			4.10	
rosenbuschite	5.70	7.27	202.5	4.32	3.70	2.28
	b/2	*c*			4.14	
	<5.66>	<7.25>	<199.0>	<4.40>	<3.95>	<2.29>
Group II						
perraultite	5.37	6.92	134.2	3.34	4.24	4.30
	a/2	*b*/2				
surkhobite	5.36	6.91	127.5	3.33	4.19	4.30
	a/2	*b*/2	135.7			
bafertisite	5.30	6.82	147.8	3.38	4.18	4.23
	a/2	*b*/2				
hejtmanite-P	5.36	6.91	129.7	3.41	4.15	4.19
	a	*b*				
hejtmanite-C	5.36	6.91	142.4	3.56	4.22	4.18
	a/2	*b*/2				
yoshimuraite	5.39	7.00	150.3	3.46	4.32	3.89
	a	*b*				
bussenite	5.40	7.02	149.3	3.45	4.31	3.42
	a	*b*				
	<5.36>	<6.93>	<140.6>	<3.42>	<4.23>	<4.07>
Group III						
lamprophyllite-2*M*	5.37	7.06	134.1	2.87	4.41	3.05*
	c	*b*				
lamprophyllite-2O	5.38	7.08	134.5	2.89	4.44	3.05*
	c	*b*				
barytolamprophyllite	5.41	7.10	135.4	2.92	4.43	3.31*
	c	*b*				
nabalamprophyllite	5.41	7.11	135.8	2.99	4.34	3.16*
	c	*b*				
innelite	5.38	7.14	139.6	2.74	4.49	4.06*
	c	*b*				
epistolite	5.46	7.17	135.6	2.85	4.39	2.40**
	a	*b*				
vuonnemite	5.50	7.16	134.7	2.92	4.40	2.31**
	a	*b*				
	<5.42>	<7.12>	<135.7>	<2.88>	<4.41>	<3.33>* <2.36>**
Group IV						
murmanite	5.38	7.05	136.6	2.87	4.43	2.51
	a	*b*				
lomonosovite	5.49	7.11	135.0	2.90	4.38	2.38
	a	*b*				
quadruphite	5.42	7.08	136.5	2.92	4.38	2.37
	a	*b*				
sobolevite	5.41	7.08	137.1	2.90	4.37	2.35
	b	*a*				
polyphite	5.39	7.06	137.0	2.93	4.38	2.68
	a	*b*				
	<5.42>	<7.08>	<136.4>	<2.90>	<4.39>	<2.40>

* A^P = Ba, Sr; ** A^P = Na.

The Topology of the TS Block. II. Its General Formula

I will write the general formula of the TS block as a combination of O and two H sheets, plus *P* sites. As all structures with a TS block are characterized by two minimal translations, their formula should be based on a planar cell with $t_1 \approx 5.5$ and $t_2 \approx 7$ Å (shown in red in Fig. 4).

Labeling of the anion sites

In the O sheet, there are four cation and eight anion sites per minimal cell (Fig. 4a). Four anions are common vertices of M^O octahedra and (SiO_4) tetrahedra, two on each side of the O sheet; they are the $X^O{}_{Si}$ anions. Four anions are common vertices of M^O octahedra and two M^H and two A^P polyhedra; they are the $X^O{}_M$ and $X^O{}_A$ anions (as they belong to both sheets). The $X^H{}_{Si–M}$ anions are common O atoms of the M^H polyhedra and Si tetrahedra, and they belong only to the H sheet (Fig. 4b). Anions $X^P{}_M$, $X^P{}_A$ (Fig. 3b) and $X^P{}_B$ belong to the M^H, A^P and B^P polyhedra on the outside of the TS block [in the intermediate space (**I**) between two TS blocks].

The O sheet

The O sheet is an array of close-packed octahedra ($M^OX^O{}_2$), where M^O and X^O are cations and anions). In the minimal cell, there are four M^O cations and eight X^O anions (Fig. 4a), and the formula of the O sheet is

$$M^O{}_4\ X^O{}_8\ (= {}^{[6]}M^O{}_4\ X^O{}_8) \quad (1)$$

The H sheet

The H sheet has one (Si_2O_7) group and one M^H polyhedron in the minimal cell (Fig. 4b). I divide anions of the H sheet that are not connected to the O sheet into two groups: O atoms of (Si_2O_7) groups, and X^P anions that are apical vertices of M^H polyhedra not shared with (Si_2O_7) groups. The M^H polyhedron has one $X^P{}_M$ vertex if it is [6]-coordinated, and no $X^P{}_M$ vertices if it is [5]-coordinated. Depending on the coordination number of the cation at the M^H site, the formula of two H sheets can be written as:

$${}^{[6]}M^H{}_2\ (Si_2O_7)_2\ X^P{}_{M2} \quad (2)$$

$${}^{[5]}M^H{}_2\ (Si_2O_7)_2 \quad (3)$$

The P sites

In the minimal cell, there are one A^P polyhedron and one B^P polyhedron (Fig. 4b). The A^P site can be fully occupied, partly occupied or vacant. The B^P site can be fully occupied or vacant. The A^P and B^P atoms have coordinating anions in the O and H sheets, and these have been already included in formulae (1)–(3). The coordination of these two sites gives two possibilities:

(a) the $X^P{}_A$ and $X^P{}_B$ anions of this TS block also belong to the H sheet of the adjacent TS block. Thus I do not count these anions here (as they are counted in the adjacent TS block; note that I count only peripheral cation sites):

$$A^P{}_2\ B^P{}_2 \quad (4)$$

(b) the A^P site has only one $X^P{}_A$ anion, and this anion is not connected to the next TS block; here I take into account cations and anions:

$$A^P{}_2\ B^P{}_2\ X^P{}_{A2} \quad (5)$$

The TS block

I write the general formula of the TS block as the sum of one O sheet, two H sheets and four peripheral sites. Note that three sheets, O and two H, constitute the major skeleton of the TS block, whereas the positions of peripheral sites are not fixed. Each (Si_2O_7) group shares two common vertices with the O sheet, and two (Si_2O_7) groups (two H sheets) share four common vertices with the O sheet. I count four common X^O anions only once as part of an (Si_2O_7) group, *i.e.*, a group where the anions get maximal bond-valence from the coordinating cation, Si^{4+}. I consider four cases:

O	**+**	**2 H**	**+**	**4 P cations**	**– common anions =**	**FORMULA**	
$M^O{}_4\ X^O{}_8$	+	${}^{[6]}M^H{}_2\ (Si_2O_7)_2\ X^P{}_{M2}$	+	$A^P{}_2\ B^P{}_2$	– $X^O{}_4$	$= A^P{}_2\ B^P{}_2\ {}^{[6]}M^H{}_2\ M^O{}_4\ (Si_2O_7)_2\ X^O{}_4\ X^P{}_{M2}$	(6)
$M^O{}_4\ X^O{}_8$	+	${}^{[6]}M^H{}_2\ (Si_2O_7)_2\ X^P{}_{M2}$	+	$A^P{}_2\ B^P{}_2\ X^P{}_{A2}$	– $X^O{}_4$	$= A^P{}_2\ B^P{}_2\ {}^{[6]}M^H{}_2\ M^O{}_4\ (Si_2O_7)_2\ X^O{}_4\ X^P{}_{M2}\ X^P{}_{A2}$	(7)
$M^O{}_4\ X^O{}_8$	+	${}^{[5]}M^H{}_2\ (Si_2O_7)_2$	+	$A^P{}_2\ B^P{}_2$	– $X^O{}_4$	$= A^P{}_2\ B^P{}_2\ {}^{[5]}M^H{}_2\ M^O{}_4\ (Si_2O_7)_2\ X^O{}_4$	(8)
$M^O{}_4\ X^O{}_8$	+	${}^{[5]}M^H{}_2\ (Si_2O_7)_2$	+	$A^P{}_2\ B^P{}_2\ X^P{}_{A2}$	– $X^O{}_4$	$= A^P{}_2\ B^P{}_2\ {}^{[5]}M^H{}_2\ M^O{}_4\ (Si_2O_7)_2\ X^O{}_4\ X^P{}_{A2}$	(9)

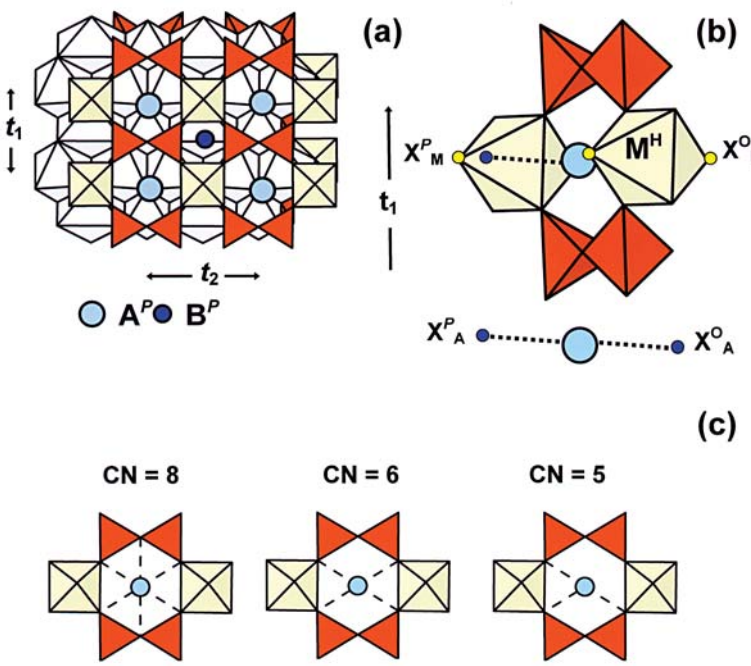

FIG. 3. The disposition of the *P* sites in the TS block showing (a) the A^P and B^P sites in large voids formed by M^H polyhedra, (Si_2O_7) groups and M^O octahedra, (b) the location of A^P–X^P_A and A^P–X^O_A bonds, and (c) the position of A^P–anion bonds in the plane of the H sheet. Legend as in Figure 1; A^P and B^P sites are large blue and smaller navy blue circles, anion sites are small navy blue and yellow circles, (A^P–anion) bonds out of the plane of the H sheet are shown as black dashed lines.

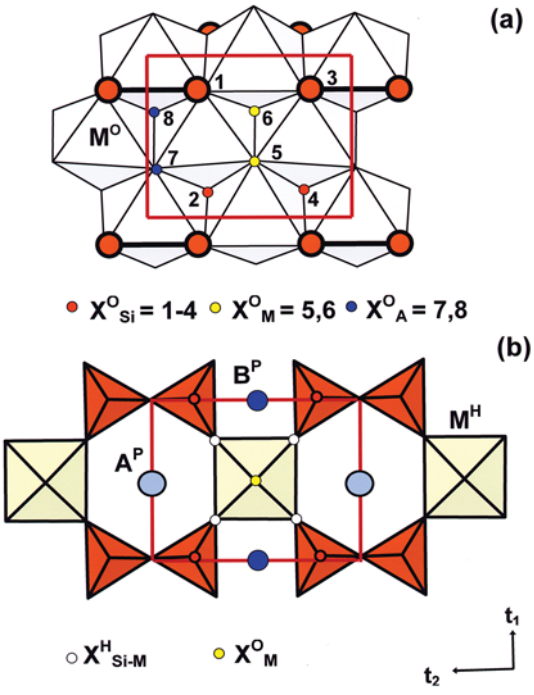

FIG. 4. Specification of the minimal cell with $t_1 \approx 5.5$ and $t_2 \approx 7$ Å translations (a) in the plane of the O sheet, and (b) in the plane of the H sheet. Legend as in Figure 2; (Si_2O_7) groups are shown schematically as two large orange circles connected by a solid black line; orange, yellow and navy blue circles indicate anions shared between O and H sheets, and they belong to M^O octahedra and (SiO_4) tetrahedra (X^O_{Si}), M^H (X^O_M) and A^P (X^O_A) polyhedra. The small white circles indicate O atoms of the H sheet shared between M^H polyhedra and (SiO_4) tetrahedra. Odd numbers in (a) signify anions shared with H-sheet polyhedra on this side, and even numbers signify anions shared with H-sheet polyhedra on the other (back) side of the O sheet. Red lines show the minimal cell.

where the M^{H} site is [6]-coordinated (formulae 6, 7) and [5]-coordinated (formulae 8, 9); the A^{P} polyhedron links to the next TS block (formulae 6, 8) or does not link to the next TS block (formulae 7, 9). These four cases can be subsumed under the following general formula for the TS block

$$A^{P}_{2}\ B^{P}_{2}\ \mathbf{M^{H}_{2}\ M^{O}_{4}\ (Si_{2}O_{7})_{2}\ X_{4+n}} \qquad (10)$$

where $X_{4+n} = X^{O}_{4} + X^{P}_{M2} + X^{P}_{A2}$ and n is the number of X^{P} anions: n = 0 where the M^{H} site is [5]-coordinated and the A^{P} polyhedron links to the next TS block; n = 2 where the M^{H} site is [6]-coordinated and the A^{P} polyhedron links to the next TS block; n = 4 where the M^{H} site is [6]-coordinated and the A^{P} polyhedron does not link to the next TS block and has one X^{P}_{A} anion. The core part of the TS block, $\mathbf{M^{H}_{2}\ M^{O}_{4}\ (Si_{2}O_{7})_{2}\ X_{4}}$, is shown in bold; the stoichiometry of this part of the TS block is invariant.

The Topology of the TS Block. III. Linkage of O and H Sheets

There are three types of linkage of two H sheets and the central O sheet. Two H sheets can be related by a pseudo-mirror plane (*m*) coinciding with the plane of the O sheet cations, or two H sheets can be shifted relative to each other. These linkages are shown in Figure 5 and are critical to an understanding of the stereochemistry of minerals with the TS block.

Linkage 1 occurs where two H sheets connect to the O sheet such that two (Si_2O_7) groups link to the *trans* edges of the same octahedron of the O sheet (Fig. 5a).

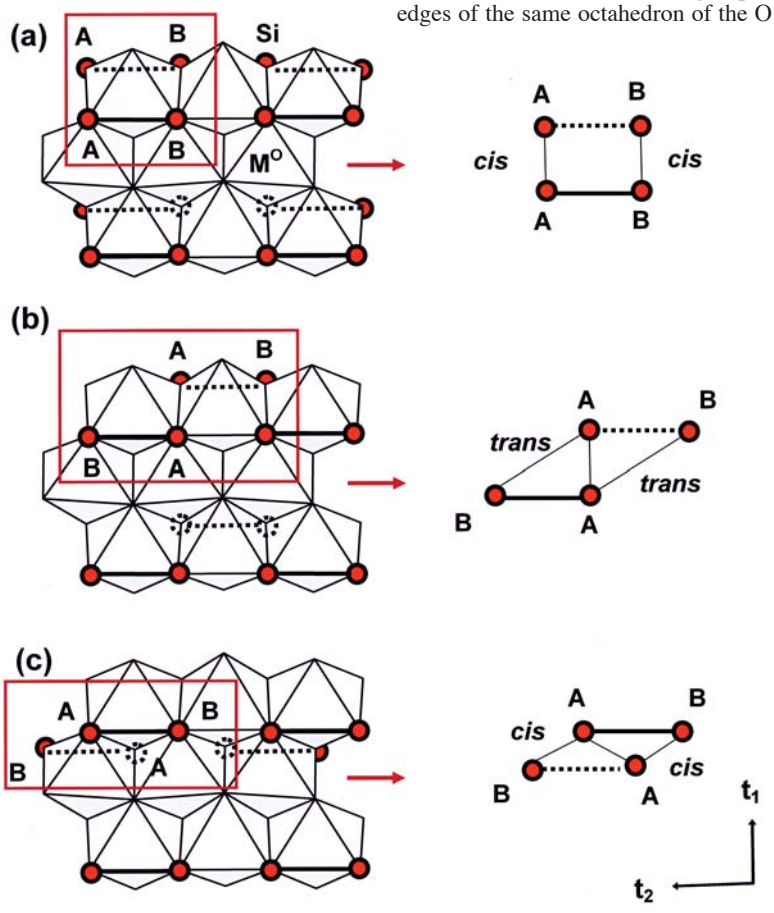

FIG. 5. Schematic representation of different linkages between O and H sheets, *i.e.*, M^{O} octahedra and [Si_2O_7] groups within one TS block; M^{H} cations are omitted for clarity. (a) Linkage 1, (b) linkage 2, (c) linkage 3. Legend as in Figure 2; (Si_2O_7) groups of two different H sheets are shown schematically as two orange circles connected by a solid (upper surface) or a dashed (lower surface) black line. The critical parts of each part of the linkage are shown by the graphs to the right of the structure illustrations.

In this case, two H sheets are related by a pseudo-mirror plane (*m*) coinciding with the plane of the O sheet.

Linkage 2 occurs where two (Si_2O_7) groups link to two octahedra adjacent along $\mathbf{t_2}$ (Fig. 5b). Two Si atoms of two different (Si_2O_7) groups (Si_A) share two anions of the O sheet that constitute a common edge between two adjacent octahedra. Another two Si atoms (Si_B) are in a *cis* position to Si_A atoms of the same group, and in a *trans* position to Si_A atoms of a different group.

Linkage 3 occurs where two (Si_2O_7) groups share common anions of the O sheet, which form edges of two octahedra adjacent approximately along $\mathbf{t_1}$ (Fig. 5c). Two Si_A atoms of two different (Si_2O_7) groups share a common edge between two adjacent octahedra. Two Si_B atoms are in a *cis* position with respect to Si_A atoms of the same group and in a *cis* position with respect to the Si_A atoms of a different group.

The Topology and Stereochemistry of the TS Block. I. Definition of Four Distinct Groups of Structures

There are three possible types of linkage between O and H sheets within one TS block (Fig. 5), and thus there are three types of topology of the TS block in the crystal structures in question, not two types of TS = HOH block, seidozerite and bafertisite, as stated by Ferraris (1997), Christiansen *et al*. (1999) and Ferraris *et al*. (2001b). As the TS block is present in all these structures, it seems logical to divide all structures into three groups on the basis of the type of linkage. However, linkage 1 shows two types of very different stereochemistry in these minerals: (a) (Si_2O_7) groups link to Na polyhedra, and (b) (Si_2O_7) groups link to Ti polyhedra. Hence I will divide these structures into four groups based on the topology *and* stereochemistry of the TS block. Figure 6 shows the different TS blocks in these four groups of structures, together with a prototype structure for each group.

In Group I, linkage 1 occurs, and two (Si_2O_7) groups link to a Na polyhedron of the O sheet (Fig. 6a). The Na atom is [8]-coordinated, the additional two anions being the bridging O atoms of (Si_2O_7) groups. The [8]-coordinated Na polyhedron shares three O anions (each three constitute two edges) with each (Si_2O_7) group. In Group II, linkage 2 occurs, and two (Si_2O_7) groups link to two M^{2+} octahedra adjacent along $\mathbf{t_2}$ (Fig. 6b). In Group III, linkage 1 occurs, and two (Si_2O_7) groups link to the Ti octahedron of the O sheet (Fig. 6c). Note that X^{O}_{Si} atoms of an (Si_2O_7) group are shared with one Ti octahedron, an adjacent Na polyhedron along $\mathbf{t_2}$ and

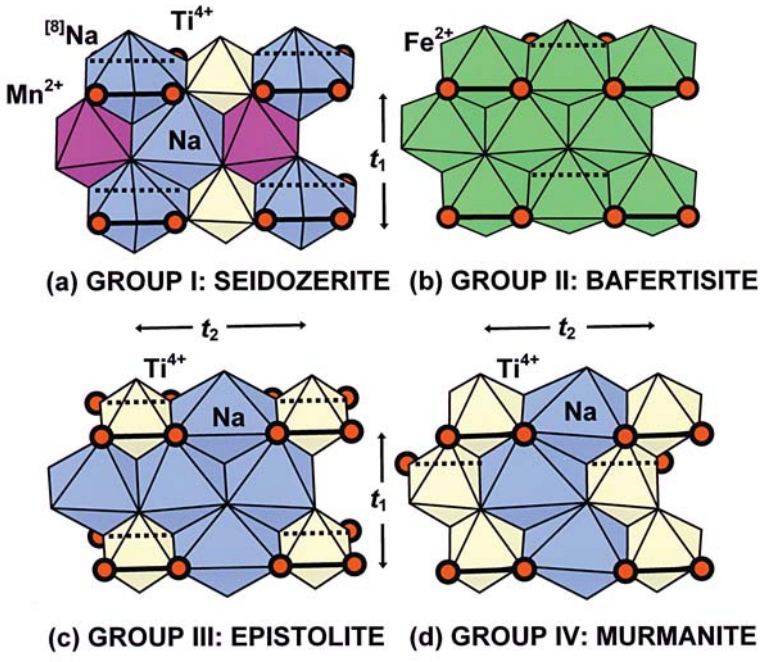

FIG. 6. The four different types of TS block based on bond topology and stereochemistry: (a) Group I, (b) Group II, (c) Group III, (d) Group IV. Only the (Si_2O_7) groups of the H sheet are shown. Legend as in Figure 4; Na, Ti, Mn^{2+}, Fe^{2+} polyhedra are navy blue, yellow, magenta and green, respectively. A prototype mineral is indicated for each group.

the third M^O octahedron, and these two O atoms are invariably coordinated as in Group I. The topology of Groups I and III is identical, but the stereochemistry is different. In Group IV, linkage 3 occurs, and two (Si_2O_7) groups link to two adjacent Ti octahedra approximately along $\mathbf{t_1}$ (Fig. 6d).

The Topology and Stereochemistry of the TS Block. II. Possible Variations in Cations of the O Sheet and the Maximal Content of Ti in the TS Block

Possible variations in cations of the O sheet

Linkage between O and H sheets requires special constraints on the composition of the O sheet. Each anion in the O sheet is a common vertex for three octahedra. At least four anions of the O sheet must have an incident bond-valence sum of 1.0 valence units (*vu*) from the cations of the O sheet in order to link to a single (Si_2O_7) group. What are the possibilities for incident bond-valence sums to be equal to 1 *vu*?

(1) Where 4 M^O = 4 M^+, 3 M^+ give 3 × 0.17 = 0.5 *vu* to any anion in the O sheet. Therefore, the O sheet cannot be formed by monovalent cations alone, as they do not give enough incident bond-valence to anions bonded to Si atoms.

(2) Where 4 M^O = 4 M^{2+}, 3 M^{2+} give 3 × 0.33 = 1.0 *vu* to any anion in the O sheet. This composition corresponds to Group II.

(3) Where 4 M^O = 4 M^{3+}, 3 M^{3+} give 3 × 0.5 = 1.5 *vu* to any anion in the O sheet. Therefore, the O sheet cannot be formed of trivalent cations alone, as they give an excessive bond-valence sum at anions bonded to Si^{4+} atoms.

Thus cations of the O sheet can be either all divalent (as in Group II), or they have to be of different valences.

(4) Where 4 M^O = 3 M^+ + M^{3+}, (a) 3 M^+ give 3 × 0.17 = 0.51 *vu* and (b) 2 M^+ + M^{3+} give 2 × 0.17 + 0.5 = 0.84 *vu*. All anions have insufficient incident bond-valence to be bonded to Si^{4+}.

(5) Where 4 M^O = 3 M^+ + M^{4+}, (a) 3 M^+ give 3 × 0.17 = 0.51 *vu* and (b) 2 M^+ + M^{3+} give 2 × 0.17 + 0.67 = 1.01 *vu*. The last combination (b) provides anions that can be bonded to Si^{4+}; (a) and (b) occur together in Groups I and III.

(6) Where 4 M^O = 2 M^+ + 2 M^{4+}, (a) 2 M^+ + M^{4+} give 2 × 0.17 + 0.67 = 1.01 *vu* and (b) M^+ + 2 M^{4+} give 0.17 + 2 × 0.67 = 1.5 *vu*; (a) provides anions that can be bonded to Si^{4+}, and (a) and (b) occur together in Group IV. In fact, anions of arrangement (b) are also bonded to Si^{4+}, but I will discuss this later.

Thus, there are three major cation combinations of the O sheet: 3 M^+ + M^{4+}, 4 M^{2+}, and 2 M^+ + 2 M^{4+}. Minor deviations from four compositions occur where M^{2+} substitutes for M^+ and M^{3+} substitutes for M^{4+}.

I do not exclude possible substitution of M^{5+} (primarily Nb^{5+}) for Ti^{4+} in the O sheet, and consider two cases:

(7) Where 4 M^O = 3 M^+ + M^{5+}, (a) 3 M^+ give 3 × 0.17 = 0.51 *vu*, and (b) 2 M^+ + M^{5+} give 2 × 0.17 + 0.83 = 1.17 *vu*; (b) provides anions that can be bonded to Si^{4+}.

(8) Where 4 M^O = 2 M^+ + M^{4+} + M^{5+}, (a) 2 M^+ + M^{4+} give 2 × 0.17 + 0.67 = 1.01 *vu*, (b) 2 M^+ + M^{5+} give 2 × 0.17 + 0.83 = 1.17 *vu*, and (c) M^+ + M^{4+} + M^{5+} give 0.17 + 0.67 + 0.83 = 1.67 *vu*; (a) and (b) provide anions that can be bonded to Si^{4+}.

The cluster (3 Na + Nb^{5+}) can occur in Groups I and III, and the cluster (2 Na + Ti + Nb^{5+}) can occur in Group IV.

The maximal content of Ti in the TS block

The maximal observed content of Ti in the TS block is 4 atoms per formula unit (*apfu*) in Group IV. Can it be more than 4 *apfu*; for example, 5 *apfu?* First, Ti occurs at M^H sites in the H sheet, and hence two H sheets give a maximum of 2 *apfu* of Ti. Second, how many sites can Ti occupy in the O sheet? Above, I showed that M^{4+} can occupy only two M^O sites in the O sheet. Therefore the maximal possible content of Ti in the TS block is 4 *apfu*: 2 Ti^O + 2 Ti^H.

The Topology and Stereochemistry of the TS Block. III. Consideration of Individual Groups

Next, I consider the topology and stereochemistry of the TS block in the minerals of Table 1. In Table 3, 24 minerals are divided into four groups in accord with the topology and stereochemistry of their TS block. It is difficult enough to compare these 24 structures without having to contend with sites occupied by several different chemical species. Hence I have simplified the formulae by considering only the dominant cation or anion at each site, except where stereochemistry and electroneutrality force a (fixed) double occupancy of one site. In several of the minerals listed in Table 3, the formulae originally given are not neutral, and I recalculated the chemical formula from the original chemical composition and assigned the resulting cations and anions to adhere as closely as possible to the original site-occupancies. Table 3 gives the chemical composition for each cation and anion site in the minimal cell of the TS block for all 24 minerals. The O sheet is characterized by four cation (M^O) and four anion (X^O) sites; the two H sheets, by two cation M^H sites, two (Si_2O_7) groups, oxygen (X^H_{Si}) sites that connect to another TS block, and two anion (X^P_M) sites at the periphery of the intermediate space. There are four cation sites, two A^P and two B^P sites, and a variable number of anion sites, X^P_A and X^P_B sites. Each site is characterized by the dominant cation or anion, or by two principal cations or

anions where they are approximately in a 1:1 ratio. In several cases, the composition of sites given in Table 3 differs from the general formulae given in Table 1.

Group I

There are seven minerals in this group: götzenite, hainite, seidozerite, grenmarite, rinkite, kochite, and rosenbuschite. Grenmarite, the Zr analogue of seidozerite, is the only mineral that does not have a Ti-dominant site (Table 3). However, grenmarite obeys the structural principles of Group I, and thus I consider it in this paper.

The O sheet: Figure 7 gives examples of the chemical composition and topology of the O sheet. In götzenite, one M^{O} site is occupied by Na, two M^{O} sites are occupied by Ca, and one M^{O} site is occupied by Ti (Fig. 7a). In kochite, three out of four M^{O} sites are occupied by Na, and one M^{O} site is occupied by Ti (Fig. 7b). In hainite, one M^{O} site is occupied by Na, two M^{O} sites are occupied by Na and Ca in the ratio 1 : 1, and one M^{O} site is occupied by Ti. For rinkite, I write 4 M^{O} = Na(NaCa)Ti although Na > Ca at two M^{O} sites. There is cation disorder at many sites in the crystal structure of rinkite, and to write a reasonably simple formula, I have to make an assumption, *i.e.*, write (NaCa) instead of Na_2. In seidozerite, two M^{O} sites are occupied by Na, one M^{O} site by Mn^{2+}, and one site by Ti (Fig. 7c). In grenmarite, two M^{O} sites are occupied by Na, one M^{O} site by Mn^{2+}, and one site by $(Zr_{0.54}\,Ti_{0.46})$ (instead of Ti as in seidozerite). At this particular site in grenmarite, Ti : Zr ≈ 1 : 1, *i.e.*, the content of Ti is 0.5 *apfu*. For hainite, kochite, rinkite, götzenite, grenmarite and seidozerite, the O sheet is characterized by $t_1 \approx 5.7$ and $t_2 \approx 7.3$ Å, and a cation unit M^{O}_4. In rosenbuschite, there are four types of dominant cation: Na, Ca, Ti^{4+} and Zr. At the *M*(2) sites, Na > Ca (Christiansen *et al*. 2003a), and I can write the composition of these sites as Na_2. Order of Ti and Zr along [010] causes doubling of the $t_1 \approx 5.6$ Å, *i.e.*, $b_{ros} = 11.398$ Å (see Table 1, Fig. 7d). There are two M^{O}_4 cation units in a planar cell with dimensions $2t_1$, t_2, which gives a composition of [Na_2 Na_4 Ti Zr]. In the crystal structures of Group I, Ti is dominant at one of four M^{O} sites (except for rosenbuschite and grenmarite). In rosenbuschite and grenmarite, the composition of the

TABLE 3. CHEMICAL COMPOSITION OF THE TS BLOCK

Mineral	O sheet						2H sheets				*P* sites					
	$4M^{O}$				$4X^{O}$ $2X^{O}_{A}$	$2X^{O}_{M}$	$2M^{H}$		$(Si_2O_7)_2$	X^{H}_{Si}	$2A^{P}$		$2B^{P}$		X^{P}_{M}	X^{P}_{A}	X^{P}_{B}
Group I																	
götzenite	[8]Na	Ca	Ca	Ti	F_2	(OF)	Ca	Ca	$(Si_2O_7)_2$	O_4	[7]Ca	[7]Ca	□	□	O_2	O_2	□
hainite	[8]Na	(Na | Ca)	Ti	F_2	(OF)	[Ca(Y,REE)]		$(Si_2O_7)_2$	O_4	[7]Ca	[7]Ca	□	□	O_2	O_2	□
seidozerite	[8]Na	Na	Mn^{2+}	Ti	F_2	O_2	Zr	Zr	$(Si_2O_7)_2$	O_4	[8]Na	[8]Na	□	□	O_2	O_2	□
grenmarite	[8]Na	Na	Mn^{2+}	Zr	F_2	O_2	Zr	Zr	$(Si_2O_7)_2$	O_4	[8]Na	[8]Na	□	□	O_2	O_2	□
rinkite	[8]Na	(Na | Ca)	Ti	F_2	(OF)	[7]$(Ca_{1.5}Ce_{0.5})$		$(Si_2O_7)_2$	O_8	[8]$(Ca_{1.5}Ce_{0.5})$		□	□	O_4	O_4	□
kochite	[8]Na	Na	Na	Ti	F_2	OF	Mn^{2+}	Zr	$(Si_2O_7)_2$	O_4	[8]Ca	Ca	□	□	O_2	O_2	□
rosenbuschite	[8]Na	Na	Na	{TiZr}:2	F_2	OF	Ca	Zr	$(Si_2O_7)_2$	O_4	Ca	[8]Ca	□	□	O_2	O_2	□
Group II																	
perraultite		$(Mn_5Fe^{2+}_3)$: 2			(OH)F	O_2	Ti	Ti	$(Si_2O_7)_2$		[9-10]Ba		[10]Na		(OH)	□	□
surkhobite	Mn^{2+}	Mn^{2+}	Fe^{2+}	Fe^{2+}		O_2	Ti	Ti	$(Si_2O_7)_2$		[10-12]Ba		[10]Na**		[F(OH)]$_0$	□	□
bafertisite	Fe^{2+}	Fe^{2+}	Fe^{2+}	Fe^{2+}	$(OH)_2$	O_2	Ti	Ti	$(Si_2O_7)_2$	O_8	[10-12]Ba	[10-12]Ba	□	□	$(OH)_2$	O_{10-14}	□
hejtmanite	Mn^{2+}	Mn^{2+}	Mn^{2+}	Mn^{2+}	$(OH)_2$	O_2	Ti	Ti	$(Si_2O_7)_2$	O_8	[10-12]Ba	[10-12]Ba	□	□	$(OH)_2$	O_{10-14}	□
yoshimuraite	Mn^{2+}	Mn^{2+}	Mn^{2+}	Mn^{2+}	$(OH)_2$	O_2	[5]Ti	[5]Ti	$(Si_2O_7)_2$		[11]Ba	[11]Ba	[11]Ba	[11]Ba	□	O_{10}	O_{14}
bussenite	$(Fe^{2+}$	Na)	$(Fe^{2+}$	Na)	$(OH)_2$	O_2	Ti	Ti	$(Si_2O_7)_2$		[9]Ba	[9]Ba	[11]Ba	[11]Ba	$(H_2O)_2$	O_4	$O_6F_4(H_2O)_4$
Group III																	
lamprophyllite	Na	Na	Na	Ti	$(OH)_2$	O_2	[5]Ti	[5]Ti	$(Si_2O_7)_2$	O_8	[10](Sr | Na)	□	□	□	O_8	□
barytolamprophyllite	Na	Na	Na	Ti	$(OH)_2$	O_2	[5]Ti	[5]Ti	$(Si_2O_7)_2$	O_8	[11](Ba | K)	□	□	□	O_8	□
nabalamprophyllite	Na	Na	Na	Ti	$(OH)_2$	O_2	[5]Ti	[5]Ti	$(Si_2O_7)_2$	O_8	[11]Ba	[11]Na	□	□	□	O_8	□
innelite	Na	Na	Ca	Ti	O_2	O_2	[5]Ti	[5]Ti	$(Si_2O_7)_2$		[10]Ba	[10]Ba	[11]Ba	[11]Ba	□	O_8	O_{14}
epistolite	Na	Na	Na	Ti	$(OH)_2$	O_2	Nb	Nb	$(Si_2O_7)_2$		[8]Na*	[8]Na*	□	□	$(H_2O)_2$	$(H_2O)_2$	□
vuonnemite	Na	Na	Na	Ti	(OF)	O_2	Nb	Nb	$(Si_2O_7)_2$	O_{10}	[8]Na	[8]Na	□	□	O_2	O_2	□
Group IV																	
murmanite	Na	Na	Ti	Ti	O_2	O_2	Ti	Ti	$(Si_2O_7)_2$		[8]Na	[8]Na	□	□	$(H_2O)_2$	$(H_2O)_2$	□
lomonosovite	Na	Na	Ti	Ti	O_2	O_2	Ti	Ti	$(Si_2O_7)_2$	O_{10}	[8]Na	[8]Na	□	□	O_2	O_2	□
quadruphite	Na	Na	Ti	Ti	O_2	O_2	Ti	Ti	$(Si_2O_7)_2$	O_8	Na	Na	□	□	O_2	O_2	□
sobolevite	Na	Na	(Ti | Mn^{2+})	(OF)	O_2	Ti	Ti	$(Si_2O_7)_2$	O_7	Na	[5]Na	□	□	O_2	O_2	□
polyphite	Na	Na	Ti	Ti	O_2	O_2	Ti	Ti	$(Si_2O_7)_2$	O_6	Na	Na	□	□	O_2	O_2	□

X^{O}, X^{H} and X^{P} : anions of O and H sheets and peripheral anions; X^{O}_{M} : common vertices of M^{O} and M^{H} polyhedra; X^{O}_{A} : common vertices of M^{O} and A^{P} polyhedra; X^{H}_{Si} (red and green): O atoms of 2 (Si_2O_7) groups shared with M^{H} and A^{P} polyhedra of another TS block and shared with polyhedra of the **I** block; X^{P}_{M}, X^{P}_{A} and X^{P}_{B} : apical anions of 2 M^{H}, 2 A^{P} and 2 B^{P} atoms at the periphery of the TS block; * 50% occupied; ** predicted occupancy (see Appendix C: Surkhobite); red: X^{P}_{M} and X^{P}_{A} anions shared with (Si_2O_7) groups of another TS block and joint sites shared by two TS blocks; green: X^{P}_{M} and X^{P}_{A} anions shared with polyhedra of the **I** block; { } cations are ordered *i.e.*, they do not substitute for each other; ( ) cations and anions are disordered and substitute for each other. Coordination numbers (CN) for cations are shown where CN ≠ 6.

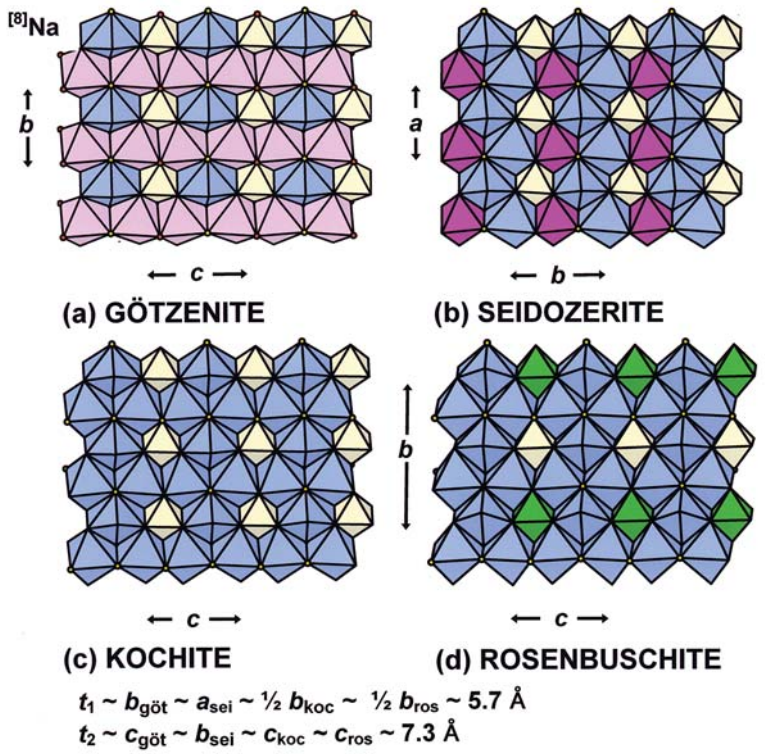

FIG. 7. Group I. Chemical composition and stereochemistry of the O sheet: (a) götzenite, (b) seidozerite, (c) kochite, (d) rosenbuschite. Ti, Zr, Mn^{2+}, Ca and Na polyhedra are yellow, green, magenta, light pink and navy blue, respectively. The F and (OF) anions are shown as small yellow and orange circles, respectively.

$M^O{}_4$ cation unit is {[Na_2 Na_4 Ti Zr] / 2} and [Na_2 Mn (Zr,Ti)], and Ti = 0.5 *apfu* or (Ti + Zr) = 1 *apfu*.

The H sheet: Figure 8 shows the main details of the stereochemistry of the H sheet. The M^H site is most commonly [6]-coordinated, except for rinkite, in which the coordination number is [7]. Where one cation is dominant at the M^H site, *e.g.*, Ca in götzenite (Fig. 8a), (Ca + REE) in hainite and rinkite, Zr in seidozerite (Fig. 8b) and grenmarite, the H sheet is characterized by two repeats, $t_1 \approx 5.7$ and $t_2 \approx 7.3$ Å. Where order of two cations at the M^H site occurs along [010], *e.g.*, Mn^{2+} and Zr in kochite (Fig. 8c), and Ca and Zr in rosenbuschite (Fig. 8d), the H sheet is characterized by a doubled length of $\mathbf{t_1}$, $2t_1$ (Figs. 8c, d). Note that such order of cations invariably occurs along the translation vector with the shorter t_1 translation.

The P sites: The A^P site is usually occupied by Ca or Na or a mixture of both. In rinkite, Ca is dominant over the rare-earth elements (REE, mainly Ce^{3+}), and the B^P site is vacant. In Group I, the A^P sites lie in the plane of the H sheet, and the coordination number varies from [6] to [8].

Linkage of O and H sheets: Linkage 1 occurs in Group I: two (Si_2O_7) groups of two H sheets link to the *trans* edges of the same octahedron of the O sheet, and two H sheets are related by a pseudo-mirror plane (*m*) coinciding with the plane of the O sheet (Figs. 9a–f). Where two (Si_2O_7) groups link to one Na polyhedron, Na is [8]-coordinated as it bonds to the bridging O atom of each (Si_2O_7) group. The Si–O–Si atoms form a reflex angle toward the O sheet. The mean ∠Si–O–Si is 199°, with a maximal value of 206.8° in rinkite (Fig. 9d) and a minimal value of 186.2° in grenmarite (Table 2). The M^H polyhedron usually links to a Ti octahedron (Figs. 9a–e), except in rosenbuschite (Fig. 9f) and grenmarite. In rosenbuschite, the Ca^H octahedron links to the Ti^O octahedron, and the Zr^H polyhedron links to the Zr^O octahedron (Fig. 9f). In grenmarite, the Zr polyhedra of the O and H sheets also share a corner. Order of cations occurs along one direction, $\mathbf{t_1}$, and causes doubling of the corresponding unit-cell parameter. Order of cations occurs primarily within the H sheet (kochite and rosenbuschite) (Figs. 9e, f), and can be accompanied by order in the O sheet (rosenbuschite) (Fig. 9f). In Group I, there

is no example of independent order in the O sheet, *i.e.*, without corresponding order in the H sheet.

Anion considerations: The X^{O}_{A} site: In Group I, two X^{O}_{A} anions are F (Table 3). Each X^{O}_{A} anion bonds to four cations, 3 M^{O} and one A^{P}, where 3 M^{O} = {$^{[8]}Na^{O}$ + 2 M^{O} (Na–Ca)}, and A^{P} is mainly Na and Ca. The X^{O}_{A} anion receives maximal bond-valence where Ca is dominant at the M^{O} and A^{P} sites. The bond-valence sum for X^{O}_{A} is 0.13 ($^{[8]}Na^{O}$) + 0.33 × 2 (2 M^{O}) + 0.33 (A^{P}) = 1.12 *vu*, and therefore the X^{O}_{A} site is invariably occupied by a monovalent anion. Why is this monovalent anion invariably F^{-}? Why does not OH^{-} occur at the X^{O}_{A} site? Absence of OH^{-} is due to insufficient space to accommodate H and its corresponding hydrogen bond.

The X^{O}_{M} site: An atom at the X^{O}_{M} site is bonded to four cations: Ti^{O} (except for rosenbuschite and grenmarite), 2 M^{O} and M^{H}. In seidozerite (**grenmarite**), Ti^{O} (**Zr^{O}**) + $(Mn^{2+})^{O}$ + Na^{O} + Zr^{H} give (formally) 1.83 *vu* and $X^{O}_{M} = O^{2-}$. In götzenite, hainite and rinkite, the X^{O}_{M} site is statistically occupied by O and F atoms in the ratio 1 : 1. In götzenite, Ti^{O} + $Ca_2{}^{O}$ + Ca^{H}, hainite, Ti^{O} + $(NaCa)^{O}$ + $[Ca_{0.5}\ (Y+REE)_{0.5}\ ]^{H}$, and rinkite, Ti^{O} + $(NaCa)^{O}$ + $[Ca_{0.75}\ Ce_{0.25}\ ]^{H}$, the cations give about 1.5 *vu*, and X^{O}_{M} = (FO). In rosenbuschite and kochite, there are two unique X^{O}_{M} sites; I label them X^{O}_{M} (1) and X^{O}_{M} (2). Anions at these sites receive the following bond-valences from their bonded cations (values taken from Christiansen *et al*. 2003a):

	X^{O}_{M} (1)	*vu*	X^{O}_{M} (2)	*vu*
rosenbuschite	**2 Zr** + 2 Na	1.66	**Ti** + 2 Na + Ca	1.36
kochite	**Ti** + **Zr** + 2 Na	1.60	**Ti** + 2 Na + Mn^{2+}	1.38

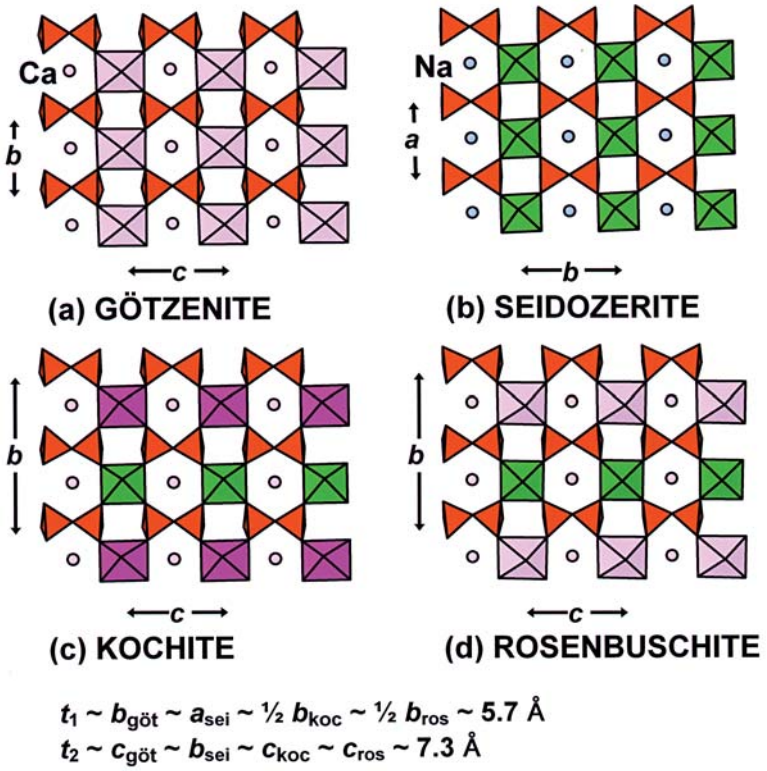

FIG. 8. Group I. Chemical composition and stereochemistry of the H sheet including *P* (= A^{P} sites): (a) götzenite, (b) seidozerite, (c) kochite, (d) rosenbuschite. Legend as in Figure 7, (SiO_4) tetrahedra are orange; Ca and Na atoms at the A^{P} site are shown as light pink and navy blue circles. Note the order among octahedrally coordinated cations in kochite and rosenbuschite.

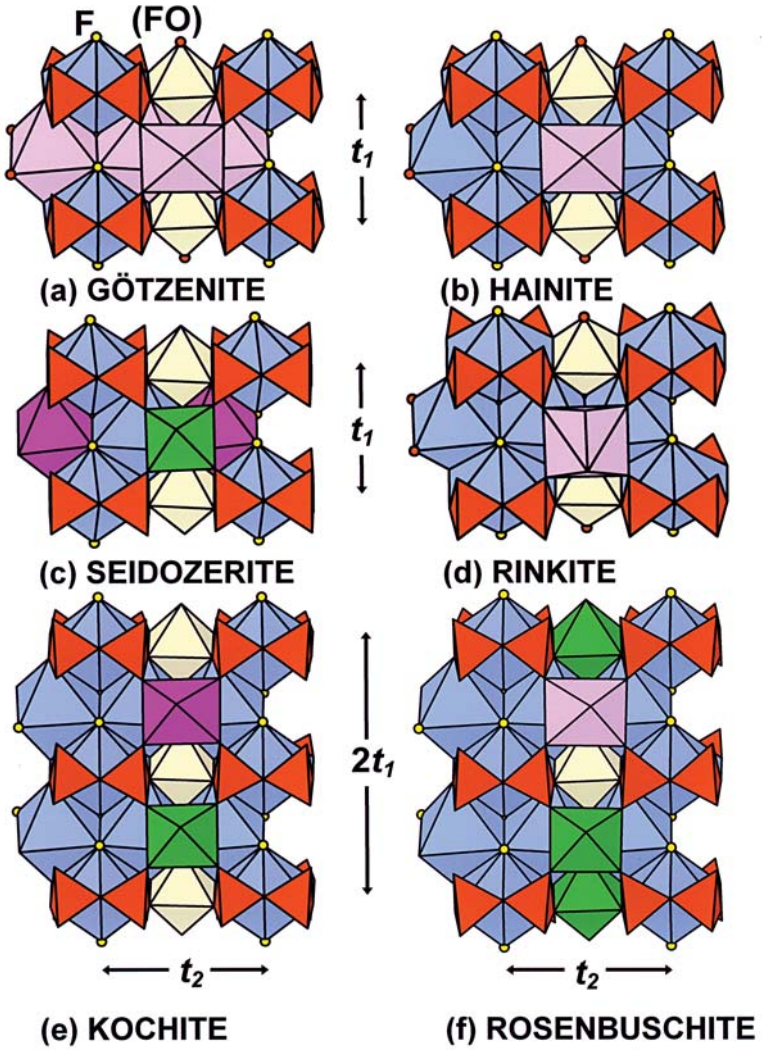

FIG. 9. Group I. Linkage of H and O sheets within one TS block: (a) götzenite, (b) hainite, (c) seidozerite, (d) rinkite, (e) kochite, (f) rosenbuschite. Legend as in Figure 8; A^P sites are not shown. Note the double value of t_1 in kochite and rosenbuschite.

I expect the O and F atoms to be ordered at these two sites, and Christiansen *et al*. (2003a) reported values that support this conclusion: $X^O{}_M$ (1) = O^{2-} and $X^O{}_M$ (2) = F^-. As for the $X^O{}_A$ site, the monovalent anion is also invariably F^-, and for the same reason.

Group II

There are six minerals in this group: bafertisite, hejtmanite [which has two polytypes, with monoclinic symmetry; they are designated hejtmanite-C (C-centered lattice) and hejtmanite-P (primitive lattice) in Table 1], perraultite, surkhobite, bussenite and yoshimuraite.

The O sheet: Figure 10 illustrates the chemical composition and topology of the O sheet. In three minerals, four M^O sites are occupied by cations of the same type: Fe^{2+} in bafertisite (Fig. 10a), and Mn^{2+} in hejtmanite and yoshimuraite. In perraultite (Fig. 10b) and surkhobite, there is Fe^{2+}–Mn^{2+} order in the O sheet: ($Mn^{2+}{}_5$ $Fe^{2+}{}_3$) in perraultite and [($Fe^{2+}{}_4$ $Mn^{2+}{}_4$) with Fe^{2+} slightly dominant over Mn^{2+}] in surkhobite (Table 3). In bussenite (Fig. 10c), Fe^{2+}, Mn^{2+} and Na are statistically distributed over three sites: $M(1) = Na_{1.0}$

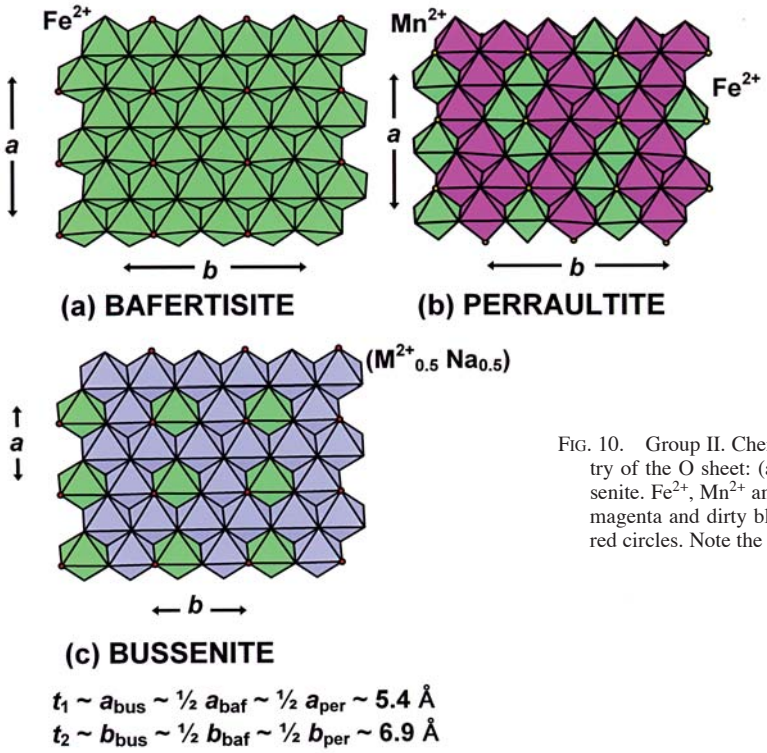

FIG. 10. Group II. Chemical composition and stereochemistry of the O sheet: (a) bafertisite, (b) perraultite, (c) bussenite. Fe^{2+}, Mn^{2+} and $(M^{2+}_{0.5}\ Na_{0.5})$ octahedra are green, magenta and dirty blue, (OH) groups are shown as small red circles. Note the difference in unit-cell dimensions.

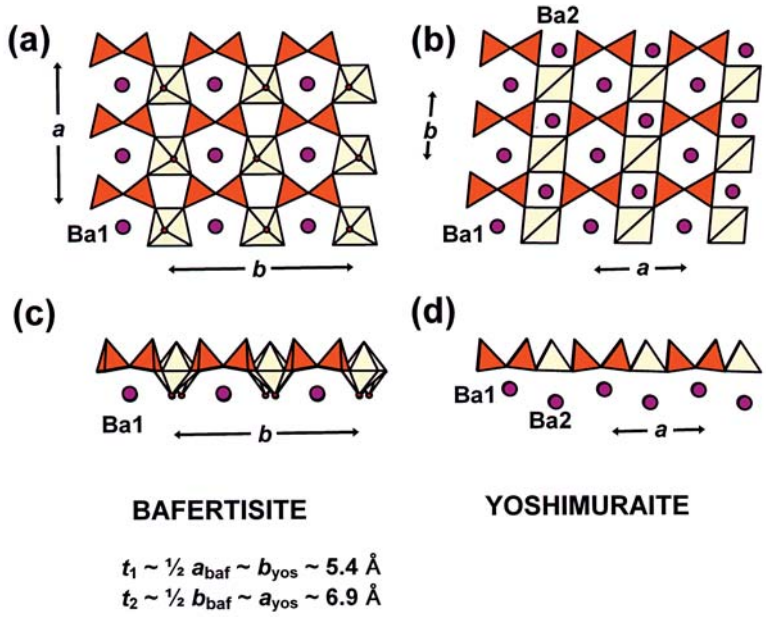

FIG. 11. Group II. Chemical composition and stereochemistry of the H sheet and *P* sites. The H sheet is viewed perpendicular to the plane of the TS block in: (a) bafertisite and (b) yoshimuraite, and viewed along the t_2 translation in bafertisite (c) and yoshimuraite (d). Legend as in Figure 2; Ba atoms are shown as magenta circles.

$Mn^{2+}_{0.55}\ Fe^{2+}_{0.45}$, $M(2) = Fe^{2+}_{0.5}\ Na_{0.4}\ Mn^{2+}_{0.1}$ and $M(3) = Na_{0.5}\ Fe^{2+}_{0.4}\ Mn^{2+}_{0.1}$ (Zhou *et al*. 2002). Thus the O sheet in bussenite is characterized by $M^{O}_{4} = [(Fe^{2+}_{1.35}\ Mn^{2+}_{0.75})_{\Sigma 2.10} + Na_{1.9}]_{\Sigma 4.00}$, *i.e.*, $M^{2+} : Na \approx 1 : 1$ with a slight prevalence of M^{2+} cations.

The H sheet: The M^{H} site is occupied solely by Ti. The M^{H} site is [6]-coordinated in bafertisite, hejtmanite, perraultite, surkhobite and bussenite (Fig. 11a), and [5]-coordinated in yoshimuraite (Fig. 11b). The mean ∠Si–O–Si is 140.6°, and the mean O–O distance in the H sheet is 4.23 Å compared to 199.0° and 3.95 Å in Group I. A smaller size of the M^{H} cation, Ti ($^{[6]}r$ = 0.605 Å), compared to [7]- and [6]-coordinated Ca, Mn^{2+}, Zr^{4+} ($^{[6]}r$ = 1.03, 0.95, 0.83 and 0.72 Å, Shannon 1976), forces the (Si_2O_7) group to tilt more in order to promote linkage between the O and H sheets.

The P sites: In all structures of Group II, the A^P site is occupied mainly by [9] – [12]-coordinated Ba, with subordinate Sr, Ca and K (Figs. 11a, b). The Ba atoms are too large to fit the A^P site in the plane of the H sheet, and they are shifted away from that plane (Figs. 11c, d). The Ba^P–X^{O}_{A} distance varies from 3.43 Å in bussenite to 4.30 Å in perraultite, and Ba is definitely not bonded to an anion of the O sheet, except for bussenite. Bussenite has the shortest Ba–X^{O}_{A} distance at 3.42 Å. This distance is an average of two distances, 2.96 and 3.89 Å, distances from two sites 50% occupied by Ba (dominant), Sr and Ca: $Ba_{0.47}\square_{0.54}$ and $Sr_{0.32}Ca_{0.12}\square_{0.56}$, and ~0.9 Å apart. The B^P site is vacant in bafertisite (Figs. 11a, c) and hejtmanite, occupied by [10]-coordinated Na in perraultite and surkhobite, and by [11]-coordinated Ba in yoshimuraite (Fig. 11d) and bussenite. The B^P site is shifted out of the plane of the H sheet more than the A^P site. The cations at the B^P site are invariably bonded to the four X^{H}_{Si-M} anions of the H sheet. In Group II, the *P* sites form cation layers in the intermediate space between two TS blocks.

Linkage of O and H sheets: In Group II, only linkage 2 occurs: two (Si_2O_7) groups link to two octahedra adjacent along $\mathbf{t_2}$ (Fig. 12). With this type of linkage, all M^{O} octahedra share common vertices with polyhedra of the H sheet: one half of the M^{O} octahedra with four (SiO_4) tetrahedra and one M^{H} polyhedron, and the other half of the M^{O} octahedra with two (SiO_4) tetrahedra and two M^{H} (= Ti) octahedra (Fig. 12). Therefore, there are two types of octahedron in the O sheet with regard to linkage to the H sheet: half the M^{O} octahedra share five, and the other half, six common vertices with the polyhedra of the H sheet.

Anion considerations: In Group II, the O sheet is of the form $M^{2+}_{4}\ X^{O}_{8}$; four X^{O} anions belong to (Si_2O_7) groups, and they are O atoms. The A^P site is too far away to be bonded to any anion of the O sheet, and the X^{O}_{A} anion receives bond valence only from three M^{2+} atoms of the O sheet: $0.33 \times 3 = 1$ *vu*. Therefore, X^{O}_{A} is a monovalent anion, *e.g.*, (OH) group in bafertisite (Table 3, Fig. 12). The bond-valence sum for the X^{O}_{M} anion is 0.67 ($^{[6]}Ti^{H}$) + 0.33×3 ($3\ M^{O}$) = 1.67 *vu*; therefore, the X^{O}_{M} site is invariably occupied by an O atom. One can write the composition of the O sheet as $M^{2+}_{4}\ X^{O}_{8} = M^{2+}_{4}\ O_6\ X^{-}_{2}$, where $X^{-} = (OH)^{-}, F^{-}$.

Group III

There are six minerals in this group: lamprophyllite (which has two polytypes, one with orthorhombic symmetry and the other with monoclinic symmetry; they are designated as lamprophyllite-2*O* and lamprophyllite-2*M*), barytolamprophyllite, nabalamprophyllite, innelite, epistolite and vuonnemite.

The O sheet: One M^{O} site is occupied by Ti (Table 3). In epistolite, nabalamprophyllite and vuonnemite, three other M^{O} sites are occupied by Na (Fig. 13a). In lamprophyllite and barytolamprophyllite, one site is occupied solely by Na, whereas two other sites are occupied by Na and M^{2+} [$(Na_{1.30}\ Mn^{2+}_{0.36}\ Fe^{2+}_{0.22}\ Mg_{0.12})$ and $(Na_{1.20}\ Fe^{2+}_{0.40}\ Mn^{2+}_{0.40})$ in lamprophyllite and barytolamprophyllite, respectively], with $Na > M^{2+}$; the ideal composition of the O sheet is 3Na + Ti. In innelite, there are two Na^{O} and one Ca^{O} sites. Therefore, Na is the dominant cation of the O sheet in Group III.

The H sheet: The M^{H} site is occupied by Ti^{4+} or Nb^{5+}. In epistolite and vuonnemite, M^{H} corresponds to [6]-coordinated Nb (Fig. 13b). Niobium is coordinated by six O atoms in vuonnemite and by five O atoms and an H_2O group in epistolite. In lamprophyllite, barytolamprophyllite, nabalamprophyllite and innelite, M^{H} corresponds to [5]-coordinated Ti (Table 3, Fig. 13c).

The P sites: In three structures with [5]-coordinated Ti in the H sheet, there is one A^P site, and it is occupied by $(Sr_{1.18}Na_{0.66}Ca_{0.12})$ = (SrNa) (lamprophyllite-2*M* and lamprophyllite-2*O*) and $[(Ba_{0.84}\ Sr_{0.21})^{2+}\ K^{+}_{0.98}]_{\Sigma 2.03}$ = (BaK) (barytolamprophyllite). In the structure of nabalamprophyllite, there are two A^P sites: the [11]-coordinated *Ba* (Fig. 13c) and [11]-coordinated *Na* sites. The latter site is in fact 0.5 Na + 0.3 Ba + 0.15 K + 0.05 Sr. The prevalence of monovalent cations (Na + K) over divalent cations (Ba + Sr) shows that site to be "Na"-dominant, *i.e.*, a *Na* site. In the crystal structure of innelite, there are two A^P and two B^P sites, Ba being the dominant cation at each site.

In structures with [6]-coordinated Nb, the A^P site is occupied by [8]-coordinated Na (vuonnemite and epistolite) (Fig. 13b). In epistolite, the A^P site is 50% occupied, and thus its composition is (Na□) (Table 3). Figures 13d and 13e show the different positioning of the A^P sites relative to the H sheet: in epistolite (= vuonnemite), Na atoms are in the plane of the H sheet (Fig. 13d), whereas in nabalamprophyllite, the Ba atoms are shifted toward the intermediate space between two TS blocks (Fig. 13e).

Linkage of O and H sheets: The linkage of O and H sheets is topologically the same as in Group I: two (Si_2O_7) groups link to *trans* edges of the same octahedron of the O sheet, and therefore two H sheets are

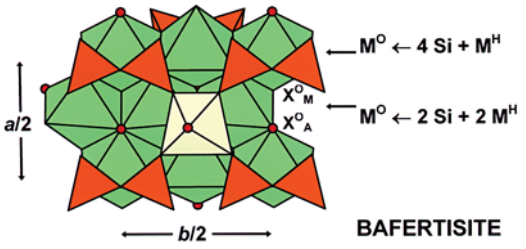

FIG. 12. Group II. Linkage of H and O sheets within one TS block. Legend as in Figure 11. The Fe^{2+} octahedra are green; rows of two types of M^O octahedra (they link to different polyhedra) are shown by arrows.

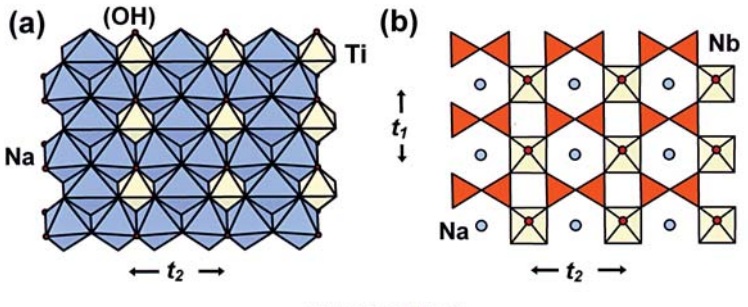

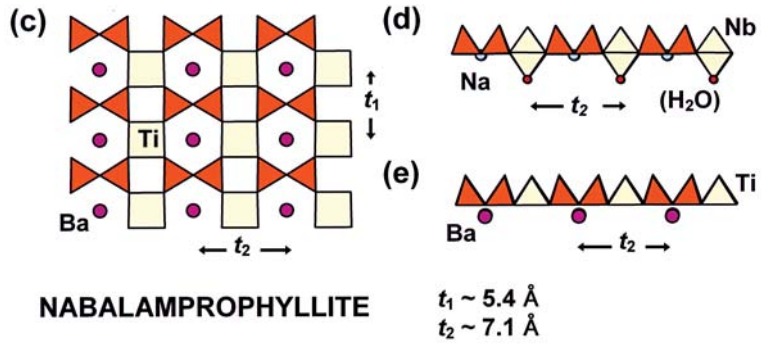

FIG. 13. Group III. Typical O sheet in (a) epistolite and two types of H sheet in (b) epistolite and (c) nabalamprophyllite viewed perpendicular to the plane of the sheets and down $\mathbf{t_1}$ (d, e). The Na octahedra of the O sheet are navy blue, Nb and Ti polyhedra are yellow, Na and Ba atoms at the A^P site and (OH) and (H_2O) groups are shown as navy blue, magenta and small and large red circles, respectively.

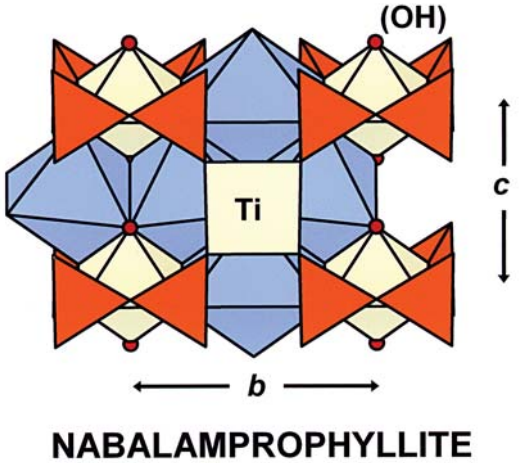

FIG. 14. Group III. Linkage of H and O sheets within one TS block. Legend as in Figure 13.

related by a pseudo-mirror plane (*m*) coinciding with the plane of the cations of the O sheet (Fig. 14). Here, two (Si_2O_7) groups link to the *trans* edges of a small Ti^O octahedron, as compared to a large Na^O octahedron in Group I. The mean ∠Si–O–Si is 135.7°, and the mean O–O distance of the (Si_2O_7) group in the O sheet is 2.88 Å *versus* 140.6° and 3.42 Å in Group II. As the M^H cation is the same in Groups II and III, the size of the (Si_2O_7) group is not influenced by the size of the M^H polyhedron (see further discussion on Groups I and III). The size of the (Si_2O_7) group adjusts to the size of the M^O octahedron to which (Si_2O_7) groups link, *i.e.*, the size of the M^O cation; it is Mn^{2+} or Fe^{2+} in Group II ($^{[6]}r$ = 0.83 and 0.78 Å), and Ti in Group III ($^{[6]}r$ = 0.605 Å).

Anion considerations: In the O sheet of the form $M^O_4 X^O_8$, four X^O anions belong to (Si_2O_7) groups, and they are O atoms, X^O_{Si} = O. Concerning the other four anions of the O sheet, the X^O_M anion receives bond valence from three M^O cations of the O sheet and the M^H atom. Formal bond-strength calculations (Pauling 1929) give bond-valence sums for the anion at the X^O_M site from 1.31 to 1.47 *vu* (Table 4). It is an excessive sum for a monovalent anion and an inadequate sum for a divalent anion. To satisfy the bond-valence requirements of the X^O_M anion, one bond, M^H–X^O_M, becomes very short, 1.68–1.77 Å (Table 4) compared to the mean value of <Ti(Nb)^H–ϕ>, 1.90–2.01 Å. Shortening of this bond increases more than twice the bond-valence contribution from the M^H atom. The bond-valence sum increases to 1.97–2.14 *vu*; therefore the X^O_M site can be occupied by O atoms, and in Group III, X^O_M corresponds to O^{2-}.

The X^O_A site invariably contains monovalent anions. The X^O_A anion receives bond-valence from four cations, 3 M^O cations of the O sheet (one of them $^{[6]}Ti^O$) and the A^P atom. In epistolite and vuonnemite, A^P corresponds to $^{[8]}Na^P$. In epistolite, X^O_A receives bond valence from $^{[6]}Ti^O$ + 2 $^{[6]}Na^O$ + $^{[8]}Na^P$, 0.67 + 0.33 + 0.125 = 1.13 *vu*, and X^O_A corresponds to $(OH)^-$. In vuonnemite, the bond-valence sum is 1.38 *vu*, and 2 X^O_A corresponds to (OF) (Ercit *et al.* 1998). In lamprophyllite, barytolamprophyllite, nabalamprophyllite and innelite, X^O_A receives bond valence from $^{[6]}Ti^O$ + 2 $^{[6]}M^O$ + $^{[10–11]}A^P$. The contribution from the A^P cation is negligible because A^P–X^O_A is a long bond: 3.05–4.06 Å. In nabalamprophyllite, the X^O_A anion receives bond valence from $^{[6]}Ti^O$ + 2 $^{[6]}Na^O$, *i.e.*, 1.00 *vu*, and X^O_A corresponds to $(OH)^-$. In lamprophyllite, the X^O_A anion receives bond valence from $^{[6]}Ti^O$ + $^{[6]}(Na_{1.30}\ Mn^{2+}_{0.36}\ Fe^{2+}_{0.22}\ Mg_{0.12})^O$, *i.e.*, 1.33 and 1.23 *vu* in 2*O* and 2*M* polytypes, respectively, and X^O_A has to be $(OH)^-$. In barytolamprophyllite, the X^O_A anion receives bond valence from $^{[6]}Ti^O$ + $^{[6]}(Na_{1.20}\ Fe^{2+}_{0.40}\ Mn^{2+}_{0.40})^O$, *i.e.*, 1.07 *vu*, and X^O_A has to be $(OH)^-$. However, Rastsvetaeva *et al.* (1995a) presented this site as (O,OH) with the bond-valence sum incident at the O(1) = X^O_A equal to 1.02 *vu*.

Where the X^O_A site is fully occupied by monovalent anions, the content of F^- is usually less than 1 *apfu*, and OH^- is a dominant species, and $(OH)^-$ + F^- = 2 *apfu*, ideally $(OH)^-_2$: $(OH)_2$ in lamprophyllite (Krivovichev *et al.* 2003) and barytolamprophyllite (Rastsvetaeva *et al.* 1995a), $(OH)_{1.67}F_{0.51}$ in nabalamprophyllite (Rastsvetaeva & Chukanov 1999), $(OH)_{1.44}F_{0.56}$ in epistolite (Sokolova & Hawthorne 2004).

As I noted before, in Group III, the X^O_A site is occupied by a monovalent anion (except for innelite, the only mineral where X^O_A corresponds to O^{2-} (Chernov *et al.* 1971). The bond-valence sums at the O(2) and O(26) sites (the X^O_A sites in innelite) are 1.65 and 1.03 *vu*. Moreover, the chemical composition reported by Chernov *et al.* (1971) and Kravchenko *et al.* (1961) contains H_2O. This is a strong indication that the X^O_A sites in innelite contain monovalent anions. The crystal structure of innelite should be re-investigated.

Group IV

There are five minerals in this group: murmanite, lomonosovite, quadruphite, polyphite and sobolevite.

TABLE 4. BOND-VALENCE (*vu*) VALUES FOR THE X^0_M SITE IN GROUP-III MINERALS

	$3M^0$					Σ_1	M^H				Σ_2	Σ_3 *	$M^H - X^0_M$ (Å)	<M^H – φ> (Å)
	Na	Na	Na	(Na	M^{2+})***		$^{[5]}$Ti	$^{[6]}$Nb	$^{[5]}$Ti*	$^{[6]}$Nb*				
lamprophyllite-2*M*	0.17			0.25	0.25	0.67	0.8		1.44		1.47	2.11	1.684	1.9
lamprophyllite-2*O*	0.17			0.25	0.25	0.67	0.8		1.41		1.47	2.08	1.69	1.9
barytolamprophyllite	0.17			0.25	0.25	0.67	0.8		1.35		1.47	1.87	1.703	1.91
nabalamprophyllite	0.17	0.17	0.17			0.51	0.8		1.47		1.31	2.14	1.677	1.916
epistolite	0.17	0.17	0.17			0.51		0.83		1.46	1.34	1.97	1.77	2.01
vuonnemite	0.17	0.17	0.17			0.51		0.83		1.52	1.34	2.02	1.756	2.001

* calculated with bond-valence parameters for Ti^{4+} and Nb^{5+} from Brown (1981). ** φ: unspecified anion.
*** (Na M^{2+}) = ($Na_{1.30}\ Mn^{2+}_{0.36}\ Fe^{2+}_{0.22}\ Mg_{0.12}$) for lamprophyllite after Krivovichev *et al.* (2003) and ($Na_{1.2}\ Fe^{2+}_{0.4}\ Mn^{2+}_{0.4}$) for barytolamprophyllite after Rastsvetaeva *et al.* (1995a).

The O sheet: There are two Ti^{O} and two Na^{O} sites in the O sheet, with Ti:Na = 1:1. This is the maximal possible content of Ti in the O sheet. In all structures, the composition of the O sheet is almost the same, neglecting a high content of Mn^{2+} in sobolevite, which substitutes for Ti and gives $[2\,Na + (TiMn^{2+})]^{O}$. There are two types of chains of edge-sharing octahedra within the O sheet: the Ti^{O} octahedra form a brookite-like $(Ti_2O_8)^{8-}$ chain, and the Na^{O} octahedra form a chain of the same topology. The O sheet is shown in Figure 15a.

The H sheet: The M^{H} site is occupied solely by Ti, as in Groups II and III. Titanium is [6]-coordinated by O atoms in all structures (Fig. 15b) except for murmanite, where it has five O atoms and an (H_2O) group.

The P sites: The A^{P} site is occupied by [8]-coordinated Na in murmanite and lomonosovite. In lomonosovite, all ligands are O atoms, whereas in murmanite, seven ligands are O atoms and the X^{P}_{A} site is occupied by an (H_2O) group. The A^{P} site can be also [6]- or [5]-coordinated. For example, in quadruphite, polyphite and sobolevite, coordination numbers are [6] and [5] and [6], respectively. The B^{P} site is vacant.

Linkage of O and H sheets: In Group IV, linkage 3 occurs, and two (Si_2O_7) groups link to two next-nearest-neighbor Ti octahedra in a "brookite" chain (Fig. 15). Each Ti octahedron links to two (Si_2O_7) groups: it shares one edge with two tetrahedra of the first (Si_2O_7) group and a vertex with one tetrahedron of the second (Si_2O_7) group. The M^{H} (= Ti) octahedron shares a common vertex with three octahedra of the O sheet: two Na^{O} octahedra and one Ti^{O} octahedron. The mean ∠Si–O–Si is 136.4°, and the mean O–O distance of the (Si_2O_7) group in the O sheet is 2.90 Å, almost identical to that in Group III (Table 2).

Anion considerations: In Group IV, the O sheet is of the form $M^{O}_4\,X^{O}_8$. Four X^{O} anions belong to (Si_2O_7) groups, and they are O atoms. The X^{O}_{M} and X^{O}_{A} anions receive bond valence from two Ti atoms and two Na atoms, and formal bond-strength calculations give about 1.67 *vu*. Therefore all anions of the O sheet are O atoms, except in sobolevite. In sobolevite, with $(TiMn^{2+})^{O}$, two of four X^{O} sites are statistically occupied by O and F atoms, (OF). Substitution of Mn^{2+} for Ti requires substitution of F for O: $Ti^{4+} + 2\,O^{2-} \rightarrow Mn^{2+} + O^{2-} + F^{-}$ (Table 3). This substitution couples to the substitution $Mn^{2+} \rightarrow Na^{+}$ elsewhere in the structure of sobolevite.

Close Packing of Cations in the TS Block

Close packing of cations has been discussed recently in detail for polyphite and sobolevite (Sokolova *et al.* 2005). This is an important feature discussed for further consideration in the context of the hierarchy of structures with the TS block.

The O sheet in any TS block has the form $[MX_2]$, and hence the M^{O} cations and X^{O} anions are close packed and occur at the vertices of a 3^6 net; each cation has six nearest neighbors at approximately equal distances (Fig. 16a). Although in the H sheet, different polyhedra are present, and the cations of the H sheet, together with the A^{P} cations that occur approximately in the plane of the H sheet, are also close-packed and arranged in accord with a 3^6 net (Fig. 16b). Note that the close-packed H layer occurs where A^{P} sites coincide with the plane of the H sheet or are shifted from it insignificantly. On one side of the H sheet, anions are close-packed (they are common with the O sheet), and on the other side, they are not close-packed. In each layer, there are four cations in the minimal cell. Three layers of the TS block constitute a three-layered or cubic close-packing with an *ABC* sequence (Fig. 16c). Cation–cation distances within a layer vary from 2.9 to 4.2 Å, depending on the type of cation.

Hierarchy of Structures with the TS Block

There are several possible relations between TS blocks in a particular structure. From the structures considered here, it seems clear that (1) in a structure, the TS block is invariably the same, (2) the H sheets of one TS block are identical, (3) the TS blocks can either link or not link directly, (4) there are two types either of self-linkage or of the intermediate space between two TS blocks. The TS block has a three-layered structure, and moreover it has three close-packed layers of cations forming the *ABC* sequence. All atoms occurring in the space between two TS blocks, I designate the *intermediate* (**I**) *block* by analogy with the TS block. Usually, the **I** block is an arrangement of alkali and alkali-earth cations, (H_2O) groups and oxyanions $(PO_4)^{3-}$, $(SO_4)^{2-}$ and $(CO_3)^{2-}$.

In this paper, I will show that the TS block propagates close-packing of cations into the **I** block. I will define two types of close-packed layers of the cations in the **I** block, and will use m as the number of close-packed layers of cations, *i.e.*, m = number of **I** layers in the **I** block. The number of intermediate layers (m) varies from 1 to 6 in the structures examined here.

To establish the structural hierarchy for the 24 minerals, I divide all structures first on the basis of type of linkage of the TS blocks (as they are major structural units), and second, on the basis of topology and size of the **I** block.

Two types of self-linkage of TS blocks are observed:

(1) Two TS blocks share common edges of M^{H} and A^{P} polyhedra and common vertices of M^{H}, A^{P} and Si^{H} polyhedra of H sheets belonging to two TS blocks. There are no additional atoms between the two blocks.

(2) Two TS blocks link through common vertices of $^{[6]}M^{H}$ polyhedra, and additional atoms occur in the intermediate space between these two blocks.

If TS blocks do not link directly, there are also two possibilities:

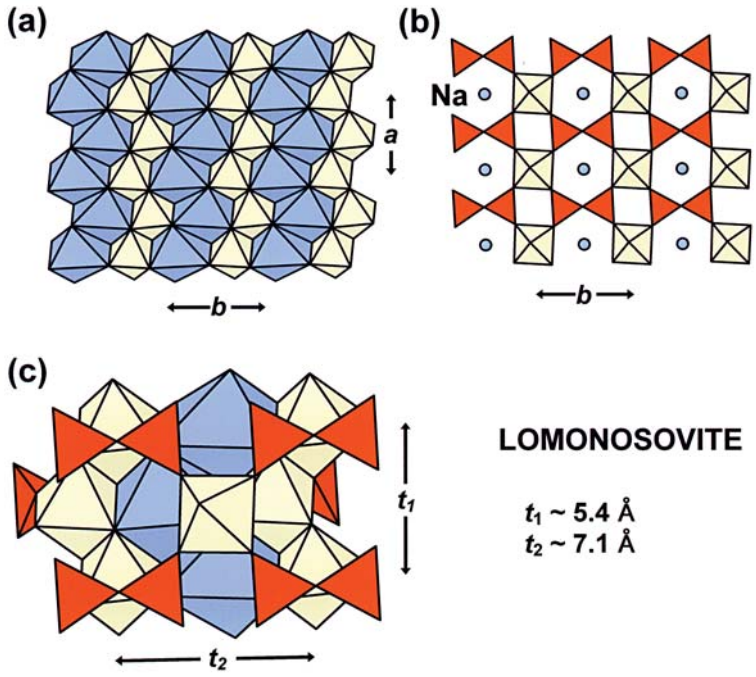

FIG. 15. Group IV. Typical O (a) and H (b) sheets (*P* sites are included), and their linkage (c) in lomonosovite. Legend as in Figure 13.

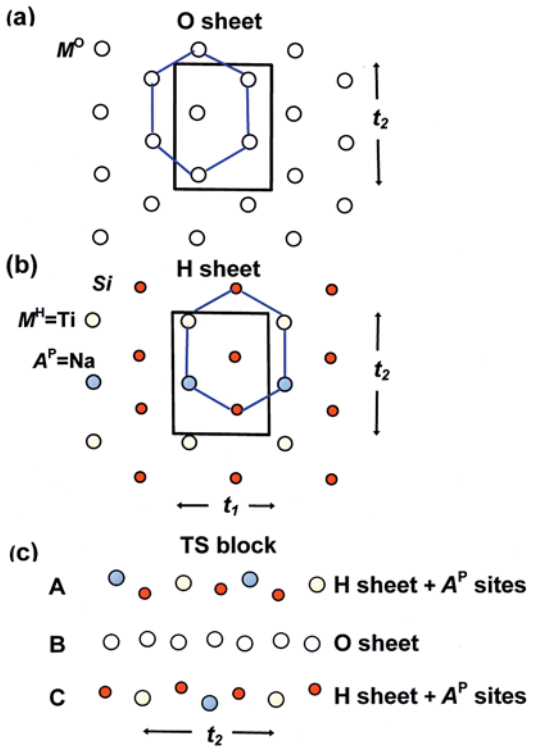

FIG. 16. The close-packed layers of cations in the TS block: (a) the close-packed layer of M^O cations of the O sheet, (b) the close-packed layer of M^H and Si atoms of the H sheet and A^P cations, (c) three close-packed layers of the TS block viewed down $\mathbf{t_1}$. The M^O, Na, Ti and Si atoms are shown as white, blue, yellow and orange circles, respectively. Solid black lines show the minimal cell, and the solid blue lines indicate six nearest cations around the central one in the O and H sheets.

m

(3) There are no additional atoms between two TS blocks.

(4) There are additional atoms in the intermediate space between two TS blocks.

The scheme in Figure 17 shows the hierarchy of these structures.

Case 1: TS blocks link together directly (m = 0), and they share common edges of M^H and A^P polyhedra and common vertices of M^H, A^P and Si polyhedra of H sheets belonging to adjacent TS blocks. This type of self-linkage of TS blocks occurs in Group I.

Case 2: In crystal structures of two minerals, perraultite and surkhobite (Group II), TS blocks link through common vertices of Ti octahedra, and there is one layer of cations in the intermediate space between two blocks (m = 1).

Case 3: TS blocks do not link together, and there are no additional cations between two blocks (m = 0), as in epistolite (Group III) and murmanite (Group IV).

Case 4: There are additional layers of cations between two TS blocks in thirteen minerals of Groups II–IV, and the number of **I** layers varies from 1 to 6.

The chemical composition of the **I** block is shown in Table 5. In accord with Table 3, Table 5 gives the chemical composition of each **I** layer in the minimal cell. Next, I consider specific details of the linkage and a general chemical formula for each of the four cases outlined above.

Case 1: TS Blocks Link Directly, m = 0

Linkage of TS blocks

In all minerals of Group I, linkage of two TS blocks occurs *via* common vertices and edges of the polyhedra of two H sheets (A^P sites are in the plane of the H sheet). Three minerals, seidozerite, grenmarite and rinkite, have monoclinic symmetry; four minerals, kochite, rosenbuschite, hainite and götzenite, have triclinic symmetry (space group $P\bar{1}$). In seidozerite, grenmarite, kochite, rosenbuschite, hainite and götzenite, each M^H and A^P polyhedron of one H sheet shares one vertex ($X^P{}_M$ and $X^P{}_A$ anions) with an (Si_2O_7) group of the H sheet of another TS block (Fig. 18a). Also, M^H and A^P polyhedra of one H sheet each share two edges with an M^H polyhedron and an A^P polyhedron in the adjacent H sheet. Two H sheets are shifted relative to each other along $\mathbf{t_1}$ by approximately half of the edge length of a Si tetrahedron (Fig. 18b), with the result that O ($X^H{}_{Si-M}$) atoms of an (Si_2O_7) group have coordination numbers

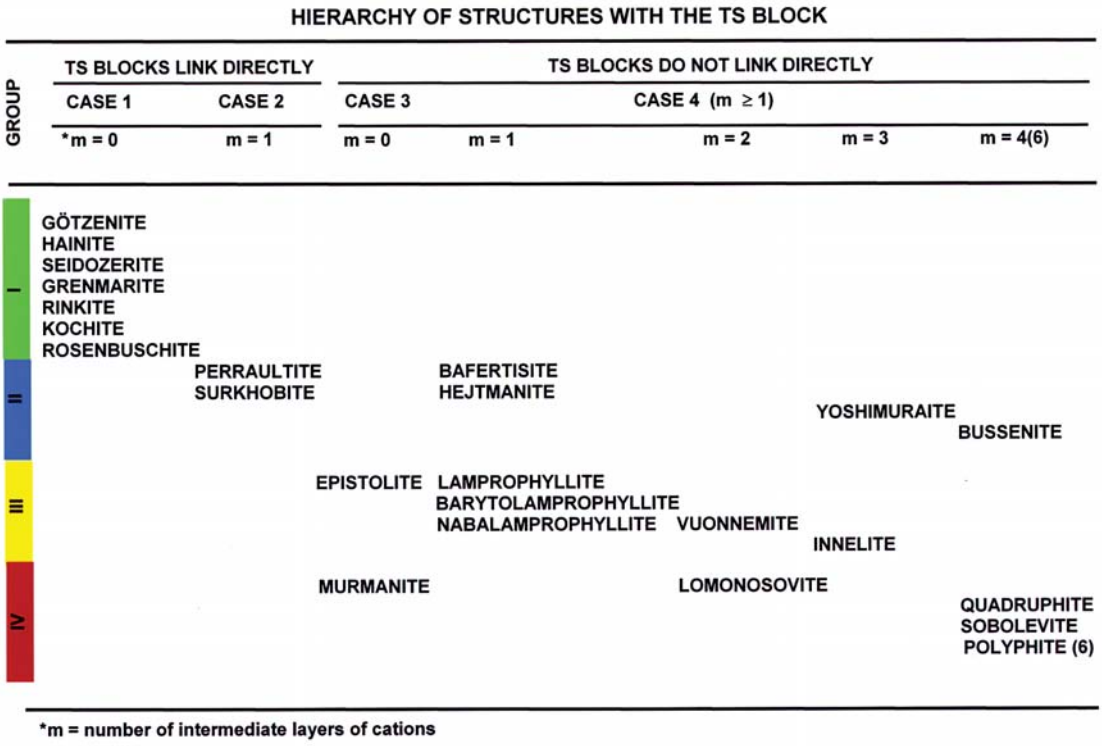

FIG. 17. Hierarchy of structures with the TS block.

TABLE 5. STEREOCHEMISTRY AND CHEMICAL COMPOSITION OF THE **I** BLOCK

Mineral	m	Composition of individual **I** layers						$X^{H,P}$, $X^{H,I}$, X^{H}_{Si}	Total
		1	2	3	4	5	6		
perraultite	1	BaNa							BaNa
surkhobite	1	BaNa*							BaNa*
bafertisite	1	Ba_2							Ba_2
hejtmanite	1	Ba_2							Ba_2
lamprophyllite	1	(SrNa)							(SrNa)
baryto-lamprophyllite	1	(BaK)							(BaK)
naba-lamprophyllite	1	BaNa							BaNa
yoshimuraite	3	Ba_2	O_4 P_2	O_4 Ba_2					$Ba_4(PO_4)_2$
innelite	3	Ba_2	O_4 S_2	O_4 Ba_2					$Ba_4(SO_4)_2$
bussenite	4	(H_2O) Ba_2	O_3 NaC	F_2 NaC	O_3 Ba_2	(H_2O)			$Ba_4Na_2(CO_3)_2F_2(H_2O)_2$
vuonnemite	2	O_7 Na_3P	O_4 Na_3P	O_7				O_{14}	O_{10} $Na_6(PO_4)_2$
lomonosovite	2	O_7 Na_3P	O_4 Na_3P	O_7				O_{14}	O_{10} $Na_6(PO_4)_2$
quadruphite	4	O_6 Na_3P	O_4 (CaNa)NaP	O_4F_2 (CaNa)NaP	O_4 Na_3P	O_6		O_{12}	O_8 $Na_8(CaNa)_2(PO_4)_4F_2$
sobolevite	4	O_6 Na_3P	O_4 $(Na_2Ca)P$	O_4F_2 (NaCaMn)P	O_4 Na_3P	O_5		O_{11}	O_7 $Na_8(Na_2Ca)(NaCaMn)(PO_4)_4F_2$
polyphite	6	O_5 Na_3P	O_4 (NaCa)CaP	O_4F_2 (NaCa)NaP	O_4 (NaCa)NaP	F_2O_4 (CaNa)NaP	O_4 Na_3P O_5	O_{10}	O_6 $Na_6(Na_4Ca_2)_2(PO_4)_6F_4$

m: number of **I** layers between two TS blocks. In green: $X^{H,P}$: anions of two H sheets shared with atoms at the *P* sites; $X^{H,I}$: anions of two H sheets shared with **I** layers; X^{H}_{Si}: O atoms of **I** and P layers shared with (Si_2O_7) groups of two TS blocks. In red: internal anions of the **I** block shared by two **I** layers.
* Predicted value (see Appendix C: Surkhobite).

[3] and [4]. With this type of linkage, M^H and A^P polyhedra form bands along $\mathbf{t_2}$ (*e.g.*, = **b** in seidozerite) (Fig. 18b). In seidozerite, TS blocks link along [001] to form a mixed framework of polyhedra with coordination numbers [4]–[8] (Fig. 18c). Details of the crystal chemistry of seidozerite, kochite, rosenbuschite, hainite and götzenite as minerals of the rosenbuschite group can be found in Christiansen *et al*. (2003a).

In rinkite, $^{[7]}M^H$ and $^{[8]}A^P$ sites have the same composition, $(Ca_{0.75}REE_{0.25})$, and $2M^H + 2A^P$ atoms constitute (Ca_3Ce) in total. In the rinkite structure, the $^{[7]}M^H$ and $^{[8]}A^P$ polyhedra share a common edge with an (SiO_4) tetrahedron of the (Si_2O_7) group of the adjacent H sheet (Fig. 19a). Therefore, all O ($X^H_{Si–M}$) atoms of an (Si_2O_7) group have a coordination number of [4]. Adjacent H sheets are shifted relative to each other along $\mathbf{t_1}$ by approximately one edge of a Si tetrahedron (Fig. 19b). In rinkite, the $^{[7]}M^H$ and $^{[8]}A^P$ polyhedra share common edges to form an individual layer between two O sheets of different TS blocks (similar to seidozerite). Thus in rinkite, TS blocks link to each other along [001] to form a mixed framework in which cations have coordination numbers of [4] to [8] (Fig. 19c).

General chemical formula

In all structures where TS blocks link directly, the M^H polyhedron is commonly [6]- or [7]-coordinated, and one can use formula (7) for the TS block: $A^P_2\ B^P_2\ ^{[6]}M^H_2\ M^O_4\ (Si_2O_7)_2\ X^O_4\ X^P_{M2}$. In the minerals of this group, the A^P and M^H polyhedra of one TS block share their vertices with (Si_2O_7) groups of another TS block, the X^P anions are common with O atoms of (Si_2O_7) groups of another block, and I do not count them in the formula. Also, the B^P sites are vacant in Group I, and I modify formula (7) accordingly:

$$A^P_2\ B^P_2\ ^{[6]}M^H_2\ M^O_4\ (Si_2O_7)_2\ X^O_4\ X^P_{M2} - X^P_{M2} - B^P_2 = A^P_2\ ^{[6]}M^H_2\ M^O_4\ (Si_2O_7)_2\ X^O_4 \quad (11)$$

Formula (11) is a general formula for the seven minerals of Group I, including rinkite with a [7]-coordinated M^H polyhedron. As an example, I write the formula of seidozerite: A^P = Na, $M^H = Zr_2$, $M^O_4 = Na_2$ + Mn + Ti, $X^O_4 = O_2 + F_2$, which gives $Na_2\ Zr_2\ Na_2\ Mn\ Ti\ (Si_2O_7)_2\ O_2\ F_2$, $Z = 2$ (see Table 3 for details). In a more general way, one can write it as $Na_4\ Zr_2\ Mn\ Ti\ (Si_2O_7)_2\ O_2\ F_2$. The formulae of götzenite, hainite, kochite and rosenbuschite are revised in Appendix D.

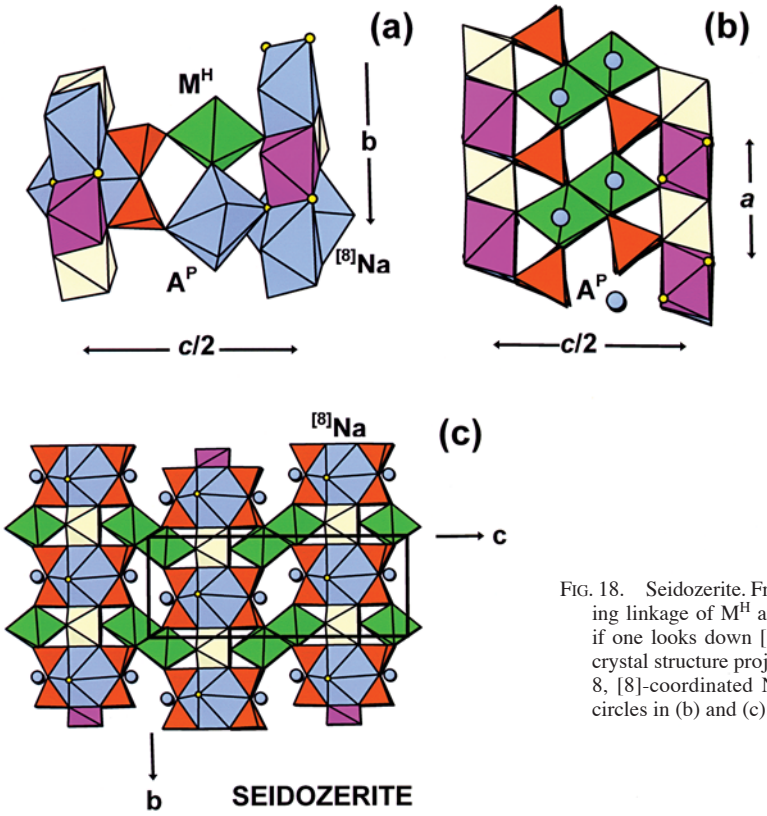

FIG. 18. Seidozerite. Fragments of the crystal structure showing linkage of M^H and A^P polyhedra to an (Si_2O_7) group if one looks down [100] (a) and down [010] (b); (c) the crystal structure projected onto (100). Legend as in Figure 8, [8]-coordinated Na (= A^P) atoms are shown as blue circles in (b) and (c).

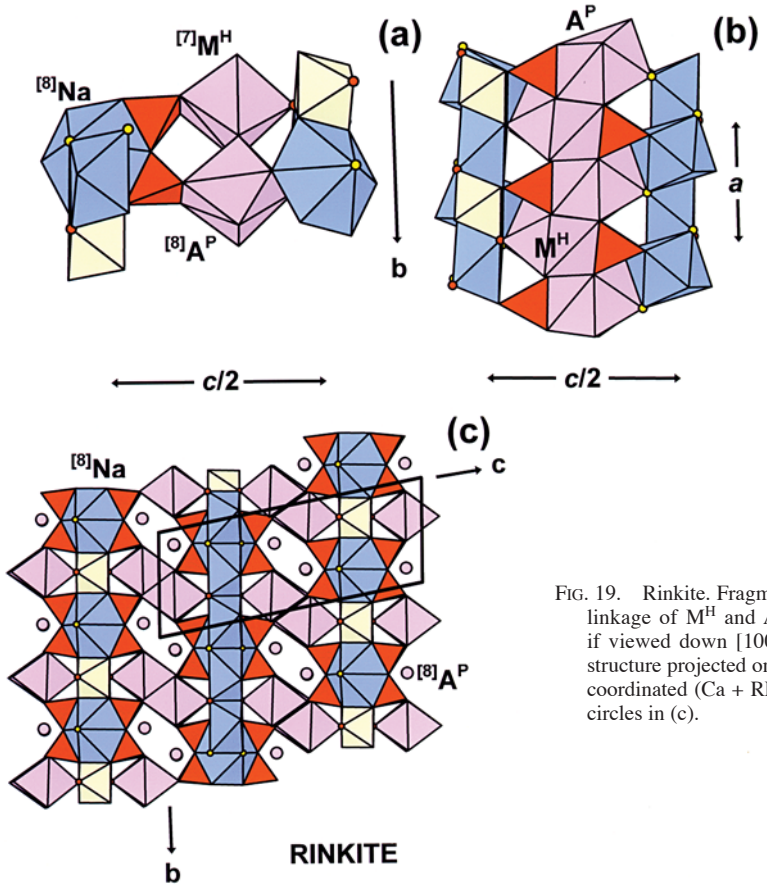

FIG. 19. Rinkite. Fragments of the crystal structure showing linkage of M^H and A^P polyhedra and an (Si_2O_7) group if viewed down [100] (a) and [010] (b); (c) the crystal structure projected onto (100). Legend as in Figure 8; [8]-coordinated (Ca + REE) (= A^P) atoms are shown as pink circles in (c).

CASE 2: TS BLOCKS LINK DIRECTLY, m = 1

*Cation sites of the **I** layer*

There are two minerals, perraultite and surkohbite, in which the TS blocks link to each other through common vertices of M^H octahedra, M^H = Ti. Two TS blocks are related to a pseudo-mirror plane (*m*), and every two *P* sites of adjacent TS blocks merge into one site in which TS blocks link together (Fig. 20a). Barium is the dominant constituent at the A^P sites in both minerals, and Na and Ca are the dominant constituents at the B^P sites in perraultite and surkhobite, respectively. The *P* sites form an intermediate (**I**) layer located in the space intermediate between two TS blocks. All distances from a P cation to anions of the O sheet are greater than 4 Å, and here I do not consider *P* sites as part of the TS block. It is interesting that the P atoms form close-packed layers, *i.e.,* each cation is surrounded by six other cations, and distances between all of them are approximately the same, about 4.9–5.5 Å.

In the crystal structure of perraultite, there are two unique close-packed **I** layers: one occurs at $z \approx 0$ and comprises the *A*(1), *A*(2) and *A*(6) sites (Fig. 20b); the other occurs at $z \approx 0.5$ and comprises the *A*(3), *A*(4) and *A*(5) sites (Fig. 20c). In total, Ba is dominant at the *A*(1–3) sites, and Na is dominant at the *A*(4–6) sites, giving the composition of two **I** layers as BaNa, *Z* = 8 (Table 5). The situation is analogous in surkhobite: three A^P and three B^P sites give BaCa, *Z* = 8 (Table 5). In the **I** layer of the perraultite-type structure, there are two cations in the minimal cell (compared to the four sites in each of the close-packed layers of cations within a TS block). Both types of layers, with two and four atoms in the minimal cell, retain the t_1 translation. In a layer with four atoms in the minimal cell, the t_2 repeat is a ½ t_2 translation, and in a layer with two atoms, the t_2 repeat is the t_2 translation (*cf.* Figs. 20b, c and 16a, b).

General chemical formula

I will use formula (7) for the TS block, $A^P_2\ B^P_2\ {}^{[6]}M^H_2\ M^O_4\ (Si_2O_7)_2\ X^O_4\ X^P_{M2}$. If two TS blocks share

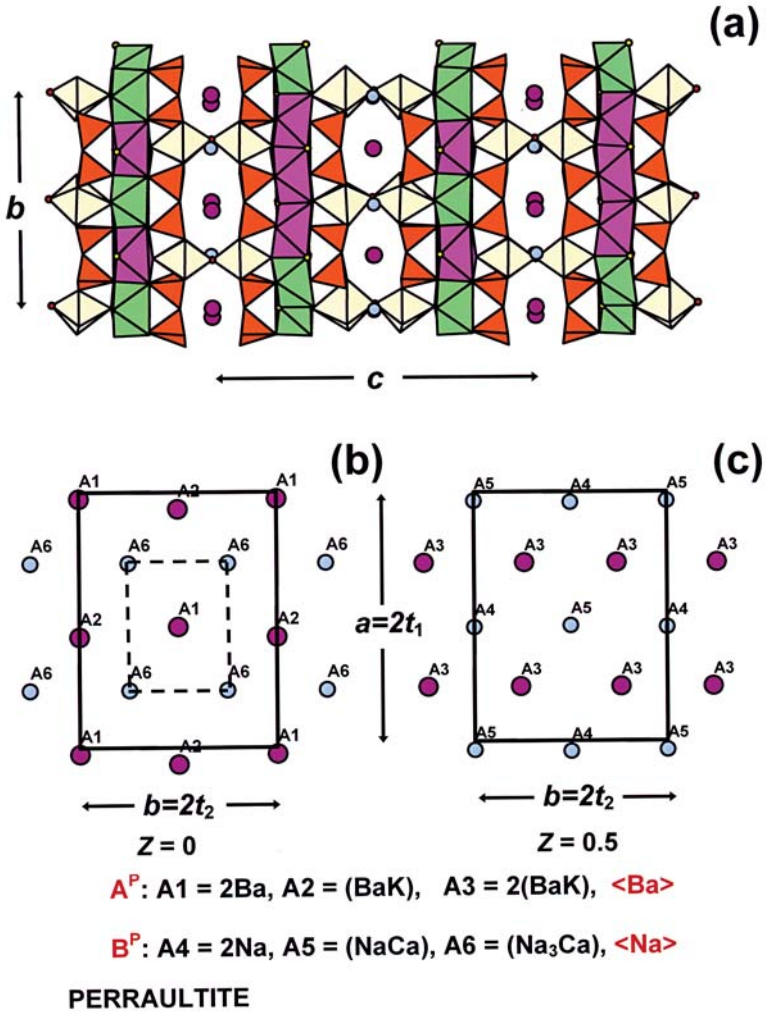

FIG. 20. Perraultite. General view of the crystal structure viewed down [100] (a), close-packed **I** layers of cations at $z = 0$ (b) and $z = 0.5$ (c). Legend as in Figure 12; the Mn^{2+} octahedra are magenta, and the Ba and Na atoms at the *P* sites are shown as large magenta and smaller blue circles. The minimal cell is shown by dashed lines in (b).

A^P and B^P cations and $X^P{}_M$ anions, and each two of these sites merge into one, then their number changes from 2, as in formula (7), to 1. In this case, the formula for the perraultite-type structure is:

$$A^P\ B^{P\ [6]}M^H{}_2\ M^O{}_4\ (Si_2O_7)_2\ X^O{}_4\ X^P{}_M \qquad (12)$$

The chemical formulae of perraultite and surkhobite

In accord with the general formula for case 2, the formula of perraultite must be written as Ba Na Ti_2 $(Mn^{2+}{}_{2.5}Fe^{2+}{}_{1.5})$ $(Si_2O_7)_2$ O_2 $(OH)_2$ F, $Z = 8$ (see Table 3 for site populations) or, ideally, Ba Na Ti_2 $Mn^{2+}{}_4$ $(Si_2O_7)_2$ O_2 $(OH)_2$ F. This formula represents the chemical composition and stoichiometry of the mineral more precisely than the formula $(Na,Ca)_2$ $(Ba,K)_2$ $(Mn,Fe)_8$ $[(Ti,Nb)_4O_4(OH)_2$ $[Si_2O_7]_4$ $(OH,F)_4$ (Yamnova *et al*. 1998). Note that the cell dimensions given by Yamnova *et al*. (1998) in the abstract of the paper and later in their Table 1 and the text, and repeated in ICSD file 87533, *a* 10.731, *b* 13.841, *c* 24.272 Å, β 121.19°, space group *C*2, do not reproduce the interatomic distances reported in their paper. I designate the cell given in the abstract

and Table 1 as cell 1. Yamnova *et al*. (1998) stated that "monoclinic symmetry of the crystal allows to choose another unit cell similar to that of the Canadian mineral" [Chao (1991) gave *a* 10.820, *b* 13.843, *c* 20.93 Å, β 95.09° for perraultite] "two unit cells being related as follows: **a'** = **a**, **b'** = **b**, **c'** = **a** + **c**, where *c*' = 20.845 Å, β 95.06°." I refer to this cell (**a'**, **b'**, **c'**) as cell 2. As Yamnova *et al*. (1998) gave atom coordinates that correspond to cell 2 [and to the unit cell given in Chao (1991)], I conclude that cell 2 is the correct cell and ICSD need to correct file 87533 accordingly: *a* 10.731, *b* 13.841, *c* 20.845 Å, β 95.06°, space group *C*2.

I assigned site populations for surkhobite in accord with Rozenberg *et al*. (2003); the resulting chemical formula of surkhobite is Ba Ca Ti_2 ($Fe^{2+}_2Mn^{2+}_2$) (Si_2O_7)$_2$ O_2 (OH) F_2, *Z* = 8 or, ideally, Ba Ca Ti_2 Fe^{2+}_4 (Si_2O_7)$_2$ O_2 (OH) F_2. Both these formulae have an excess charge of +1, indicating that there is something wrong with the previously accepted formula of surkhobite. See Appendix C: Surkhobite, for a prediction of a more accurate chemical formula. The chemical formula of surkhobite must be Na Ba Ti_2 Fe^{2+}_4 (Si_2O_7)$_2$ O_2 (OH) F_2, and the corresponding site-occupancies are given in Table 3.

Case 3: TS Blocks Do Not Link Directly, m = 0

Structure topology

Epistolite and murmanite are very interesting examples of how topology and stereochemistry of a particular TS block can be independent of the intermediate species, *e.g*., (H_2O) groups. Epistolite and murmanite have TS blocks of different topology and chemistry (Sokolova & Hawthorne 2004). There is one unique TS block in the unit cell of epistolite (Fig. 21a) and murmanite (Fig. 21b). Two adjacent TS blocks do not link directly; they repeat along the **c** direction and are connected by hydrogen bonds between (H_2O)–(H_2O)

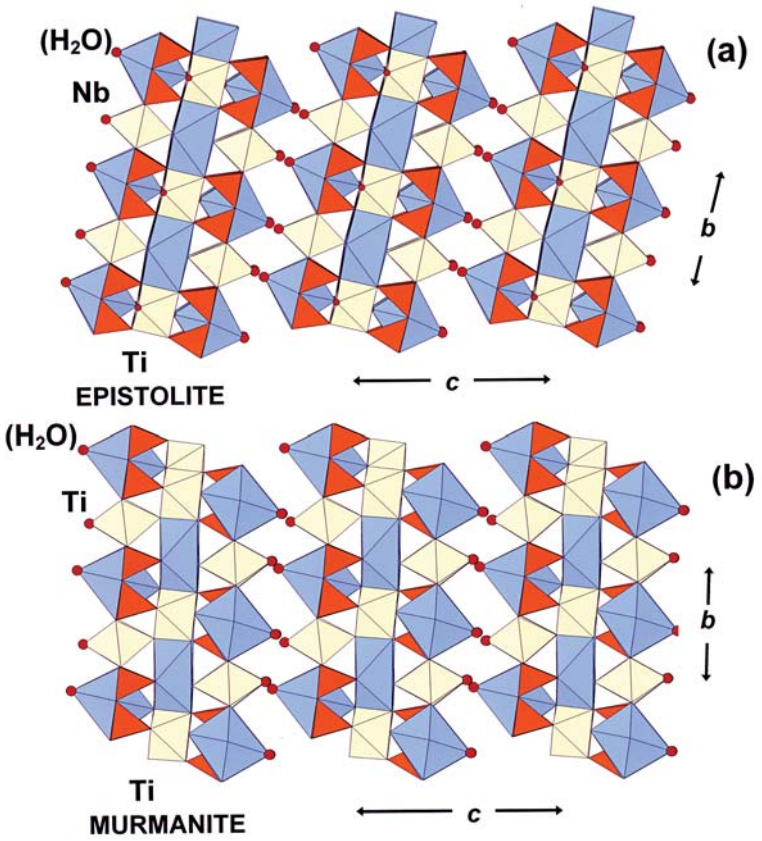

FIG. 21. General view of the crystal structure of (a) epistolite, and (b) murmanite. Legend as in Figure 14; the [6]- and [8]-coordinated Na polyhedra are navy blue, and the (H_2O) and (OH) groups are shown as large and small red circles.

groups and (H_2O)–O atoms of adjacent TS blocks. The (H_2O) groups are ligands of M^H and A^P atoms, and they occupy the X^P_M and X^P_A sites. Apparently, (H_2O) groups prevent self-polymerization of TS blocks, in accord with Hawthorne (1992), who emphasized that (H_2O) prevents polymerization of structural units.

Hydrogen bonding

The H atoms of the (OH) groups of the O sheets and (H_2O) groups in epistolite and murmanite have not been located (Sokolova & Hawthorne 2004, Khalilov 1989). There is no possibility of sp^3 hybridization-type hydrogen bonding within the arrangement of bonds constrained by $P\bar{1}$ symmetry. A stereochemically sensible scheme has been derived with $P1$ symmetry (Sokolova & Hawthorne 2004), and it seems probable that hydrogen bonding does not obey $P\bar{1}$ symmetry.

General chemical formula

The crystal structures of epistolite and murmanite consist exclusively of TS blocks, and a general formula for these minerals is identical to formula (8), in which the B^P site is vacant:

$$A^P_2\ B^P_2\ {}^{[6]}M^H_2\ M^O_4\ (Si_2O_7)_2\ X^O_4\ X^P_{M2}\ X^P_{A2} - B^P_2 = A^P_2\ {}^{[6]}M^H_2\ M^O_4\ (Si_2O_7)_2\ X^O_4\ X^P_{M2}\ X^P_{A2} \quad (13)$$

Structural formulae for epistolite and murmanite

Site occupancies for the TS block in epistolite and murmanite (Table 3) provide the following information with which to write their formulae:

Mineral	*O sheet*				*2H sheets*		P *cations and anions*		
	4 M^O		4 X^O		2 M^H	$(Si_2O_7)_2$	2 A^P	X^P_{M2}	X^P_{A2}
epistolite	Na_3	Ti	$(OH)_2$	O_2	Nb_2	$(Si_2O_7)_2$	$^{[8]}$Na □	$(H_2O)_2$	$(H_2O)_2$
murmanite	Na_2	Ti_2	O_2	O_6	Ti^{4+}_2	$(Si_2O_7)_2$	$^{[8]}Na_2$	$(H_2O)_2$	$(H_2O)_2$

The chemical formulae of epistolite and murmanite are $(Na\,\square)\ Nb_2\ Na_3\ Ti^{4+}\ (Si_2O_7)_2\ O_2\ (OH)_2\ (H_2O)_4$ and $Na_2\ Ti^{4+}_2\ Na_2\ Ti^{4+}_2\ (Si_2O_7)_2\ O_4\ (H_2O)_4$, and the simplified ideal (end-member) chemical formulae of epistolite and murmanite are $Na_4\ Nb_2\ Ti^{4+}\ (Si_2O_7)_2\ O_2\ (OH)_2\ (H_2O)_4$ and $Na_4\ Ti^{4+}_4\ (Si_2O_7)_2\ O_4\ (H_2O)_4$. Murmanite and epistolite are related by the substitution $Na^P_2 + Ti^H_2 + Ti^O + O^{2-}_2 \rightarrow (Na\square)^p + Nb^H_2 + Na^O + (OH)^-_2$.

Case 4: TS Blocks Do Not Link Directly, m = 1 – 6

In the thirteen structures of Groups II–IV, the number of **I** layers varies from 1 to 6 (Fig. 17). For bafertisite, hejtmanite, lamprophyllite, barytolamprophyllite and nabalamprophyllite, m = 1; for vuonnemite and lomonosovite, m = 2; in yoshimuraite and innelite, m = 3; in bussenite, quadruphite and sobolevite, m = 4, and in polyphite, m = 6. As I have shown above for perraultite (and surkhobite), the **I** cations can be close-packed. There are four sites in the close-packed layers of cations within a TS block, and there are two cations in the minimal cell in perraultite. Where the **I** cations are large, *i.e.*, Ba^{2+}, Sr^{2+}, K^+, they can be close-packed, with <cation–cation> distances of ~ 4.9–5.4 Å, with two atoms per minimal cell. Where **I** cations are smaller, *e.g.*, Na^+, Ca^{2+}, Mn^{2+}, Mg^{2+}, they can be expected to be close-packed, with <cation–cation> distances of ~ 2.9–4.2 Å, with four atoms per minimal cell (as in the TS block itself). Where the two types of cations occur together in the **I** block, it is more probable that their arrangement will correspond to those of larger cations, as occurs in perraultite, where both Ba and Na are present.

I will consider structures with a specific number of **I** layers (m) increasing from one to six, and will examine the close-packed layers in each case.

*m = 1 **I** layers*

There is one **I** layer in bafertisite, hejtmanite, lamprophyllite, barytolamprophyllite and nabalamprophyllite. Topologically, bafertisite is identical to hejtmanite.

Lamprophyllite, barytolamprophyllite and nabalamprophyllite: Lamprophyllite and barytolamprophyllite are very similar to nabalamprophyllite. In the three minerals, the M^H site is occupied by [5]-coordinated Ti, and the A^P sites are shifted from the TS block to the **I** layer. The formula of the TS block (excluding A^P sites) is $^{[5]}M^H_2\ M^O_4\ (Si_2O_7)_2\ X^O_4 = Ti_2\ Na\ (Na_{1.3}\ Mn_{0.36}Fe_{0.22}Mg_{0.12})\ Ti\ O_2\ (Si_2O_7)_2\ (OH)_2$ for lamprophyllite (Krivovichev *et al.* 2003), $\{Na[Na_{1.2}(Fe^{2+}, Mn^{2+})_{0.8}][Ti(O,OH)_2]\}\ \{[Si_2O_7]_2[Ti_2O_2]$ for barytolamprophyllite (Rastsvetaeva *et al.* 1995a) and $Ti_2\ Na_3\ Ti\ (Si_2O_7)_2\ (OH)_2\ O_2$ for nabalamprophyllite (Rastsvetaeva & Chukanov 1999). I suggest writing the formula of the TS block for lamprophyllite and barytolamprophyllite as $Ti_2\ Na_3\ Ti\ (Si_2O_7)_2\ O_2\ (OH)_2$ (I showed above that the X^O_A site in barytolamprophyllite is occupied by

monovalent anions, and hence there are 2 OH groups *pfu*). The total charge of the TS block is –3 in lamprophyllite, barytolamprophyllite and nabalamprophyllite, and hence the total charge of the **I** block is +3. In lamprophyllite, barytolamprophyllite and nabalamprophyllite, there is one distorted layer of cations between adjacent TS blocks (Fig. 22a). In lamprophyllite, these cations are close-packed parallel to (100), and there are two cation sites per minimal cell (Fig. 22b). Krivovichev *et al*. (2003) gave the composition of this A^P_2 site as 1.18 Sr + 0.66 Na + 0.2 Ca, and the site has an aggregate positive charge +3.26 *vu* (for two atoms). One can present this site as an end-member composition, with two major constituents, (Sr Na), with a total charge of +3. The TS blocks and **I** layers of (Sr Na) atoms alternate in the **a** direction in the crystal structure of lamprophyllite (Fig. 22c). In barytolamprophyllite, Rastsvetaeva *et al*. (1995a) gave the composition of this A^P_2 site as 0.98 K + 0.84 Ba + 0.21 Sr, and the site has an aggregate positive charge +3.08 (for two atoms). They presented this site as (K Ba) with a total charge of +3. As divalent cations [1.19 (Ba + Sr)] prevail over a monovalent cation, 0.98 K, I suggest to write the site as (Ba K).

In the crystal structure of nabalamprophyllite, there is the same alternation of TS blocks and **I** layers. For nabalamprophyllite, Rastsvetaeva & Chukanov (1999) gave $A^P(1)$ = 1.0 Ba and $A^P(2)$ = 0.33 Ba + 0.30 Na + 0.12 K + 0.05 Sr + 0.20 □. In a later description, Chukanov *et al*. (2004) revised the site assignments for $A^P(2)$ as 0.30 Ba + 0.50 Na + 0.15 K + 0.05 Sr and presented these two sites as Ba(Na,Ba). As I showed above, the charge of the TS block is –3. At the $A^P(2)$ site in nabalamprophyllite, (Na + K) are dominant over (Ba + Sr), with Na > K, and hence I can write $A^P(2)$ = Na. Then the **I** layer has a chemical composition of [Ba Na] with a total charge of +3.

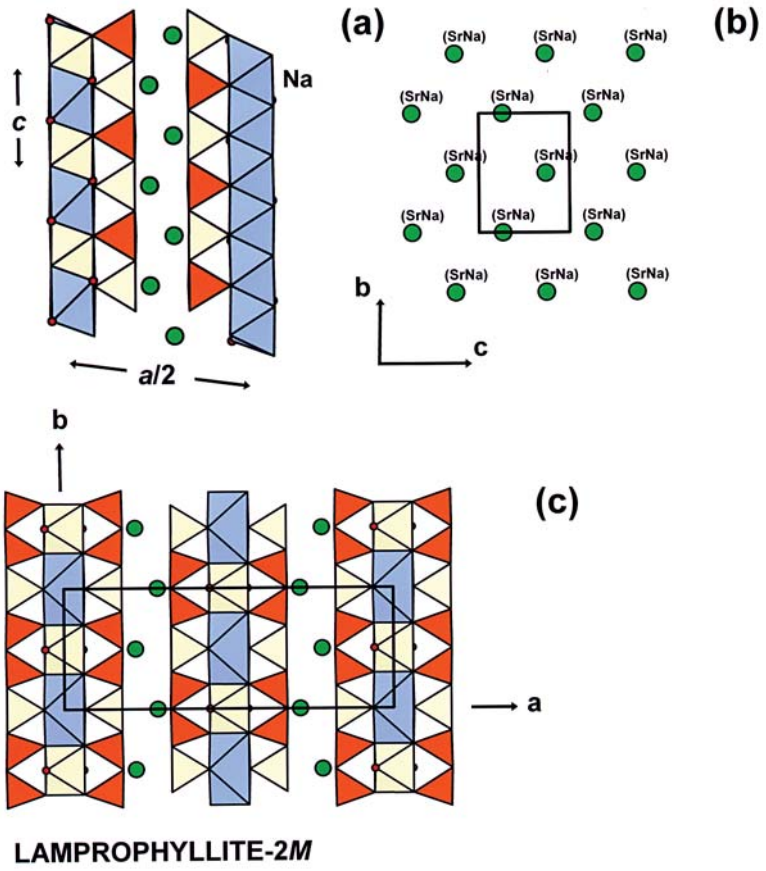

FIG. 22. Lamprophyllite-2*M*. Fragments of the crystal structure showing the (Sr Na) atoms in the **I** layer between two TS blocks (a) and projected onto (100) (b); the structure is projected onto (001). Legend as in Figure 13.

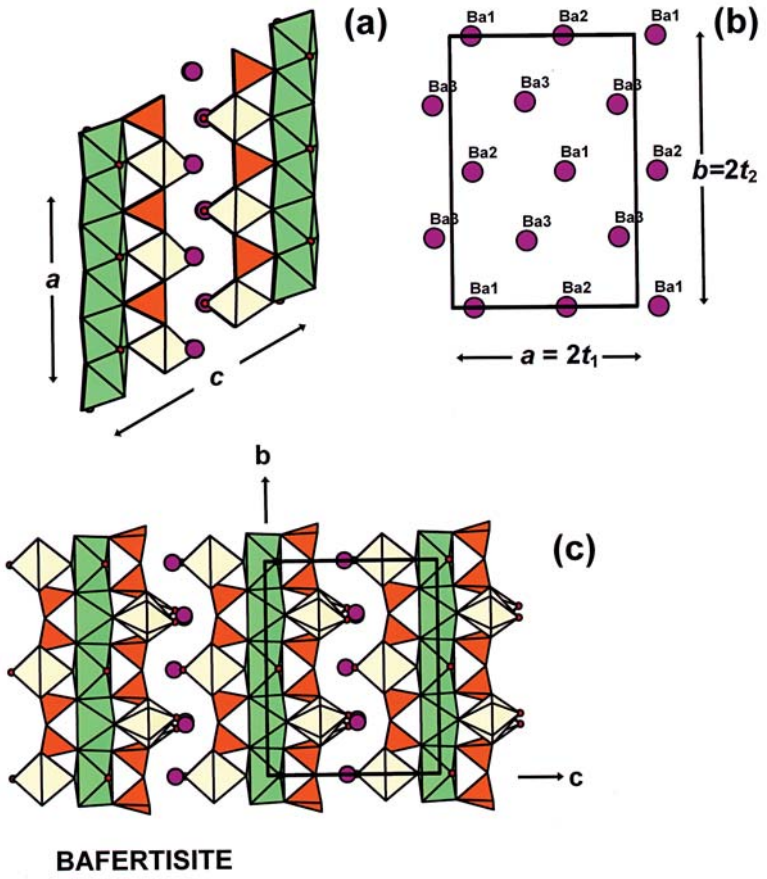

FIG. 23. Bafertisite. Fragments of the crystal structure showing the Ba atoms of the **I** layer between two TS blocks (a) and projected onto (001) (b); (c) the structure projected onto (100). Legend as in Figure 12; Ba atoms are shown as magenta circles.

In lamprophyllite and barytolamprophyllite, Sr and Na, and Ba and K, respectively, are disordered over one site; the **I** layer is (Sr Na) and (Ba K), and the space groups are *Pnmn* and *C*2/*m*. In nabalamprophyllite, Ba and Na are ordered at two sites, the **I** layer is [Ba Na], and the space group is *P*2/*m*. It is not clear to me what causes the Na–Ba order in the structure of nabalamprophyllite. The $A^P(1)$ and $A^P(2)$ sites are located on different sides of the TS block: one side is dominated by Ba, and the other one is dominated by Na (Fig. 13). To my knowledge, this is the only case where the TS block is characterized by chemically different *P* sites on each side.

Bafertisite and hejtmanite: The [6]-coordinated M^H site is occupied by Ti, the A^P sites are dominated by Ba, and the latter are shifted from the H sheets to form the **I** layer. Consider the Ti as [5]-coordinated; one can write the chemical composition of the TS block (minus the *P* sites) as $^{[5]}M^H_2\ M^O_4\ (Si_2O_7)_2\ X^O_4 = Ti_2\ Fe^{2+}_4\ (Si_2O_7)_2\ O_2\ (OH)_2$ for bafertisite and $Ti_2\ Mn^{2+}_4\ (Si_2O_7)_2\ O_2\ (OH)_2$ for hejtmanite. In each case, the total charge of the TS block is –2, and therefore the total charge of the **I** block must be +2. In bafertisite (and in hejtmanite), one **I** layer of cations occurs between adjacent TS blocks (Fig. 23a). There are two cation sites per minimal cell in a close-packed layer in bafertisite (Fig. 23b), and the total charge of the two constituent cations must be +2 to compensate the negative charge of the TS block. There are three possibilities: (1) the A^P cations are monovalent, *e.g.*, $2K^+$, (2) the A^P cations are divalent, *e.g.*, Ba^{2+}, and each A^P cation is accompanied by an (OH) group, *e.g.*, 2[Ba(OH)], or (3) one A^P cation is monovalent, another is divalent, and divalent cations are accompanied by (OH) groups: $A^{P2+}\ A^{P+}\ (OH)^-$. For bafertisite (and hejtmanite), the second possibility occurs: the cations of the **I** layer are Ba^{2+}, and they are

accompanied by (OH) groups at the X^{P}_{M} sites. The Ti atom at the M^{H} site is [6]-coordinated by five O atoms and an (OH) group (Figs. 23a, c). Two Ba^{2+} and two $(OH)^{-}$ give the interlayer charge of +2. In the crystal structure of bafertisite, TS blocks and **I** layers of Ba atoms are stacked along **c** (Fig. 23c).

General formula: There are two formulae for the TS block, (9) and (7), that can be used to produce the formulae of these four minerals (note that the B^{P} sites are vacant): for lamprophyllite, barytolamprophyllite and nabalamprophyllite

$$(9)\ A^{P}_{2}\ B^{P}_{2}\ {}^{[5]}M^{H}_{2}\ M^{O}_{4}\ (Si_2O_7)_2\ X^{O}_{4} - B^{P}_{2} = A^{P}_{2}\ {}^{[5]}M^{H}_{2}\ M^{O}_{4}\ (Si_2O_7)_2\ X^{O}_{4} \quad (14)$$

and for bafertisite and hejtmanite

$$(7)\ A^{P}_{2}\ B^{P}_{2}\ {}^{[6]}M^{H}_{2}\ M^{O}_{4}\ (Si_2O_7)_2\ X^{O}_{4}\ X^{P}_{M2} - B^{P}_{2} = A^{P}_{2}\ {}^{[6]}M^{H}_{2}\ M^{O}_{4}\ (Si_2O_7)_2\ X^{O}_{4}\ X^{P}_{M2} \quad (15)$$

The chemical formulae of bafertisite, hejtmanite, lamprophyllite, barytolamprophyllite and nabalamprophyllite: The chemical formulae of

bafertisite $Ba_2\ Ti_2\ Fe^{2+}_4\ (Si_2O_7)_2\ O_2\ (OH)_4$

and of

hejtmanite $Ba_2\ Ti_2\ Mn^{2+}_4\ (Si_2O_7)_2\ O_2\ (OH)_4$

are identical to those given in Guan *et al*. (1963) and Rastsvetaeva *et al*. (1991b) (see Table 1). The chemical formulae of

lamprophyllite $(Sr\ Na)\ Ti_2\ Na_3\ Ti\ (Si_2O_7)_2\ O_2\ (OH)_2$,

barytolamprophyllite
$(Ba\ K)\ Ti_2\ Na_3\ Ti\ (Si_2O_7)_2\ O_2\ (OH)_2$

and of

nabalamprophyllite
$Ba\ Na\ Ti_2\ Na_3\ Ti\ (Si_2O_7)_2\ O_2\ (OH)_2$

are similar to the end-member formula given in the description of nabalamprophyllite as a new mineral by Chukanov *et al*. (2004), Ba (Na,Ba) {Na_3 Ti [Ti_2 O_2 $(Si_2O_7)_2$] $(OH,F)_2$}. However, inspection of the data for barytolamprophyllite shows that in some cases, there is a significant mismatch between structure refinement and microprobe data, *e.g*., in Rastsvetaeva *et al*. (1995a). The crystal chemistry of barytolamprophyllite needs reconsideration, and this work is in progress.

*m = 2 **I** layers*

In vuonnemite and lomonosovite, there are two **I** layers between adjacent TS blocks. Each layer consists of [4]- to [7]-coordinated Na polyhedra and (PO_4) tetrahedra. In the **I** layer, Na polyhedra share vertices, edges and corners, whereas (PO_4) tetrahedra share common vertices with Na polyhedra (Fig. 24c). These two layers are parallel to (001) and related by an inversion center (Figs. 24a, b). Therefore, the topology and chemical composition of these two **I** layers of polyhedra in each structure are identical. All cations in this **I** layer are close-packed, and there are four cations, 3 Na^{+} + P^{5+}, in the minimal cell (Fig. 24d). Two **I** layers link together through common vertices of Na and P polyhedra to form the **I** block in vuonnemite and lomonosovite. There are four O sites responsible for this linkage in each **I** layer; these are designated as internal anions of the **I** block. Alternating TS and **I** blocks along **c** build up the crystal structures of vuonnemite and lomonosovite (Figs. 25a, b).

General formula: A general formula for minerals with two **I** layers (m = 2) each containing four cations requires consideration of the **I**-layer anions. I write the formula of the TS block using formula (8) $A^{P}_{2}\ B^{P}_{2}\ {}^{[6]}M^{H}_{2}\ M^{O}_{4}\ (Si_2O_7)_2\ X^{O}_{4}\ X^{P}_{M2}\ X^{P}_{A2}$ and site populations from Table 3 (note that the B^{P} site is vacant):

vuonnemite
$Na^{P}_{2}\ {}^{[6]}Nb^{H}_{2}\ Na^{O}_{3}\ Ti^{O}\ (Si_2O_2\underline{O}_5)_2\ (FO)^{O}\ O^{O}_{2}\ \underline{O}^{P}_{4}$

lomonosovite
$Na^{P}_{2}\ {}^{[6]}Ti^{H}_{2}\ Na^{O}_{2}\ Ti^{O}_{2}\ (Si_2O_2\underline{O}_5)_2\ O^{O}_{4}\ \underline{O}^{P}_{4}$

The total charge of the TS block (excluding peripheral X^{P} anions) in vuonnemite and lomonosovite is zero, and thus the total charge of the **I** block has to be zero in order to satisfy the electroneutrality principle. Polyhedra of the **I** layer link to polyhedra of the H sheet through common vertices, edges and faces, and they share seven O atoms with each H sheet. The $(Si_2O_7)_2$ group is written as $(Si_2O_2\underline{O}_5)_2$ to show that five O atoms (underlined) are shared with adjacent **I** layers. I underline the other four X^{P} anions ($\underline{O}^{P}_{4}$) to show that they also are shared with the **I** layer (see footnote, Table 3). In total, each **I** layer shares seven O atoms with the adjacent H sheet; four O atoms are common vertices of (PO_4) tetrahedra and Na polyhedra of the **I** layer, and they are internal anions of each **I** layer (Fig. 24c). These four anions are internal, as they are not bonded to any cation of the TS block (doubly underlined later in the text). Four cations, 3 Na^{+} + P^{5+}, and eleven anions, 11 O^{2-}, give the composition of one **I** layer, *i.e*., $[Na_3\ P\ \underline{O}_4\ \underline{O}_7]^{14-}$ (Table 5). Common sense tells me to keep small oxyanions intact, *e.g*., (PO_4), (Si_2O_7); although these groups have anions from both **I** layer and H sheet, (PO_4) groups are assigned to the **I** block and (Si_2O_7) groups are assigned to the TS block. To do this, I consider $\underline{O}^{P}_{4}$ anions not as a part of the TS block (Table 3) but as a part of the **I** block.

As a result, the composition of the **I** block is the composition of two **I** layers minus four internal anions

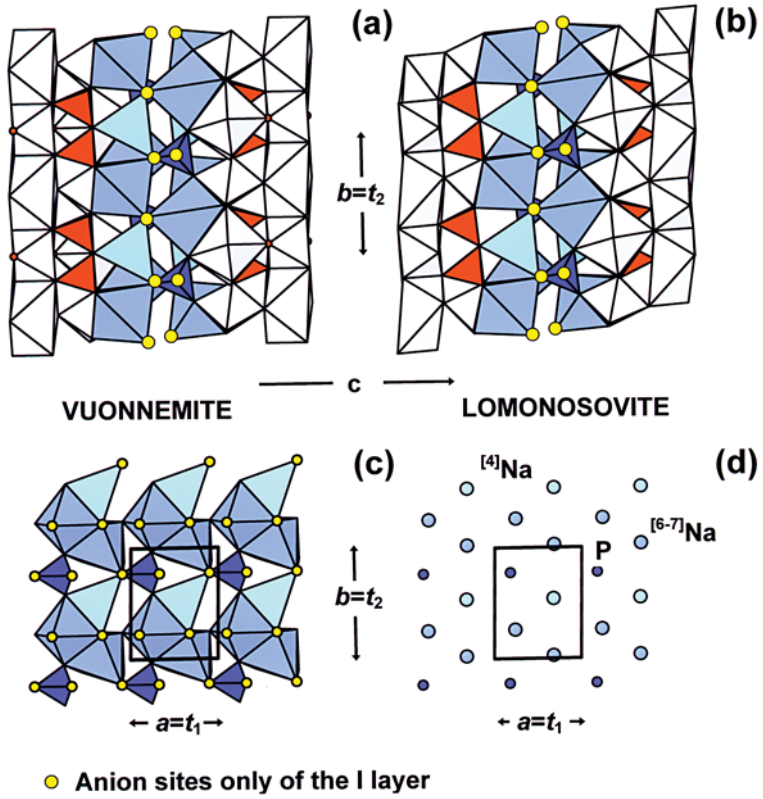

FIG. 24. Fragments of the crystal structure of vuonnemite (a) and lomonosovite (b) showing two **I** layers between two TS blocks, an **I** layer projected onto (001) as Na and P polyhedra (c), and a close-packed arrangement of cations (d). All polyhedra of the TS block are white except for orange (SiO_4) tetrahedra. In the **I** layers, (PO_4) groups are purple, [4]- and [6–7]-coordinated Na polyhedra are greenish blue and navy blue; the [(OH,F)O] sites are shown as small orange circles. Internal anion sites of the **I** block are the large yellow circles.

(as each pair of internal anion sites merge into one site) and ten anions shared with (Si_2O_7) groups:

$$2 \times [Na_3\, P\, \underline{O}_4\, \underline{O}_7] - \underline{O}_4 - \underline{O}_{10} = Na_6\,(PO_4)_2$$

The total charge of the **I** block is zero. Note that the **I** block has $\underline{O}^P{}_4$ previously listed in the formula of the TS block at the beginning of this section, and hence $\underline{O}^P{}_4$ must be subtracted from the TS block before the TS block and **I** block are summed to give the final formula:

vuonnemite

$$Na^P{}_2\, {}^{[6]}Nb^H{}_2\, Na^O{}_3\, Ti^O\, (Si_2O_7)_2\, (FO)^O\, O^O{}_2 + Na_6\,(PO_4)_2 =$$

$$Na_6\, Na_2\, Nb_2\, Na_3\, Ti\, (Si_2O_7)_2\, (PO_4)_2\, (FO)\, O_2$$

lomonosovite

$$Na^P{}_2\, {}^{[6]}Ti^H{}_2\, Na^O{}_2\, Ti^O{}_2\, (Si_2O_7)_2\, O^O{}_4 + Na_6\,(PO_4)_2 =$$

$$Na_6\, Na_2\, Ti_2\, Na_2\, Ti_2\, (Si_2O_7)_2\, (PO_4)_2\, O_4$$

The general formula for the structures with **I** layers containing four cation sites (3*Na* and *P*) can be written as

$$A^I{}_{3m}\, A^P{}_2\, {}^{[6]}M^H{}_2\, M^O{}_4\, (Si_2O_7)_2\, (PO_4)_m\, X^O{}_4 \qquad (16)$$

where m = number of **I** layers, A^I = cations of the **I** layers, except for P^{5+}, which are written as (PO_4) groups.

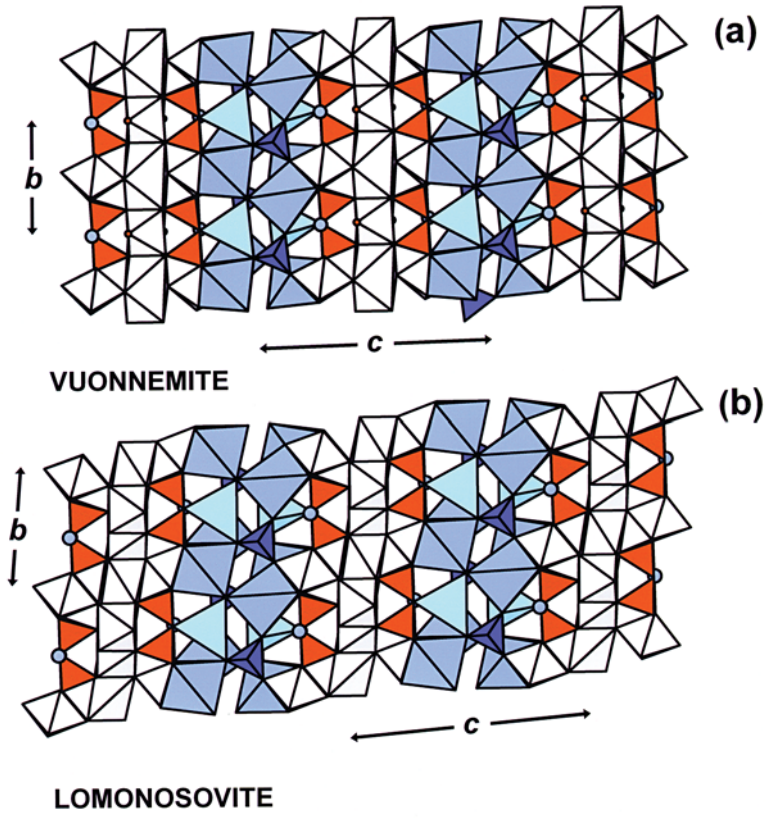

FIG. 25. General view of the crystal structure of (a) vuonnemite, and (b) lomonosovite. Legend as in Figure 24; [8]-coordinated Na^P atoms are shown as navy blue circles.

*m = 3 **I** layers*

Three **I** layers occur in yoshimuraite and innelite. The topology of the **I** block in both structures is identical: the Ba atoms constitute a close-packed layer (Fig. 26a) identical to that in bafertisite and hejtmanite (Fig. 23b). There are two Ba atoms per minimal cell (Table 5) that occupy the A^P and B^P sites, which are strongly shifted into the **I** block: Ba–X^O_A distances are 3.89 and 4.06 Å (Table 2). The (PO_4) and (SO_4) tetrahedra constitute another layer in yoshimuraite (Fig. 26b) and innelite, with the P (S) atoms arranged as a close-packed layer. In these two structures, the layer of tetrahedral oxyanions is intercalated between two layers of Ba atoms (Fig. 26c). The [10]- and [11]-coordinated Ba atoms are bonded to O atoms of (TO_4) tetrahedra and polyhedra of the H sheets. Each O atom of a (TO_4) group is bonded to two or three Ba atoms. The ideal composition of the **I** block in yoshimuraite is $[Ba_4 (PO_4)_2]^{2+}$, and in innelite, it is $[Ba_4 (SO_4)_2]^{4+}$ (Table 5). In fact, there are similarities in chemical composition of these two blocks, as the *P* site in yoshimuraite has a composition 0.5 P + 0.3 S + 0.2 Si with a total charge of +5.1 (McDonald *et al*. 2000). Therefore, the TS block has a negative charge of –2 in yoshimuraite, and –4 in innelite. As noted before, the topology of the TS block is different in yoshimuraite (Group II, Figs. 11b, d) and innelite (Group III, Figs. 13c, e). Alternation of **I** and TS blocks along the 14.75 Å axis produces the crystal structures of yoshimuraite (Fig. 26c) and innelite. To accommodate the three-layered **I** block, the TS blocks shift relative to each other in innelite, with $\gamma = 99.00°$ *versus* $\alpha = 89.98°$ in yoshimuraite (Table 1).

General formula: I use formula (8), $A^P_2\ B^P_2\ ^{[5]}M^H_2\ M^O_4\ (Si_2O_7)_2\ X^O_4$, and add the complex oxyanions $(TO_4)_2$:

$$A^P_2\ B^P_2\ ^{[5]}M^H_2\ M^O_4\ (Si_2O_7)_2\ (TO_4)_2\ X^O_4 \qquad (17)$$

where T = P, Si. I write the formulae with site populations taken from Tables 3 and 5:

yoshimuraite $Ba_2\,Ba_2\,Ti_2\,Mn_4\,(Si_2O_7)_2\,(PO_4)_2\,O_2\,(OH)_2$

innelite $Ba_2\,Ba_2\,Ti_2\,Na_2\,Ca\,Ti\,(Si_2O_7)_2\,(SO_4)_2\,O_4$

The chemical composition and chemical formula of innelite need revision, as pointed out above.

*m = 4 **I** layers*

There are three minerals that contain four **I** layers, bussenite, quadruphite and sobolevite. The composition and topology of the **I** block in bussenite are very different from those in quadruphite and sobolevite.

Bussenite: Bussenite is the only mineral considered here that contains (CO_3) groups. There are seven cation sites in the **I** block. There are two [6]-coordinated *Na* sites, *Na*(1) and *N*a(2), each has a multiplicity of 2, and each is 50% occupied by Na, giving 2 × (Na□) = 2 Na. The [11]-coordinated *Ba*(1) site is occupied by 1.6 Ba + 0.4 K, ideally Ba_2. The [9]-coordinated *Ba*(2) site is approximately 50% occupied by Ba: 0.94 Ba + 1.06 □. The [7]-coordinated *M*(4) site also is half-occupied: 0.64 Sr + 0.42 K + 0.94 □. There is a short distance between *Ba*(2) and *M*(4) sites, 0.92 Å, and one can treat these two sites effectively as one site, 0.94 Ba + 0.64 Sr + 0.42 K; divalent cations are dominant at this site, Ba > Sr, so ideally it is Ba_2. There is one [3]-coordinated *C* site fully occupied by C, which gives 2 C *apfu*. The Na octahedra form convoluted chains extending along [100] (Figs. 27a, b). In a chain, two Na polyhedra at the same level along [100] share a common face to form a dimer. Each dimer shares edges with one dimer and faces with other next-nearest dimers. The combination of two dimers corresponds to a sequence of two [F(1)–F(2)] edges defining the *a* repeat and giving an *a* cell-parameter of 5.399 Å. The Na polyhedra and Ti octahedra of the H sheet share common vertices, which are (H_2O) groups. The Na–O–F–(H_2O) chains are connected *via* (CO_3) groups along [010] (Figs. 27a, b). Each (CO_3) group shares one edge with an Na octahedron of one chain and a vertex with an Na octahedron of another chain. The size of the **I** cations varies extensively: r [$^{[6]}$Na] = 0.99, r [$^{[11]}$Ba] = 1.57, r [$^{[3]}$C] = –0.08 Å (Shannon 1976), but they are arranged as close-packed layers. There are layers of Ba(1) and [Ba(2) + M(4)] atoms between sheets of Na octahedra and (CO_3) groups and TS blocks. In total, there are four layers of cations in the **I** block. Layers 1 and 4 (Fig. 27a) are related by an inversion center and consist of Ba(1) and Ba(2) [= Ba(2) + M(4)] atoms, as in bafertisite and yoshimuraite. There are two atoms, Ba(1) and Ba(2), per minimal cell (Table 5). The Na(1), Na(2) and C atoms constitute layers 2 and 3, which are also related by an inversion centre. As the Na(1) and Na(2) sites are only 50% occupied, there are also two cations, Na^+ and C^{4+}, per minimal cell (Fig. 27c). Thus two Ba layers, two Na–C layers, and F atoms in between layers 2 and 3 give the composition of the **I** block in bussenite as 2 × Ba_2 + 2 × [Na (CO_3)] + F_2 = $[Ba_4\,Na_2\,(CO_3)_2\,F_2]^{4+}$. I include in the latter formula the two (H_2O) groups that are shared with the adjacent TS block, to give the composition of the **I** block: $[Ba_4\,Na_2\,(CO_3)_2\,F_2\,(H_2O)_2]^{4+}$ (see Table 5). Therefore the TS block must have a charge of 4^-. I write the formula of the TS block using formula (6), $A^P_2\,B^P_2\,{}^{[6]}M^H_2\,M^O_4\,(Si_2O_7)_2\,X^O_4\,X^P_{M2}$, and site populations from Table 3:

$$\begin{array}{cccccc} {}^{[6]}M^H_2 & M^O_4 & (Si_2O_7)_2 & X^O_4 & X^P_{M2} \rightarrow \\ Ti_2 & (M^{2+}\,Na)_2 & (Si_2O_7)_2 & O_2 & (OH)_2\,(H_2O)_2. \end{array}$$

The total charge is –4. I add TS and **I** blocks, and consider $(H_2O)_2$ once, as it is shared by two blocks:

$$Ba_2\,Ba_2\,(Na\square)_2\,\underline{Ti_2}\,(\underline{Fe^{2+}}\,\underline{Na})_2\,(\underline{Si_2O_7})_2\,(CO_3)_2\,\underline{O_2}\,(\underline{OH})_2\,(\underline{H_2O})_2\,F_2,$$

which corresponds to the general formula

$$A^P_2\,B^P_2\,A^I_{2m}\,M^H_2\,M^O_4\,(Si_2O_7)_2\,(CO_3)_m\,X^O_4\,X^P_2\,F_m \qquad (18)$$

where m represents the number of **I** layers not containing *P* sites.

m = 4 (*quadruphite and sobolevite*) *and m = 6* (*polyphite*) ***I** layers*

I consider quadruphite and sobolevite with m = 4 and polyphite with m = 6 together, as they are closely structurally related. The main constituents of the **I** block are alkali cations and (PO_4) groups. There are two different parts of the **I** block. The outer parts of the **I** block are sheets of Na polyhedra and (PO_4) groups adjacent to the TS block (Fig. 28). In quadruphite, these two outer **I** layers differ in coordination of Na, which can be [4]-, [6]- and [7]-coordinated (Figs. 28a, b). In polyphite, two outer **I** layers are symmetrically equivalent, related by the inversion center and containing [4]- and [5]-coordinated Na polyhedra (Fig. 28c). In sobolevite, there are two outer **I** layers; one is identical to an outer layer in polyphite, another, to an outer layer in quadruphite. In each outer **I** layer, there are four cations per minimal unit cell, and they are arranged as a close-packed layer (Fig. 28d). Each Na–P–O layer has a composition $[Na_3\,P\,O_{11}]^{3-}$. The Na–P–O layers in quadruphite, polyphite and sobolevite are similar to the **I** layers in vuonnemite and lomonosovite.

The inner part of the **I** block contain trimeric clusters of octahedrally coordinated alkali cations. Sokolova (1997) designated it as a *nacaphite block*, as it is topologically identical and chemically very close to the crystal structure of nacaphite, Na (NaCa) (PO_4) F (Sokolova *et al.* 1989, Sokolova & Hawthorne 2001). Sokolova & Hawthorne (2001) designated this part of the **I** block as the *AC block* to emphasize the key role played by alkalis in the structure of these minerals. The

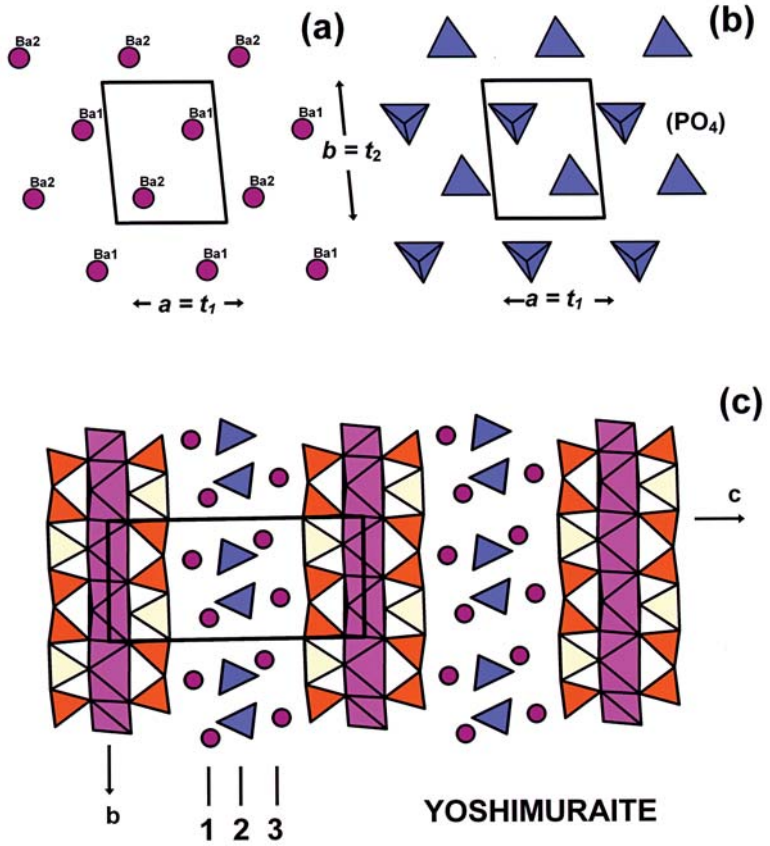

FIG. 26. The crystal structure of yoshimuraite: a close-packed layer of Ba atoms (a), and a close-packed layer of P atoms is presented as (PO_4) tetrahedra (b), a general view of the structure projected onto (100). The Ba atoms and Mn^{2+} polyhedra are magenta, the (PO_4) tetrahedra are purple, [5]-coordinated Ti polyhedra and Si tetrahedra are yellow and orange, and lines 1, 2, and 3 show three layers of the **I** block.

presence of the trimeric cluster in a series of crystal structures indicates its high stability as a structural motif and testifies to a highly alkaline environment of formation (Sokolova & Hawthorne 2001). Each cluster consists of three octahedra that share a central common edge; in the cluster, each two octahedra share a common face. Trimeric clusters link together to form a convoluted chain of octahedra (Fig. 29a) that extends in the $\mathbf{t_1}$ direction. Clusters adjacent in the chain are rotated ~60° relative to each other and connect by sharing both faces and edges. The chain shows pseudohexagonal symmetry described by the 6_3 axis oriented along the sequence of [F(1)–F(2)] common edges that defines the central axis of the chain. Combination of two clusters corresponds to a sequence of two [F–F] edges defining the t_1 repeat. The chains extend along the $\mathbf{t_1}$ direction, and link in the plane based on t_1 and t_2 by sharing octahedron corners, and triplets are further linked through (PO_4) tetrahedra that point alternately up and down $\mathbf{t_1}$ (Figs. 29b–e).

In the crystal structures of quadruphite, polyphite and sobolevite, the trimeric structure of the **I** block links through outer Na–P–O layers to two TS blocks, forming a mixed cation framework (*e.g.*, as in quadruphite, Fig. 30a). The trimeric structure shares four O atoms with each outer layer of polyhedra, and the latter shares eight, six and seven O atoms with an H sheet of two TS blocks in quadruphite, polyphite and sobolevite, respectively (Table 5). The number of O atoms shared by the polyhedron of the outer layer of the **I** block and (Si_2O_7) groups depends on coordination of cations of the outer layer.

All cations of the **I** block in quadruphite, polyphite and sobolevite are arranged in close-packed layers. In quadruphite, there are four layers: layers 1 and 4

correspond to the **I** layers adjacent to two TS blocks, and layers 2 and 3 correspond to the trimeric structure (Figs. 29b, 30a). Within the trimeric structure, there are two layers in quadruphite (Figs. 30b, c) and sobolevite, and four layers in polyphite. Therefore, the central part of the **I** block is twice as large in polyphite compared to that in quadruphite and sobolevite.

Each layer contains four cation sites and is characterized by <cation–cation> separations of ~3.4 Å. Table 5 gives ideal site-populations for each **I** layer. In the trimeric structure of the **I** block in quadruphite (space group $P1$), the four sites are Ca-dominant (with Ca slightly greater than Na), two sites are Na-dominant, and one can write the composition of the trimeric structure as $Na_2\,(Ca_2\,Na_2)\,(PO_4)_2\,F_2$. In polyphite (space group $P\bar{1}$), two chains of trimeric clusters are related by an inversion center. Within the trimeric structure, four sites are Na-dominant, and two sites are Ca-dominant, and one can write the composition of the trimeric structure as 2 $[Na_4\,Ca_2\,(PO_4)_2\,F_2]$. Maximal Na–Ca order occurs in sobolevite (space group Pc). There are two sites solely occupied by Na and one site solely occupied by Ca (Figs. 29c, d): Na_2Ca. There are two Ca-dominant sites with a significant amount of Mn^{2+} and a Na-dominant site, so one can write the composition of these three sites as (Na Ca Mn), and the composition of the trimeric structure is $[Na_2\,Ca\,(Na\,Ca\,Mn)\,(PO_4)_2\,F_2]$.

General formula for CASE 4: TS BLOCKS DO NOT LINK DIRECTLY, m = 4 and 6: Earlier, I showed that the general formula for structures with **I** layers, which contain four cation sites (3 Na and P), can be written as $A^{I}_{3m}\,A^{P}_{2}\,{}^{[6]}M^{H}_{2}\,M^{O}_{4}\,(Si_2O_7)_2\,(PO_4)_m\,X^{O}_{4}$, which

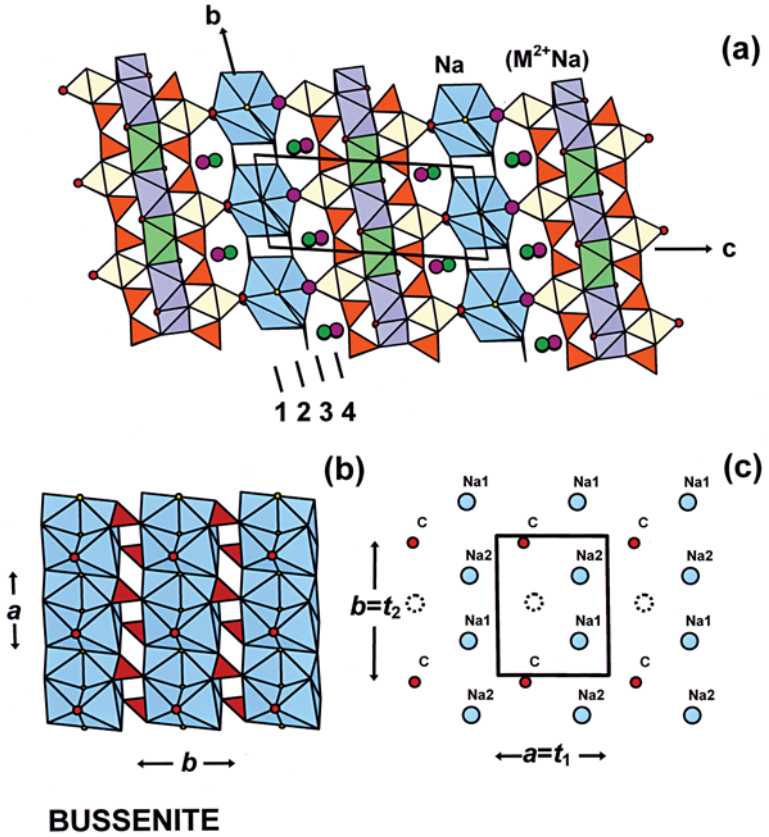

FIG. 27. Bussenite. General view of the crystal structure projected onto (100) (a), linkage of chains of Na octahedra and (CO_3) groups (b), a close-packed layer of Na and C atoms (c). Legend as in Figures 10 and 11; Na octahedra and (CO_3) groups of the **I** block are light blue and red, and Ba, Sr and Na atoms of the **I** block are shown as magenta, green and light blue circles in (a) and (c); (OH) and (H_2O) groups and F atoms are shown as small and medium red circles and small yellow circles in (a); C atoms are shown as red circles, and vacant sites of the **I** layers 2 and 3 are shown as dashed black circles in (c); short lines 1–4 show the position of four **I** layers.

TABLE 6. OPTIMAL FORMULAE OF MINERALS WITH THE TS BLOCK

	F1	F2	General formula	Structural formula	Mineral formula
Group I					
götzenite	6	11	$A^{P}_{2}\,M^{H}_{2}\,M^{O}_{4}\,(Si_2O_7)_2\,X^{O}_{4}$	$Ca_2Ca_2NaCa_2Ti(Si_2O_7)_2OF_3$	$NaCa_6\mathbf{Ti}(Si_2O_7)_2OF_3$
hainite	6	11		$Ca_3(Y,REE)Na(NaCa)Ti(Si_2O_7)_2OF_3$	$Na_2Ca_4(Y,REE)\mathbf{Ti}(Si_2O_7)_2OF_3$
seidozerite	6	11		$Na_2Zr_2Na_2MnTi(Si_2O_7)_2O_2F_2$	$Na_4MnZr_2\mathbf{Ti}(Si_2O_7)_2O_2F_2$
grenmarite	6	11		$Na_2Zr_2Na_2MnZr(Si_2O_7)_2O_2F_2$	$Na_4MnZr_3(Si_2O_7)_2O_2F_2$
rinkite	6	11		$Ca_3REENa(NaCa)Ti(Si_2O_7)_2OF_3$	$Na_2Ca_4REE\mathbf{Ti}(Si_2O_7)_2OF_3$
kochite	6	11		$Ca_2MnZrNa_3Ti(Si_2O_7)_2OF_3$	$Na_3Ca_2MnZr\mathbf{Ti}(Si_2O_7)_2OF_3$
rosenbuschite	6	11		$Ca_4Ca_2Zr_2Na_2Na_4TiZr(Si_2O_7)_4O_2F_6$	$Na_6Ca_6Zr_3\mathbf{Ti}(Si_2O_7)_4O_2F_6$
Group II					
perraultite	6	12	$A^{P}\,B^{P}\,M^{H}_{2}\,M^{O}_{4}\,(Si_2O_7)_2\,X^{O}_{4}\,X^{P}_{M}$	$BaNaTi_2(Mn_{2.5}Fe^{2+}_{1.5})(Si_2O_7)_2O_2(OH)_2F$	$NaBaMn_4\mathbf{Ti_2}(Si_2O_7)_2O_2(OH)_2F$
surkhobite	6	12		$BaNaTi_2(Fe^{2+}_2\,Mn_2)(Si_2O_7)_2O_2(OH)F_2$	$NaBaFe^{2+}_4\mathbf{Ti_2}(Si_2O_7)_2O_2(OH)F_2$
bafertisite	6	15	$A^{P}_{2}\,M^{H}_{2}\,M^{O}_{4}\,(Si_2O_7)_2\,X^{O}_{4}\,X^{P}_{M2}$	$Ba_2Ti_2Fe^{2+}_4(Si_2O_7)_2O_2\,(OH)_4$	$Ba_2Fe^{2+}_4\mathbf{Ti_2}(Si_2O_7)_2O_2(OH)_4$
hejtmanite	6	15		$Ba_2Ti_2Mn^{2+}_4(Si_2O_7)_2O_2(OH)_4$	$Ba_2Mn^{2+}_4\mathbf{Ti_2}(Si_2O_7)_2O_2(OH)_4$
yoshimuraite	8	17	$A^{P}_{2}\,B^{P}_{2}\,M^{H}_{2}\,M^{O}_{4}\,(Si_2O_7)_2\,(TO_4)_2\,X^{O}_{4}$	$Ba_2Ba_2Ti_2Mn_4(Si_2O_7)_2(PO_4)_2O_2(OH)_2$	$Ba_4Mn^{2+}_4\mathbf{Ti_2}(Si_2O_7)_2(PO_4)_2O_2(OH)_2$
bussenite	6	18	$A^{P}_{2}\,B^{P}_{2}\,A^{I}_{2m}\,M^{H}_{2}\,M^{O}_{4}\,(Si_2O_7)_2(CO_3)_m\,X^{O}_{4}\,X^{P}_{2}\,F_m$	$Ba_2Ba_2(Na\square)_2Ti_2(M^{2+}Na)_2(Si_2O_7)_2(CO_3)_2O_2(OH)_2(H_2O)_2F_2$	$Na_4Ba_4Fe^{2+}_2\mathbf{Ti_2}(Si_2O_7)_2(CO_3)_2O_2(OH)_2(H_2O)_2F_2$
Group III					
lamprophyllite	8	14	$A^{P}_{2}\,M^{H}_{2}\,M^{O}_{4}\,(Si_2O_7)_2\,X^{O}_{4}$	$(SrNa)Ti_2Na_3Ti(Si_2O_7)_2O_2(OH)_2$	$Na_3(SrNa)\mathbf{Ti_3}(Si_2O_7)_2O_2(OH)_2$
barytolamprophyllitee	8	14		$(BaK)Ti_2Na_3Ti(Si_2O_7)_2O_2(OH)_2$	$Na_3(BaK)\mathbf{Ti_3}(Si_2O_7)_2O_2(OH)_2$
nabalamprophyllite	8	14		$BaNaTi_2Na_3Ti(Si_2O_7)_2O_2(OH)_2$	$Na_4Ba\mathbf{Ti_3}(Si_2O_7)_2O_2(OH)_2$
innelite	8	17	$A^{P}_{2}\,B^{P}_{2}\,M^{H}_{2}\,M^{O}_{4}\,(Si_2O_7)_2\,(TO_4)_2\,X^{O}_{4}$	$Ba_2Ba_2Ti_2Na_2CaTi(Si_2O_7)_2(SO_4)_2O_4$	$Na_2CaBa_4\mathbf{Ti_3}(Si_2O_7)_2(SO_4)_2O_4$
epistolite	7	13	$A^{P}_{2}\,M^{H}_{2}\,M^{O}_{4}\,(Si_2O_7)_2\,X^{O}_{4}\,X^{P}_{M2}\,X^{P}_{A2}$	$(Na\square)Nb_2Na_3Ti(Si_2O_7)_2O_2(OH)_2(H_2O)_4$	$Na_4\mathbf{TiNb_2}(Si_2O_7)_2O_2(OH)_2(H_2O)_4$
vuonnemite	7	16	$A^{I}_{3m}\,A^{P}_{2}\,M^{H}_{2}\,M^{O}_{4}\,(Si_2O_7)^{H}_{2}\,(PO_4)_m\,X^{O}_{4}$	$Na_6Na_2Nb_2Na_3Ti(Si_2O_7)_2\,(PO_4)_2O_3F$	$Na_{11}\mathbf{TiNb_2}(Si_2O_7)_2(PO_4)_2O_3F$
Group IV					
murmanite	7	13	$A^{P}_{2}\,M^{H}_{2}\,M^{O}_{4}\,(Si_2O_7)_2\,X^{O}_{4}\,X^{P}_{M2}\,X^{P}_{A2}$	$Na_2Ti_2Na_2Ti_2(Si_2O_7)_2O_4(H_2O)_4$	$Na_4\mathbf{Ti_4}(Si_2O_7)_2O_4(H_2O)_4$
lomonosovite	7	16	$A^{I}_{3m}\,A^{P}_{2}\,M^{H}_{2}\,M^{O}_{4}\,(Si_2O_7)_2\,(PO_4)_m\,X^{O}_{4}$	$Na_8Na_2Ti_2Na_2Ti_2(Si_2O_7)_2(PO_4)_2O_4$	$Na_{10}\mathbf{Ti_4}(Si_2O_7)_2(PO_4)_2O_4$
quadruphite	7	20	$A^{I}_{3m}\,A^{T}_{3t}\,A^{P}_{2}\,M^{H}_{2}\,M^{O}_{4}\,(Si_2O_7)_2\,(PO_4)_{m+t}\,X^{O}_{4}\,F_t$	$Na_8Na_2(CaNa)_2Na_2Ti_2Na_2Ti_2(Si_2O_7)_2(PO_4)_4O_4F_2$	$Na_{14}Ca_2\mathbf{Ti_4}(Si_2O_7)_2(PO_4)_4O_4F_2$
sobolevite	7	20		$Na_6(Na_2Ca)(NaCaMn)Na_2Ti_2Na_2TiMn(Si_2O_7)_2(PO_4)_4O_3FF_2$	$Na_{13}Ca_2Mn_2\mathbf{Ti_3}(Si_2O_7)_2(PO_4)_4O_3F_3$
polyphite	7	20		$Na_6(Na_4Ca_2)_2Na_2Ti_2Na_2Ti_2(Si_2O_7)_2(PO_4)_6O_4F_4$	$Na_{16}Ca_4\mathbf{Ti_4}(Si_2O_7)_2(PO_4)_6O_4F_4$

F1: formulae 6, 7 and 8 of the TS block: (6) $A^{P}_{2}\,B^{P}_{2}\,{}^{[6]}M^{H}_{2}\,M^{O}_{4}\,(Si_2O_7)_2\,X^{O}_{4}\,X^{P}_{M2}$, (7) $A^{P}_{2}\,B^{P}_{2}\,{}^{[6]}M^{H}_{2}\,M^{O}_{4}\,(Si_2O_7)_2\,X^{O}_{4}\,X^{P}_{M2}\,X^{P}_{A2}$, (8) $A^{P}_{2}\,B^{P}_{2}\,{}^{[5]}M^{H}_{2}\,M^{O}_{4}\,(Si_2O_7)_2\,X^{O}_{4}$.
F2: general formulae (11–18, 20) describe groups of minerals of different topology. Formula (19) describes the trimeric structure of the **I** block: $A^{T}_{3t}(PO_4)_tF_t$.
I block: m: number of **I** layers, t: number of **I** layers within the trimeric structure, A^{I}_{3m} and A^{T}_{3t}: cations of the **I** layers except for P^{5+}; *T* cations: P, S; $M^{2+} = Fe^{2+}$, Mn^{2+} for bussenite.
Formula of rosenbuschite is given for a doubled minimal cell.

corresponds to formula (16), where m = 2; A^I are cations of the **I** block different from P^{5+}. Quadruphite, polyphite and sobolevite each contain two such **I** layers, and formula (16) applies to the TS block plus two adjacent **I** layers. The only part of the complete structure not yet considered is the trimeric structure in the central part of the **I** block. The trimeric structure has its mineral analogue, nacaphite, Na (NaCa) (PO_4) F (Z = 4). By analogy with nacaphite, one can write the composition of the trimeric structure as

nacaphite (Z = 2) Na_2 $(NaCa)_2$ $(PO_4)_2$ F_2

quadruphite Na_2 $(CaNa)_2$ $(PO_4)_2$ F_2

sobolevite (Na_2Ca) (NaCaMn) $(PO_4)_2$ F_2

polyphite $(Na_4Ca_2)_2$ $(PO_4)_4$ F_4.

Thus the general composition of the trimeric structure may be written as

$$A^T{}_{3t}\,(PO_4)_t\,F_t \qquad (19)$$

where t represents the number of cation layers, and A^T are the cations different from P^{5+}. I can now write the general formula for minerals with trimeric structures as the sum of formulae (16) and (19):

$$A^I{}_{3m}\,A^T{}_{3t}\,A^P{}_2\,{}^{[6]}M^H{}_2\,M^O{}_4\,(Si_2O_7)_2\,(PO_4)_{m+t}\,X^O{}_4\,F_t \qquad (20)$$

where m is number of **I** layers adjacent to the TS block, t is the number of **I** layers in the trimeric structure, and $A^I{}_{3m}$ $A^T{}_{3t}$ are the cations of the m and t layers of the **I** block different from P^{5+}.

The formulae for quadruphite, sobolevite and polyphite: I write the formulae for these minerals in accord with the general formula (20):

general formula	$\mathbf{A^I{}_{3m}}$	$\mathbf{A^T{}_{3t}}$	$\mathbf{A^P{}_2}$	$\mathbf{{}^{[6]}M^H{}_2}$	$\mathbf{M^O{}_4}$	$\mathbf{(Si_2O_7)_2}$	$\mathbf{(PO_4)_{m+t}}$	$\mathbf{X^O{}_4}$	$\mathbf{F_t}$
quadruphite	Na_6	$Na_2\,(CaNa)_2$	Na_2	Ti_2	$Na_2\,Ti_2$	$(Si_2O_7)_2$	$(PO_4)_4$	O_4	F_2
sobolevite	Na_6	(Na_2Ca) (NaCaMn)	Na_2	Ti_2	Na_2 TiMn	$(Si_2O_7)_2$	$(PO_4)_4$	O_3F	F_2
polyphite	Na_6	$(Na_4Ca_2)_2$	Na_2	Ti_2	$Na_2\,Ti_2$	$(Si_2O_7)_2$	$(PO_4)_6$	O_4	F_4

Formulae of Minerals with the TS Block

In Table 6, I list nine general formulae [(11)–(18), (20)] for structures of different topology. To obtain these formulae, I used formulae (6)–(8) for the TS block and have added the formula content of the **I** block, *i.e.*, I have used a polysomatic approach to derive a general formula. It is easy to notice that formula (16) is part of formula (20): (16) = (20)–(19), where the latter is the formula for the trimeric structure. Therefore, one can describe the chemical composition of the minerals with the TS block with eight formulae, (11–15), (17), (18), (20). In accordance with the general formulae, one can write structural formulae for all minerals (see Table 6). To obtain a simpler chemical formula, I write the mineral formulae in a common systematic way: from alkaline to alkaline-earth cations, from low valence to high valence, then list oxyanions, $(Si_2O_7)_2$, (PO_4), (SO_4), (CO_3), followed by anions: O atoms, (OH) groups and F atoms, and (H_2O) groups. Mineral formulae are listed in the last column of Table 6. These formulae are written in a unified way, they are compact, they provide an understanding of the chemical composition of each mineral, and they allow the general features of these minerals to be identified easily. I compare these structural formulae with those presented in Table 1 (where they are from the latest work on the relevant structure). Certainly, structural formulae in this work (Table 6) are simpler and give a better idea of chemical composition. Moreover, the mineral formulae revised in this work are more accurate than those given in the recent issue of Fleischer's Glossary of Mineral Species (Table A5 in Appendix E). In particular, I had to revise formulae of götzenite, kochite, rosenbuschite and hainite to give a better correlation with EMPA data, particularly the F content (Appendix D). Analysis of mineral formulae indicates that: (1) The composition of the **I** block in surkhobite has to be Na Ba. Re-examination of the chemical composition of surkhobite is desirable, and this work is in progress. (2) All chemical formulae of minerals of Group III contain monovalent anions, (OH) or F, except innelite, strongly suggesting that the formula of innelite is wrong. Work is currently under way to check this prediction.

Stereochemistry of Titanium

Inspection of Table 6 clearly shows that the Ti content of the minerals varies systematically from one Group to another. This is a very important feature. I divided all minerals with the TS block into four groups based on the topology and stereochemistry of the TS block. Apparently, the topology and stereochemistry of the TS block are strongly related to the content of Ti. First, a definition; where I refer to Ti, I mean *Ti-dominant site*; this site may also contain Nb^{5+}, Ta^{5+},

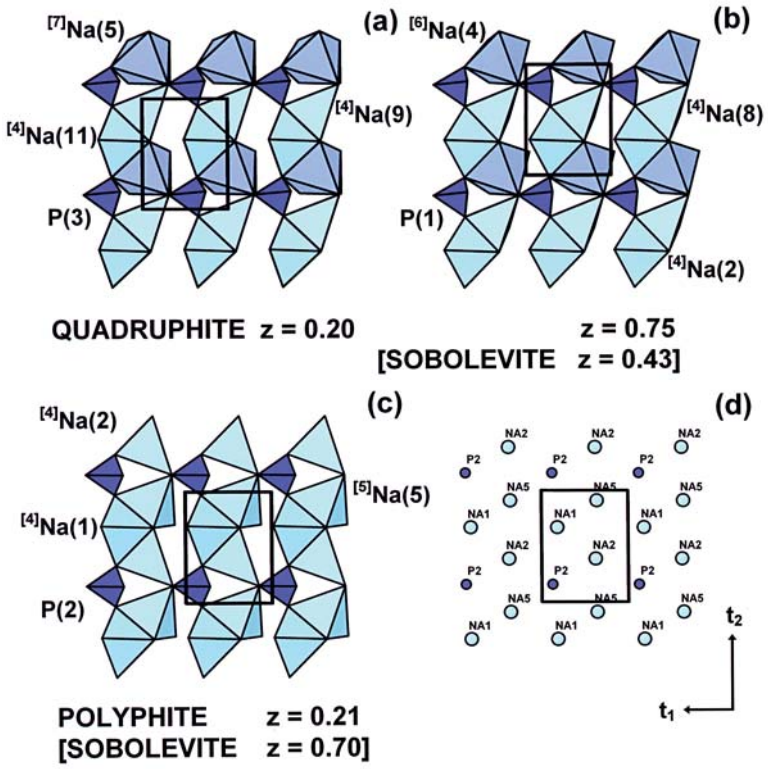

FIG. 28. A sheet of Na polyhedra and P tetrahedra in the **I** block in (a) quadruphite, z ≈ 0.20, (b) quadruphite, z ≈ 0.75 = sobolevite, z ≈ 0.43; (c) polyphite, z ≈ 0.21 = sobolevite, z ≈ 0.70. The close-packed layer of Na and P atoms in polyphite, z = 0.21 (d). In this diagram, the TS block is below the sheet of Na polyhedra and P tetrahedra. The [4]- and [5]-coordinated Na polyhedra are greenish blue, [6]-coordinated Na polyhedra are light navy blue, P tetrahedra are purple. Na and P atoms are greenish blue and purple circles in (d).

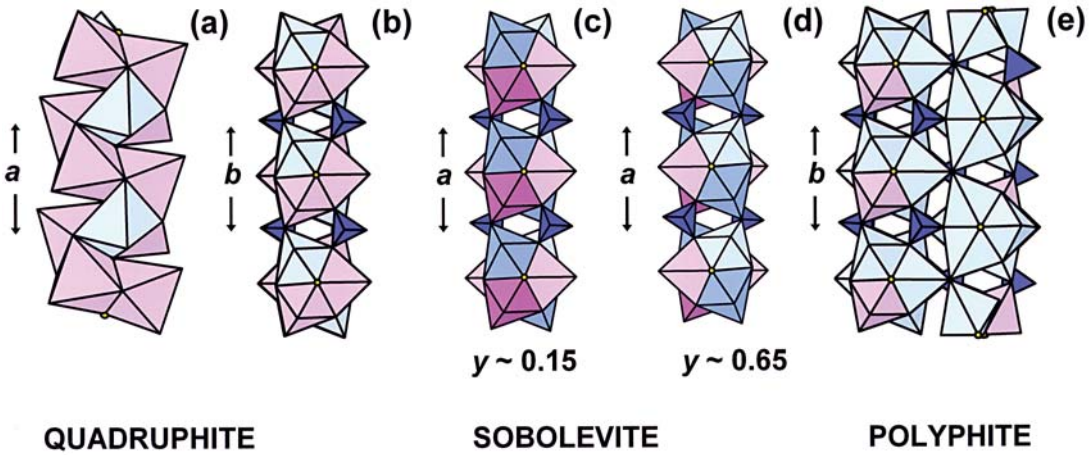

FIG. 29. Fragment of the **I** block: (a) the convoluted chain of trimeric clusters of octahedra in the crystal structure of quadruphite, (b) the linkage of chains of trimeric clusters and (PO_4) tetrahedra in quadruphite, and (c–e) the chains of trimeric clusters and (PO_4) tetrahedra in sobolevite, $y \approx 0.15$ and $y \approx 0.65$ (c) and (d), and polyphite (e). The Na, Na-dominant, Ca and Ca-dominant octahedra are navy blue, pale blue, bright pink and pale pink, respectively; P tetrahedra are purple, and F atoms are shown as small yellow circles.

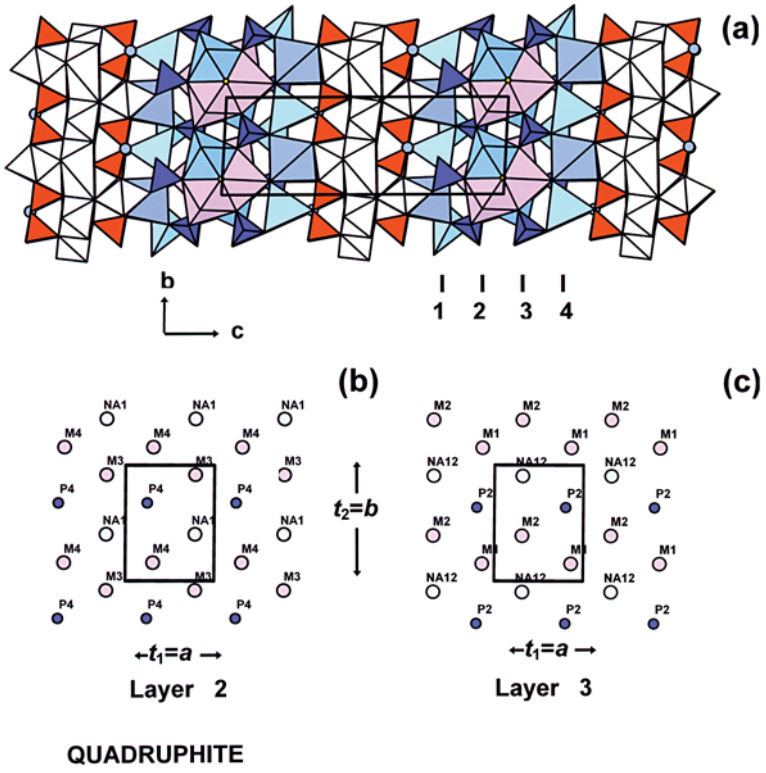

FIG. 30. The crystal structure of quadruphite: a general view of the crystal structure projected onto (100) (a), and close-packed layers 2 and 3 of M, Na and P atoms at z ≈ 0.92 (b), z ≈ 1.06 (c). Legend as in Figure 29. The [4]- and [5]-coordinated Na polyhedra are greenish blue; the Ca-dominant, Na-dominant, Na and P atoms are shown as light pink, light blue, navy blue and purple circles, respectively. The F atoms are small yellow circles. Vertical lines 1–4 show the position of close-packed layers of cations.

Zr^{4+}, Fe^{3+}, Mg^{2+} and Mn^{2+}. Each group is characterized by the same number of Ti-dominant sites per formula unit of $M^{O}_4\,M^{H}_2\,(Si_2O_7)_2$ (Tables 3, 6). In the majority of minerals of Group I, the content of Ti is equal to 1 *apfu*, and there is usually one $^{[6]}Ti^{O}$ site in the O sheet of the TS block. In Group II, Ti is equal to 2 *apfu*, and it is invariably dominant at the M^{H} site in the H sheet. In Group III, Ti is equal to 3 *apfu*, and it is dominant at the M^{H} site in the H sheet (2 *apfu*) and at one $^{[6]}M^{O}$ site in the O sheet (1 *apfu*). In Group IV, Ti is equal to 4 *apfu*, and it is dominant at the $^{[6]}M^{H}$ site in the H sheet (2 *apfu*) and at two M^{O} sites in the O sheet (2 *apfu*). Furthermore, the maximal possible content of Ti in the TS block is 4 *apfu* (see discussion above).

The Ti(Nb)–O distances do not vary greatly within the $^{[6]}M^{O}$ polyhedron, but show a wide range within the M^{H} polyhedron, *i.e.*, this polyhedron can be strongly distorted. Figure 31 shows the observed M^{H}–X distances as a function of bond valence incident at X from other cations. The Ti–X distances increase as the bond valence required to satisfy the valence-sum rule at the X anions decreases. The bond-valence curves for Ti^{4+}–O and Nb^{5+}–O are also shown in Figure 31a, where it can be seen that the data for both Ti^{4+}–O and Nb^{5+}–O distances in these structures follow the corresponding bond-valence curves, *i.e.*, they agree with the valence-sum rule for occupancy of the M^{H} site by Ti^{4+} and Nb^{5+}. It is particularly notable that the Ti^{4+}–O bond-valence varies from ~0.3 to 1.5 *vu*, an extremely wide range of bond valence, with Ti^{4+}–O distances varying from 2.30 to 1.68 Å. Figure 31a clearly shows three groups of Ti(Nb)–O distances for M^{H} polyhedra. The shortest distances are from the M^{H} cation to X^{O}_{M} (an anion common to the O and H sheets). Intermediate distances occur between the M^{H} cation and four $X^{H}_{Si–M}$ anions of an (Si_2O_7) group of the H sheet. The longest distances occur between the M^{H} cation and the X^{P}_{M} anion (Fig. 31a). Figure 31b shows the environment of the M^{H} cation, which can be [5]- or [6]-coordinated. Excluding the M^{H} cation, each X^{O}_{M} anion receives bond valence from three M^{O}

atoms of the O sheet, each X^{H}_{Si-M} anion receives bond valence from one Si atom, and the X^{P}_{M} anion (if M^{H} is [6]-coordinated) receives bond valence from the cations of the **I** block (if an **I** block is present). The shortest M^{H}–X^{O}_{M} distances occur in Group III, where Ti^{H} is [5]-coordinated. The sum of bond valences from three M^{O} cations is very low (formally, it does not exceed 0.68 *vu*); therefore, $^{[5]}$Ti must provide the remaining bond-valence required, resulting in a very short Ti^{H}–X^{O}_{M} distance. I consider this issue specifically for Group III (see Table 4). The longest M^{H}–X^{P}_{M} distances occur in the crystal structure of epistolite, where Nb^{5+} is the dominant cation at the M^{H} site and is bonded to an (H_2O) group. Figure 31a shows that the main variation of bond valence (and corresponding distances) is associated with the X^{O}_{M} anion. The distortion of the M^{H} polyhedron allows Ti^{H} to satisfy the bond-valence requirements of the coordinating anions. The wide range in Ti(Nb)–O bond lengths is one of the major factors that allows the chemical composition of the TS block to change drastically while retaining close packing of the cations and accommodating various intermediate species.

Orthoericssonite [Ba ($Mn_{1.5}Fe^{2+}_{0.5}$) Fe^{3+} (Si_2O_7) O (OH): Moore (1971), Matsubara (1980), Appendix B] is a good example to show that Ti is an important element of the TS block. Orthoericssonite has an HOH structure with Mn^{2+} and Fe^{2+} as cations of the O sheet (as in Group II), $^{[5]}M^{H} = Fe^{3+}$, there is no Ti in its HOH block, which has a topology described by linkage 1 (as in Groups I and III). The graph in Figure 31a shows that the distance from the M^{H} (= Fe^{3+}) cation to X^{O}_{M} (light blue square) in orthoericssonite is longer than distances Ti^{4+}–X^{O}_{M} in Group II (blue circles), and hence X^{O}_{M} receives a smaller incident bond-valence from Fe^{3+} than is necessary for linkage 2. However, distortions of polyhedra in orthoericssonite are different from those in Groups I and III (linkage 1). Therefore, the crystal structure of orthoericssonite exhibits linkage 1, which is unusual for the distortions of polyhedra in the TS block of Group II.

Close Packing of Cations in the **I** Block

In this paper, I have shown that in every structure, the **I** block consists of close-packed layers of cations, and the types of cations and number of layers can vary significantly. In the **I** block, there are two types of close-packed layers. The first type has four cations in the minimal cell, and this layer is similar to the cation layers of the TS block. Layers of the first type occur in vuonnemite, lomonosovite, quadruphite, sobolevite and polyphite, and contain three alkali cations and one P^{5+} (Table 5). The second type of layer has two cations in the minimal cell, commonly Ba^{2+}. The composition of the second type of layer varies in perraultite, (surkhobite?), bafertisite, hejtmanite, lamprophyllite, barytolamprophyllite, nabalamprophyllite, yoshimuraite, innelite and bussenite (Table 5). Close-packed layers of cations can be fully or partly occupied, as in bussenite. In fact, bussenite is the only mineral in which both types of layers occur: two layers of the first type contain four cation sites, which give 2 (= m) $\times$ [2 ($Na_{0.5}\square_{0.5}$) + $\square$ + C = NaC] = 2 NaC (Fig. 27c), and two layers of the second type contain two *Ba* sites each, as in Figure 26a.

From Chemical Composition to Structure Topology. I. Different Stereochemistry Versus Identical Topology, Groups I and III

The topology of the TS block in Groups I and III is identical (linkage 1), but the stereochemistry is different. The different sizes of the M^{H} polyhedron and the dimensions of the H sheet were discussed by Egorov-Tismenko & Sokolova (1987, 1990) and Ferraris (1997).

Previous authors did not address the origin of the differences in stereochemistry of Groups I and III. Christiansen *et al*. (1999) stated that *vuonnemite* (our Group III) *contains an HOH-layer identical with that of seidozerite* (our Group I). Christiansen *et al*. (2003a) revised the crystal chemistry of the rosenbuschite group (our Group I, excluding rinkite and grenmarite) and emphasized the effect of "the size of the M^{H} cation" on the geometry of the (Si_2O_7) group. They stated "(1) the size of the M^{H} polyhedron has a significant effect upon the size and deformation of the adjacent polyhedra and (Si_2O_7) groups, (2) (Si_2O_7) groups show three modes of bending, depending on the size of two M^{H} octahedra, (3) the degree of bending relates directly to a stretching of A^{P} polyhedra and also to the interatomic distance between the A^{P} cations and X^{O}_{A}" (the labeling of atoms is taken from my work). None of these observations *explain* the differences in stereochemistry of the TS block in Groups I and III.

In Group I, the M^{H} octahedron (M^{H} = Na, Ca, Mn^{2+}, Zr^{4+}) is larger than in Group III (M^{H} = Ti). In Group I, (Si_2O_7) groups are attached to large Na polyhedra in the O sheet, and in Group III, (Si_2O_7) groups are attached to small Ti octahedra in the O sheet. Apparently, the size of the M^{H} polyhedron does not *explain* why (Si_2O_7) groups are attached to different polyhedra in Groups I and III.

The stereochemistry of the O sheet

In some minerals of Groups I and III, the composition of the O sheet is identical, *e.g.*, in kochite (Group I) and nabalamprophyllite (= lamprophyllite, barytolamprophyllite, epistolite, vuonnemite) (Group III), 4 M^{O} = 3 Na + Ti; in hainite (Group I) and innelite (Group III), 4 M^{O} represent Na + (Na Ca) + Ti. Hence *the difference in stereochemistry involved in linkage 1 (which occurs in both Groups) cannot be due to the differences in stereochemistry of the O sheet*.

The stereochemistry of the P sites

In several minerals of Groups I and III, the composition of the *P* sites is identical, *e.g.*, in seidozerite and grenmarite (Group I) and epistolite and vuonnemite (Group III), 2 A^P = 2 Na. Therefore *the difference in stereochemistry involved in linkage 1 cannot be due to the differences in stereochemistry of the P sites*.

The stereochemistry of the H sheet

The periodicity of the H sheet has to match the periodicity of the O sheet in order to form the TS block. In Group I, the M^H cation is large [Ca ($^{[6,7]}$r = 1.00, 1.06 Å), Mn^{2+} ($^{[6]}$r = 0.83 Å), Zr^{4+} ($^{[6]}$r = 0.72 Å)], whereas in Group III, the M^H cation is small [Ti ($^{[5]}$r = 0.51 Å) or Nb^{5+} ($^{[6]}$r = 0.64 Å)]. In order to compensate for these differences in size of the M^H cation in each group, the *effective* size of the (Si_2O_7) group within the H sheet [which I define as the O–O separation of the peripheral anions of the (Si_2O_7) group: $(O–O)^H$] must vary inversely as the size of the M^H polyhedron (also defined as an O–O separation within the plane of the H sheet). Figure 32a shows that there is an inverse relation between the size of the M^H polyhedron and the size of the (Si_2O_7) group within the plane of the H sheet.

The stereochemistry of linkage 1

As I noted above, the periodicity of the H sheet has to match the periodicity of the O sheet in order to form the TS block. Where the H sheet links to the O sheet, the *effective* size of the (Si_2O_7) group within the O sheet [which I define as the O–O separation of the peripheral anions of the (Si_2O_7) group: $(O–O)^O$] increases in Group I and decreases in Group III [compared to $(O–O)^H$]. Figure 32b shows that there is a direct relation between the Si–O–Si angle and the difference in effective size of the (Si_2O_7) group in the H sheet and in the O sheet: $(O–O)^H – (O–O)^O$. I define $(O–O)^H – (O–O)^O$ as the difference in the effective size of the (Si_2O_7) group, $(O–O)^{H\rightarrow O}$. The mean values of the Si–O–Si angle in Groups I and III are 199.0 and 135.7°, respectively. In Groups I and III, the mean effective size of the (Si_2O_7) group changes from the H sheet to the O sheet, $\langle(O–O)^{H\rightarrow O}\rangle$ = –0.44 and 1.53 Å, respectively. Note that in Group I, the $(O–O)^H$ varies from 4.14 to 3.78 Å, and in Group III, the $(O–O)^H$ varies from 4.34 to 4.44 Å. How can such a small variation in $(O–O)^H$ coexist with a very large change in $(O–O)^O$?

Mechanism of linkage 1

Figure 33 illustrates how the geometry of the (Si_2O_7) group changes to promote linkage of the H and O sheets. First, note that the principal geometrical difference between the (Si_2O_7) groups in Groups I and III involves the Si–O–Si angle; the length of the Si–O bonds does not vary significantly ($\langle$Si–O$\rangle \approx$ 1.62 Å). In an (Si_2O_7) group with ∠Si–O–Si = 180°, $(O–O)^H = (O–O)^O$ equals 4.32 Å (Fig. 33a). Where the (Si_2O_7) group contracts in the H sheet, the Si–O–Si angle increases and becomes reflex, and $(O–O)^O$ increases (Group I in Fig. 33b). Where the (Si_2O_7) group expands in the H sheet, ∠Si–O–Si and $(O–O)^O$ both decrease (Group III in Fig. 33d). At ∠Si–O–Si = 141.6°, the $Si–X^O_{Si}$ bonds are perpendicular to the plane of the O sheet, and $(O–O)^H_{calc}$ is equal to 4.58 Å, and $(O–O)^O_{calc}$ is equal to 3.05 Å. These calculated values correlate fairly well with the observed values for Group III, 4.41 and 2.88 Å, respectively (Table 2). Thus, variation of the Si–O–Si angle allows the (Si_2O_7) group to change its effective size in both sheets and to promote linkage of H and O sheets to form the TS block.

Figure 34 gives examples of linkage 1 in Groups I and III. The Si–O–Si atoms form a reflex angle toward the O sheet in kochite (Group I) and an acute angle toward the O sheet in nabalamprophyllite (Group III) (Figs. 34a, b). Figures 34c and 34d show the linkage of the O and H sheets in kochite and nabalamprophyllite, with the exact values for the anion separations in the (Si_2O_7) group in both sheets. In kochite, the anion separation in the O sheet is 4.37 Å, and it matches two edges of the Na polyhedron (Fig. 34c). In nabalamprophyllite, the anion separation in the O sheet is 2.99 Å, and it matches the short edge of the Ti octahedron (Fig. 34d).

Therefore, the mechanism of linkage 1 can be described as four successive steps:

(1) In response to different sizes of the M^H polyhedra, the $(O–O)^H$ edge of the (Si_2O_7) group changes its length to maintain the same periodicity in the H sheet as in the O sheet.

(2) Change of the $(O–O)^H$ edge produces a much larger inverse change in length of the $(O–O)^O$ edge of the (Si_2O_7) group (Fig. 33).

(3) Where the resulting $(O–O)^O$ edge is long, the (Si_2O_7) group links to a large Na polyhedron in the O sheet.

(4) Where the $(O–O)^O$ edge is short, the (Si_2O_7) group links to a small Ti octahedron in the O sheet.

Thus it is the size of the M^H polyhedron and the $(O–O)^H$ distance that control the size of the Si–O–Si angle and, hence, the separation of the apical anions of the (Si_2O_7) group. In turn, the separation of the apical anions of the (Si_2O_7) group controls whether the group links to a small (Ti) polyhedron or a large (Na) polyhedron in the O sheet. Thus it is the size of the M^H polyhedron (and the articulation requirements of the H and O sheets) that dictate the stereochemistry of linkage 1 in Groups I and III.

Distortions of polyhedra in the O sheet

The O sheet in Groups I and III consists of two types of chains of octahedra extending along $\mathbf{t_2}$ (Fig. 35a): (1)

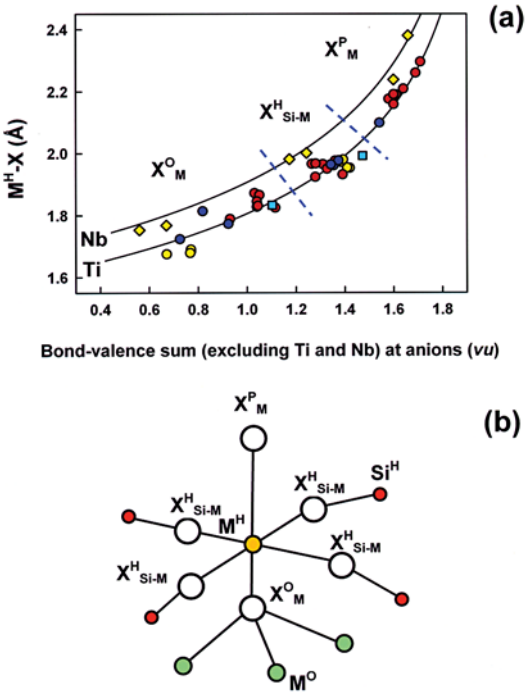

FIG. 31. The M^H–X distances (Å) *versus* bond-valence sums (excluding Ti and Nb) at X anions (*vu*), M^H = Ti, Nb (a). A schematic representation of the topology of the M^H site (b). Data for Group II (bussenite, hejtmanite-P and yoshimuraite), Group III (epistolite, vuonnemite, lamprophyllite-2*M*, lamprophyllite-2*O* and nabalamprophyllite) and Group IV (murmanite, lomonosovite, quadruphite, sobolevite and polyphite) are shown as navy blue, yellow and red circles (M^H = Ti) or diamonds (M^H = Nb). The data on orthoericssonite are shown as light blue squares. Dashed blue lines separate X^O_M, X^H_{Si-M} and X^P_M data. Solid black lines show ideal bond-valence curves for Ti^{4+} and Nb^{5+}. In diagram (b), M^H, M^O, Si^H and *X* sites are shown as medium yellow and green, small orange and large white circles.

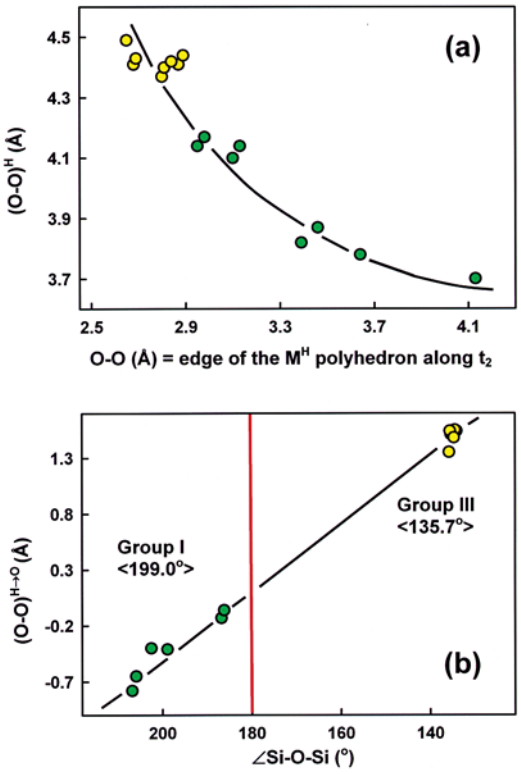

FIG. 32. Linkage 1: the effect of the size of the M^H polyhedron on the geometry of (Si_2O_7) group. (a) The O–O distance of the (Si_2O_7) group along $\mathbf{t_2}$ in the H sheet [= $(O–O)^H$] *versus* O–O edge of the M^H polyhedron, also oriented along $\mathbf{t_2}$. (b) The difference in the effective size of the (Si_2O_7) group [= $(O–O)^{H–O} = (O–O)^H – (O–O)^O$)] along $\mathbf{t_2}$ *versus* ∠Si–O–Si. Data for Groups I and III are shown as green and yellow circles; the vertical red line indicates ∠Si–O–Si = 180° in (b).

Na–Ti–Na–Ti, and (2) Na–Na–Na–Na (or other cations with valence from +1 to a mean valence of less than +2). As the radius of [6]Ti is less than that of [6]Na, the Na and Ti octahedra in chain (1) must be strongly elongate to match the periodicity of chain (2) in the $\mathbf{t_2}$ direction (this strain is visible in Fig. 35a). Therefore, in chain (1), the Ti and Na polyhedra are contracted and distances X^O_A–X^O_A (blue circles) and X^O_M–X^O_M (yellow circles) are shortened along $\mathbf{t_1}$ (both distances shown by dotted red lines in Fig. 35a). The X^O_A–X^O_A distance (blue circles, Ti octahedron) is shorter than the analogous X^O_M–X^O_M distance (yellow circles, Na octahedron). There are two possibilities to match the periodicity along $\mathbf{t_1}$: (a) the X^O_A–X^O_A and X^O_M–X^O_M distances in chain (2) have to be longer and shorter than in chain (1), or (b) ∠X^O_A–X^O_A–X^O_A and ∠X^O_M–X^O_M–X^O_M between chains (1) and (2) have to be larger and smaller, respectively. A scheme in Figure 35b shows that in epistolite, X^O_A–X^O_A = X^O_M–X^O_M = 3.1 Å, ∠X^O_A–X^O_A–X^O_A = 102° and ∠X^O_M–X^O_M–X^O_M = 91°. Thus the difference in angles X^O_A–X^O_A–X^O_A and X^O_M–X^O_M–X^O_M or different tilting of polyhedra of different size allows the periodicity along $\mathbf{t_1}$ to be retained.

The sum of the incident bond-valence at X^O_M (yellow, Ti^H + 3 Na) is greater than at X^O_A (blue, Ti^O + 2 Na), and in chain (2), the central atoms in the M^O polyhedra are displaced toward the X^O_A sites (blue) to satisfy their bond-valence requirements. As a result, the M^O cation has longer bonds to X^O_M anions (yellow) and shorter bonds to X^O_A anions (blue). In accord with bond-valence requirements, monovalent anions are

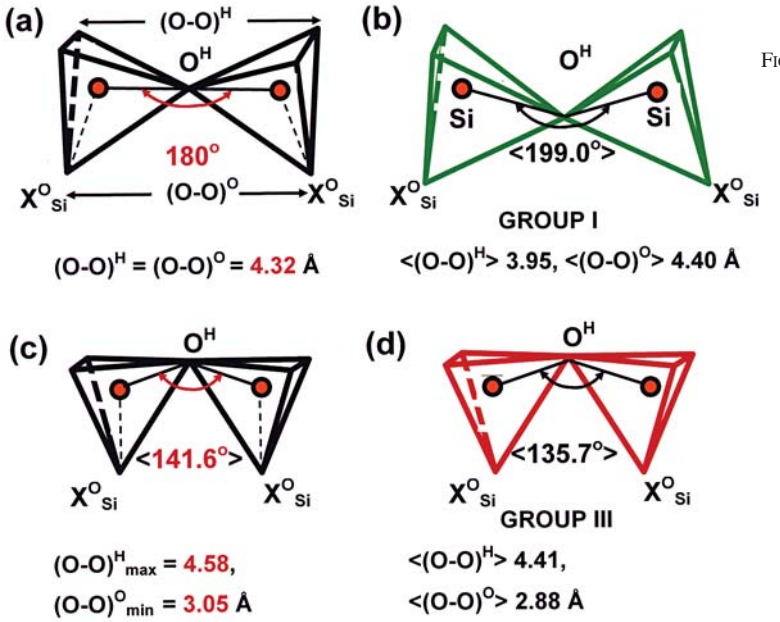

FIG. 33. Variation of $(X^{O}_{Si}–X^{O}_{si})$ [= $(O–O)^{O}$] as a function of $(O–O)^{H}$: (a) <Si–O> 1.62 Å, ∠Si–O–Si = 180° and $(O–O)^{H} = (O–O)^{O}$; (b) Group I, where $(O–O)^{H} < (O–O)^{O}$ and ∠Si–O–Si > 180°; (c) <Si–O> 1.62 Å, Si–O–Si = 141.06°, and Si–X^{O}_{Si} bonds are perpendicular to the plane of the O sheet; (d) Group III, where $(O–O)^{H} > (O–O)^{O}$ and Si–O–Si < 180° calculated for $(Si–O–Si)_{min}$ = 141.06°. All calculated and observed values are shown in red and black. The Si atoms are shown as orange circles; the Si tetrahedra are shown by black, green and red thick lines (solid and dashed). The bonds from Si atoms to a bridging O atom and to X^{O}_{Si} atoms are shown as solid and dashed thin black lines.

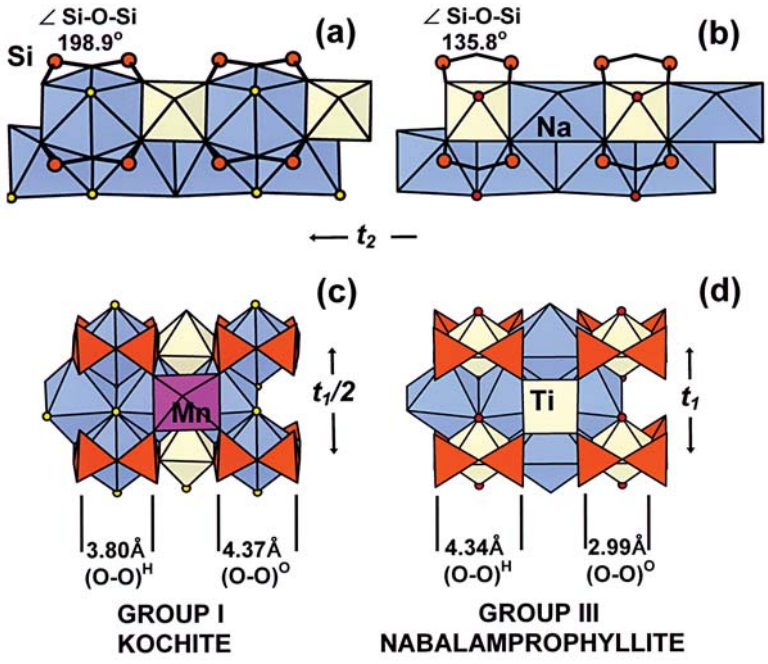

FIG. 34. Geometry and stereochemistry of the TS block in Groups I (kochite) and III (nabalamprophyllite). Geometry of an (Si_2O_7) group in kochite (a) and nabalamprophyllite (b). Fragment of a TS block in kochite (c) and nabalamprophyllite (d). Legend as in Figures 9 and 14. The Si atoms are shown as orange circles in (a) and (b).

dominant at the X^{O}_{A} sites (blue), and divalent anions are dominant at the X^{O}_{M} sites (yellow) in most structures of Groups I and III.

From Chemical Composition to Structure Topology. II. Why Linkage 2 Occurs Only with $M^{O} = M^{2+}$

In Group II, all cations of the O sheet are divalent (mainly Fe^{2+} and Mn^{2+}), and the size of these cations is similar: Fe^{2+} ($^{[6]}r = 0.78$ Å), Mn^{2+} ($^{[6]}r = 0.83$ Å), and hence all polyhedra of the O sheet are very similar in size. Figure 35c shows that in a Group-II structure, there are two crystallographically distinct M^{O} sites, $M^{O}(1)$ and $M^{O}(2)$. The $M^{O}(1)$ polyhedron shares anions with four Si tetrahedra and one M^{H} polyhedron. The $M^{O}(2)$ polyhedron shares anions with two Si tetrahedra and two M^{H} polyhedra. Two chains of octahedra extend along $\mathbf{t_2}$ and consist of (1) $M^{O}(1)$ and (2) $M^{O}(2)$ octahedra (Fig. 35c). I showed above that in Group III, $<(O–O)^{O}>$ equals 2.88 Å (M^{H} = Ti). In Group II, M^{H} consists of Ti, and $<(O–O)^{O}>$ should be similar to that in Group III. As the $Mn^{2+}(Fe^{2+})^{O}$ octahedron is larger than the Ti^{O} octahedron, both the (Si_2O_7) group and the M^{O} octahedron adjust their geometry to fit, and $<(O–O)^{O}>$ is equal to 3.42 Å.

Where an (Si_2O_7) group links to the edge of an $M^{O}(1)$ octahedron, the latter edge contracts. Therefore, where an (Si_2O_7) group links to one side of the $M^{O}(1)$ octahedron, this side is shorter compared to the other side, which retains its ideal size in chain (1). For example, in yoshimuraite, the size of the edge of the $M^{O}(1)$ octahedron along $\mathbf{t_2}$ is either 3.54 or 3.46 Å, and the latter matches an (Si_2O_7) group. In each $M^{O}(1)$ octahedron, there are four long bonds to X^{O}_{Si} and two shorter bonds to the X^{O}_{A} and X^{O}_{M} anions. The shorter X^{O}_{A}–$M^{O}(1)$–X^{O}_{M} distance is subparallel to $\mathbf{t_1}$, and four long bonds are in a plane perpendicular to $\mathbf{t_1}$. Therefore, the $M^{O}(1)$ octahedron is shortened along $\mathbf{t_1}$ and elongate along $\mathbf{t_2}$. The $M^{O}(1)$ and $M^{O}(2)$ octahedra are of the same size, and they must be distorted in the same way to form the O sheet. Although $M^{O}(2)$ octahedra do not share their edges with (Si_2O_7) groups, the $M^{O}(2)$ octahedron has to contract along $\mathbf{t_1}$ and become elongate along $\mathbf{t_2}$, as does the $M^{O}(1)$ octahedron. Note that the $M^{O}(1)$ and $M^{O}(2)$ octahedra each form a chain along $\mathbf{t_2}$. Inspection of the structures of Group II shows that $M^{O}(2)$–X^{O}_{M} bonds are the longest in the $M^{O}(2)$ octahedron, and the $M^{O}(2)$ octahedra are elongate along X^{O}_{M}–$M^{O}(2)$–X^{O}_{M} (yellow circles in Fig. 35c). Thus with linkage 2, the arrangement of the X^{O}_{M} sites allows the two types of M^{O} octahedra to be similarly distorted, and chain (2) has the same periodicity as chain (1).

If linkage 1 were to occur in Group-II minerals, then all the octahedra of chain (1) would be elongate along $\mathbf{t_2}$ and shortened along $\mathbf{t_1}$ (see Fig. 35a), and in chain (2), $M^{O}(2)$ octahedra are not elongate along $\mathbf{t_2}$ (see Fig. 35a). Thus the distortion of octahedra in chains (1) and (2) is different, and mismatch of two types of octahedra makes linkage of these two chains more difficult.

If linkage 3 were to occur in Group-II minerals, then half the octahedra in each chain would become elongate along $\mathbf{t_2}$ and half would become elongate along $\mathbf{t_1}$. The mismatch in size of M^{O} octahedra makes linkage of chains (1) and (2) into the O sheet more difficult.

From Chemical Composition to Structure Topology. III. Optimal Linkage in Group IV

In Group IV, Ti amounts to 4 *apfu*. In the H sheet, two M^{H} sites are occupied by Ti, and in the O sheet, two M^{O} sites are occupied by Ti; two M^{O} sites are occupied by Na, and Ti octahedra form brookite-like chains along $\mathbf{t_1}$. What linkages between the O and H sheets are possible with an O sheet of this stereochemistry?

(1) Consider linkage 2. Where linkage 2 occurs, (Si_2O_7) groups link to Ti and Na octahedra, the geometry of the (Si_2O_7) groups is different, and the two H sheets are different, whereas in all structures containing the TS block (except for the model of bornemanite), the two H sheets of one TS block are geometrically identical. Linkage 2 is not in accord with this observation, and hence it is unlikely that linkage 2 will occur in Group IV.

(2) Consider linkage 1 as it occurs in Group I [where (Si_2O_7) links to a Na polyhedron of the O sheet]. In Groups II–IV, to compensate for the small size of $^{[6]}M^{H}$ occupied by Ti, O–O distances in the (Si_2O_7) groups are elongate in the H sheet and contracted in the O sheet (Table 2). Because of the shortening of the O–O distance of the (Si_2O_7) group in the O sheet, (Si_2O_7) groups cannot link to a large Na polyhedron in Group IV. Thus one can exclude linkage 1 as it occurs in Group I. Two possibilities are left: (3) linkage 3, and (4) linkage 1 as it occurs in Group III.

(3) Consider linkage 3. Figure 35d shows a fragment of the structure of quadruphite, in which (Si_2O_7) groups link to two adjacent Ti octahedra in a brookite-like chain. Each Ti^{O} octahedron shares two anions (orange circles labeled 1, 2) with another Ti^{O} octahedron, one Si tetrahedron and one Na^{O} octahedron, one anion (orange circle labeled 3) with a Si tetrahedron and two Na^{O} octahedra, one anion (yellow circle labeled 4) with a Ti^{H} octahedron and two Na^{O} octahedra, and two anions (blue circles labeled 5, 6) with another Ti^{O} octahedron and two Na polyhedra, Na^{O} and Na^{P}. Each Ti^{O} octahedron has three long bonds to X^{O}_{Si} anions and three shorter bonds to two X^{O}_{A} and one X^{O}_{M} anions. In a brookite-like chain, Ti atoms are shifted away from anions with high bond-valence sums toward anions with low bond-valence sums (the red arrows in Fig. 35d show these directions), and the Ti octahedra are elongate along $\mathbf{t_1}$. To compensate for this elongation and to retain close packing of cations in the O sheet, Na^{O} octahedra are elongate along the X^{O}_{Si}–Na–X^{O}_{M} direc-

tion (solid red lines in Fig. 35d), which is perpendicular to the direction of shift of Ti atoms in the brookite chain. Hence cations of the O sheet occur at reasonably similar distances and retain their close packing. These specific distortions of the polyhedra of the O sheet allow satisfaction of bond-valence requirements on both cations and anions (most commonly O atoms) of the O sheet.

(4) Consider linkage 1 (as it occurs in Group III) in Group IV. Is the linkage of two (Si_2O_7) groups to one Ti octahedron possible, as illustrated in Figure 35a? Where two (Si_2O_7) groups link to one Ti octahedron in Group IV (Fig. 35e), the distortions of the M^O polyhedra are as in Group III: Ti and Na octahedra are shortened along $\mathbf{t_1}$ in chain (1), and cations in the chain (2) are displaced along $\mathbf{t_2}$. Compare the bond-valence sum incident at the $X^O{}_A$ anion (blue circle), as it occurs in Group IV with linkage 3 (Fig. 35d) and linkage 1 (Fig. 35e). In both cases, the $X^O{}_A$ anion receives a formal bond-valence of 1.68 *vu* from 2 Ti^O + Na^O + Na^P. In Group IV with linkage 1, the mean bond-valence sum is 1.77 *vu*, and slightly less than necessary for the O atom. This low sum occurs in spite of cooperative relaxation of two Ti atoms in a chain where shortening of Ti–$X^O{}_A$ bonds promotes a satisfaction of bond-valence requirements at the $X^O{}_A$ anion. With linkage 1, contraction of Ti(1)–$X^O{}_A$ bonds lengthens the Ti(2)–$X^O{}_A$ bonds (Fig. 35e). Therefore the bond-valence sum incident at the $X^O{}_A$ anion becomes less than with linkage 3 and does not satisfy the bond-valence requirements of this O atom.

The above requirements (1)–(4) show that the TS block with Ti = 4 *apfu* can have only one type of linkage, linkage 3.

From Chemical Composition to Structure Topology. IV. Important Features of Linkages 1–3

From the three previous sections, I make the following statements.

(1) The type of linkage in a structure is independent of the topology or chemical composition of the **I** block.

(2) *Within one TS block, H sheets are invariably identical* [and thus the geometry of the (Si_2O_7) groups also is identical]. This is a very important observation. If linkages 2 and 3 were to occur in TS blocks with an O sheet of the form 3 M^O + Ti (Ti = 1 and 3 *apfu*), the (Si_2O_7) groups of the two H sheets would be attached to chemically different polyhedra of the O sheet (in general, Na and Ti polyhedra). This type of linkage is not in accord with the above observation, and linkages 2 and 3 do not occur in Groups I and III.

(3) Linkage 2 occurs with the O sheet 4 M^O = 4 M^{2+}, where Ti^O = 0 and Ti^H = 2 *apfu*, *i.e.*, Group II.

(4) Linkage 1 cannot occur in a TS block with an O sheet of the form 2 Na + 2 Ti ($Ti^{O,H}$ = 4 *apfu*), *i.e.*, Group IV.

(5) Linkage 3 cannot occur in a TS block with an O sheet of the form 4 M^O = 4 M^{2+} (Ti^O = 0 and Ti^H = 2 *apfu*), *i.e.*, Group II.

Why Are There Only Three Types of Linkages of O and H Sheets?

After discussing the occurrence of different linkages as a function of different chemical compositions, one question remains: why are there only three types of linkage of O and H sheets? The explanation can be found in the close-packed nature of the layers of cations in the TS block. The H–O–H sheets form a three-layered close packing of cations with an *ABC* repeat (Fig. 36). If one views the TS block perpendicular to the close-packed layers (Fig. 36a), one can see the minimal cell [shown in green], four (Si_2O_7) groups in the upper H sheet, the M^H cation at the center of the minimal cell, and two A^P sites (Fig. 36b). Within the minimal cell, the M^H cation has five nearest-neighbor cations in the H sheet that underlies the O sheet. Consider the possible positions for the M^H site in the next H sheet. They are labeled 1, 2 and 3 in Figure 36b.

(1) If the M^H cation were to occupy site 1 in the second H sheet, then the two M^H cations in the *A* and *C* layers would be related by the translation ($^2/_3$ $^1/_3$ 1)*t*, where *t* is a minimal cation–cation distance in the *ABC* close packing. If the same translation were to be applied to the A^P cations and (Si_2O_7) groups, then two H sheets would also be related by this translation. The two H sheets related by the translation ($^2/_3$ $^1/_3$ 1)*t* correspond to the two H sheets in the TS block described by linkage 1 (Fig. 36c).

(2) If the M^H cation were to occupy the site labeled 2 in the second H sheet, then the two M^H cations in the *A* and *C* layers would be related by the translation ($^2/_3$ $^1/_3$ 1)*t*. Following the argument for case (1), the two H sheets related by the translation ($^2/_3$ $^2/_3$ 1)*t* correspond to the two H sheets in the TS block described by linkage 2 (Fig. 36d).

(3) If the M^H cation were to occupy the site labeled 3 in the second H sheet, then the two M^H cations in the *A* and *C* layers would be related by the translation ($^1/_3$ $^1/_3$ 1)*t*. Following the argument for case (1), the two H sheets related by the translation ($^1/_3$ $^1/_3$ 1)*t* correspond to the two H sheets in the TS block described by linkage 3 (Fig. 36e).

Thus there are only three possibilities for two H sheets to link to the central O sheet and retain *ABC* close-packing of the H, O and H layers.

Close Packing of Cations

In this paper, I have shown that (1) the TS block contains three close-packed layers of cations, and (2) the **I** block consists of close-packed layers of cations. The three types of linkage in the TS block correspond to the three possible translations between cations within

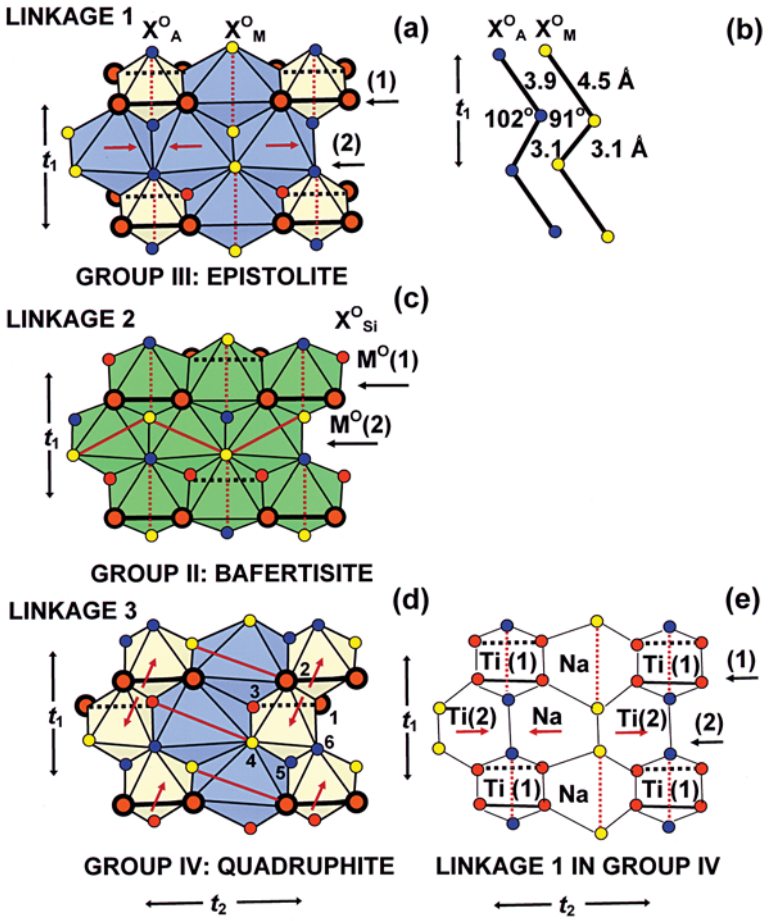

FIG. 35. Distortion of M^O octahedra in TS blocks: (a) linkage 1 in Group III, (b) detail of linkage 1 in Group III showing arrangement of anions along $\mathbf{t_1}$, (c) linkage 2 in Group II, (d) linkage 3 in Group IV, (e) linkage 1 in Group IV. Anions of the O sheet are shown as orange (X^O_{Si}), yellow (X^O_M) and navy blue (X^O_A) circles. The Fe^{2+}, Na and Ti polyhedra are green, navy blue and yellow; the Si atoms are shown as large orange circles. Directions of shortening and elongation of M^O octahedra are shown by dashed and solid red lines. Within an octahedron, the possible direction of displacement of a cation toward anions with low bond-valence sums is shown by red arrows. In (a), (c) and (e), different chains of octahedra in the O sheet are shown with horizontal black arrows. In (d), six anions of a Ti^O octahedron are labeled 1–6.

ABC close-packing. Sokolova (1997) emphasized that the occurrence of two types of blocks in one crystal structure requires similar surfaces on each block so that they can link together, and showed that there is a close relation between the topology of the surfaces of "nacaphite" and "seidozerite" blocks, *i.e.*, of the trimeric structure and the TS block. The close packing of cations in every block allows these blocks to occur in the same structure where the anion separations on the surfaces of both blocks match each other. Hence the close-packed arrangement of cations is a key feature of the minerals with the TS block.

SUMMARY

I will divide the summary into two sections: (1) previous observations that have been made on the crystal chemistry of minerals with the TS block, and (2) my new observations and new findings, first about this group of minerals in general, and second, about

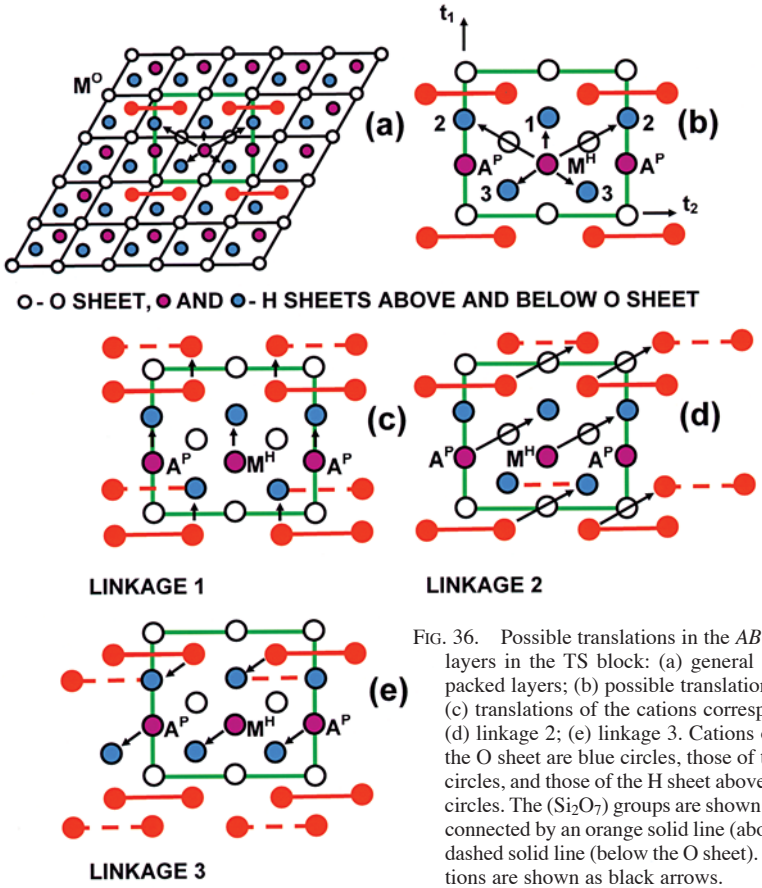

FIG. 36. Possible translations in the *ABC* sequence of cation layers in the TS block: (a) general view of three close-packed layers; (b) possible translations for the M^H cation; (c) translations of the cations corresponding to linkage 1; (d) linkage 2; (e) linkage 3. Cations of the H sheet below the O sheet are blue circles, those of the O sheet are white circles, and those of the H sheet above O sheet are magenta circles. The (Si_2O_7) groups are shown as two orange circles connected by an orange solid line (above the O sheet) and a dashed solid line (below the O sheet). Directions of translations are shown as black arrows.

specific minerals for which the current data are significantly in error.

Previous important observations

(1) The TS (*titanium silicate*) block consists of a central trioctahedral sheet between two sheets of cation polyhedra and (Si_2O_7) groups (Pyatenko *et al*. 1976). The TS block also can be described as an HOH block (Ferraris *et al*. 1997, Ferraris 1997).

(2) The linkage of O and H sheets results in two type of interstice that can host (in several structures) the *peripheral* A^P and B^P sites. These sites occur on the periphery of the TS block, they can be occupied or vacant (Pyatenko *et al*. 1976), and the constituent cations have weak bonds with anions of the O sheet.

(3) The TS block is characterized by a planar cell based on minimal lengths of translational vectors, $t_1 \approx 5.5$ and $t_2 \approx 7$ Å, and $\mathbf{t_1} \wedge \mathbf{t_2} \approx 90°$ (Egorov-Tismenko & Sokolova 1987, 1990).

(4) All structures incorporating the TS block can be considered as consisting of two types of block: the TS block itself and an intermediate (**I**) block that comprises all atoms occurring in the intermediate space between two TS blocks. These structures retain the minimal translations, $t_1 \approx 5.5$ and $t_2 \approx 7$ Å of the TS block, whereas the third translation varies depending on size of the **I** block (Egorov-Tismenko & Sokolova 1987, 1990).

The major focus of later publications on the crystal chemistry of minerals with the TS block has been the detailed description of these complicated structures and their presentation in different ways, *e.g*., somatic series (Sokolova 1997, 1998, Ferraris *et al*. 2004), homologous + somatic series (Egorov-Tismenko 1998) or polytypes of various sorts (Christiansen *et al*. 1999). The somatic approach (Ferraris *et al*. 2001b) resulted in a general mineral formula, which is detailed for the TS block, but it does not give any information about the **I** block. A detailed chemical formula for the TS block was given by Christiansen *et al*. (2003a).

New findings: general

(1) There are three topologically distinct TS blocks. There are three types of linkage of two H sheets and the central O sheet. *Type 1* occurs where two H sheets connect to the O sheet so that two (Si_2O_7) groups on opposite sides of the O sheet link to *trans* edges of the same octahedron of the O sheet. *Type 2* occurs where two (Si_2O_7) groups link to two octahedra of the O sheet adjacent along $\mathbf{t_2}$. *Type 3* occurs where two (Si_2O_7) groups link to two octahedra adjacent approximately along $\mathbf{t_1}$. This finding does not agree with the conclusion of Ferraris *et al*. (2001b) that there are only two distinct TS blocks, one seidozerite-like and the other bafertisite-like.

(2) Cations in each sheet of the TS block are arranged in a close-packed layer, where each cation is surrounded by six other cations. The three layers of the TS block constitute a three-layered or cubic close-packing of cations with an *ABC* sequence. Cation–cation distances within a layer vary from 2.9 to 4.2 Å, depending on the types of cations.

(3) The three possible linkages of H sheets and O sheets result from the close-packing of cations with the HOH = *ABC* repeat: they correspond to three possible translations between *A* and *C*, $(^2/_3\ ^1/_3\ 1)t$, $(^2/_3\ ^2/_3\ 1)t$ and $(^1/_3\ ^1/_3\ 1)t$, where *t* is the minimal cation–cation distance in the *ABC* close packing.

(4) The different types of linkages in minerals with the TS block are a result of the bond-valence requirements of anions shared by the O and H sheets, excluding the anions of the (Si_2O_7) group. The type of linkage is not related to the topology or chemical composition of the **I** block.

(5) The general formula of the TS block is $A^P_2\ B^P_2\ M^H_2\ M^O_4\ (Si_2O_7)_2\ X_{4+n}$, where the central part of the TS block is $M^H_2\ M^O_4\ (Si_2O_7)_2\ X_4$, $X_{4+n} = X^O_4 + X^P_{M2} + X^P_{A2}$, and n is the number of X^P anions; n = 0 where the M^H site is [5]-coordinated and the A^P polyhedron links to the next TS block; n = 2 where the M^H site is [6]-coordinated and the A^P polyhedron links to the next TS block; n = 4 where the M^H site is [6]-coordinated and the A^P polyhedron does not link to the next TS block and has one X^P_A ligand.

(6) Two H sheets of one TS block are invariably identical.

(7) There is only one type of TS block in a structure.

(8) The two H sheets of one TS block are attached to the O sheet in the same way.

(9) In a structure, TS blocks link to each other only in one way.

(10) There are four groups of structures, each characterized by the topology and stereochemistry of the TS block. Each group of structures has a different linkage, content and stereochemistry of Ti (= Ti + Nb).

Group I Ti = 1 *apfu*; Ti occurs in the O sheet; linkage 1;

(Si_2O_7) groups link to a Na polyhedron of the O sheet;

1 M^O = Ti; 3 M^O = mainly Na, Ca and rarely Mn^{2+}; $^{[6],[7]}M^H = Zr^{4+}$, Ca + REE, Ca, Mn^{2+};

A^P = Na, Ca, Ca + REE. The monovalent anion at the X^O_A and X^O_M sites is invariably F^-, as there is insufficient space to accommodate H and its corresponding hydrogen bond.

Group II Ti = 2 *apfu*; Ti occurs in the H sheet; linkage 2;

(Si_2O_7) groups link to two M^{2+} octahedra of the O sheet adjacent along $\mathbf{t_2}$;

4 $M^O = M^{2+} = Fe^{2+}$, Mn^{2+} and (Fe^{2+}, Mn^{2+}); $^{[5],[6]}M^H$ = Ti; A^P, B^P = Ba, Na.

Group III Ti = 3 *apfu*; Ti occurs in the O and H sheets; linkage 1;

(Si_2O_7) groups link to the Ti octahedron of the O sheet;

1 M^O = Ti; 3 M^O = mainly Na, subordinate Ca, Mn^{2+} and Fe^{2+}; A^P = Ba, Na, (Sr Na), (Ba K); B^P = Ba.

Group IV Ti = 4 *apfu*; Ti occurs in the O and H sheets; linkage 3;

(Si_2O_7) groups link to two Ti octahedra of the O sheet adjacent along $\mathbf{t_1}$; 2 M^O = Ti; 2 M^O = Na; $^{[6]}M^H$ = Ti; A^P = Na.

(11) The maximum possible content of Ti in the TS block is 4 *apfu*.

(12) The topology and stereochemistry of the TS block are strongly related to the stereochemistry of Ti. The stability of the TS block is due to an extremely wide range in Ti(Nb)–O bond lengths, 1.68–2.3 Å, which allows the composition of the TS block to vary drastically while retaining close-packing of the cations.

(13) The TS block propagates close-packing of cations into the **I** block.

(14) Only one type of the **I** block can occur in a crystal structure.

(15) There are four types of crystal structure based on the self-linkage of TS blocks.

[1] TS blocks link directly where they share common edges of M^H and A^P polyhedra and common vertices of M^H, A^P and Si polyhedra of H sheets belonging to two TS blocks. This type of self-linkage of TS blocks occurs in the crystal structures of Group I.

[2] TS blocks link through common vertices of Ti octahedra, and the **I** block has one layer of cations (m = 1).

[3] TS blocks do not link directly, additional cations do not occur in the **I** space (m = 0), and TS blocks are connected through hydrogen bonds of (H_2O) groups at the X^P sites.

TABLE 7. CORRECTED FORMULAE OF FOUR MINERALS OF GROUP I

	Christiansen *et al.* (2003a)	This work
götzenite	$Ca_2\ (Ca,Na)_2\ Ca_2\ Na\ Ti\ (Si_2O_7)_2\ F_2\ O_2$	$Na\ Ca_6\ Ti\ (Si_2O_7)_2\ O\ F_3$
hainite	$(Ca,Zr,Y)_2\ (Na,Ca)_2\ Ca_2\ Na\ Ti\ (Si_2O_7)_2\ F_2\ F_2$	$Na_2\ Ca_4\ (Y,REE)\ Ti\ (Si_2O_7)_2\ O\ F_3$
kochite	$Zr_2\ (Mn,Zr)_2\ (Na,Ca)_4\ Ca_4\ Na_2\ Ti_2\ (Si_2O_7)_4\ F_4\ O_4$	$Na_3\ Ca_2\ Mn\ Zr\ Ti\ (Si_2O_7)_2\ O\ F_3$
rosenbuschite	$Zr_2\ Ca_2\ (Na,Ca)_4\ Ca_4Na_2\ Zr\ Ti\ (Si_2O_7)_4\ F_4\ O_4$	$Na_6\ Ca_6\ Zr_3\ Ti\ (Si_2O_7)_4\ O_2\ F_6$

[4] TS blocks do not link directly, and there are additional layers of cations, the **I** block, between adjacent TS blocks (m = 1–6).

(16) Each type of structure [1]–[4] can be characterized by a general formula:

[1] $A^P_2\ M^H_2\ M^O_4\ (Si_2O_7)_2\ X^O_4$;

[2] $A^P\ B^P\ M^H_2\ M^O_4\ (Si_2O_7)_2\ X^O_4\ X^P_M$;

[3] $A^P_2\ M^H_2\ M^O_4\ (Si_2O_7)_2\ X^O_4\ X^P_{M2}\ X^P_{A2}$;

[4] $A^P_2\ {}^{[5]}M^H_2\ M^O_4\ (Si_2O_7)_2\ X^O_4$
and $A^P_2\ {}^{[6]}M^H_2\ M^O_4\ (Si_2O_7)_2\ X^O_4\ X^P_{M2}$, m = 1;

$A^P_2\ B^P_2\ {}^{[5]}M^H_2\ M^O_4\ (Si_2O_7)_2\ (TO_4)_2\ X^O_4$, m = 3;

$A^P_2\ B^P_2\ A^I_{2m}\ M^H_2\ M^O_4\ (Si_2O_7)_2$
$(CO_3)_m\ X^O_4\ X^P_2\ F_m$, m = 4;

$A^I_{3m}\ A^T_{3t}\ A^P_2\ M^H_2\ M^O_4\ (Si_2O_7)_2$
$(PO_4)_{m+t}\ X^O_4\ F_t$, m = 2,4,6,

where m and t refer to the number of cation layers in the **I** block.

New findings: specific minerals

(1) For four minerals of Group I, formulae have been corrected for better correlation with results of chemical analyses, especially with respect to the content of F (Table 7).

(2) Surkhobite should have an **I** block of the composition Na Ba (as in perraultite), not Ca Ba as commonly written. The chemical composition of the mineral has to be re-investigated. The formula of surkhobite must be changed from $\{[Ba_{1.65}K_{0.35}]\ [Ca_{1.2}Na_{0.8}]\}\ \{[Fe_4]\ [Mn_{3.7}Na_{0.3}]\}\ \{[Ti_{3.2}\ (Zr,Nb)_{0.8}\ O_4\ F\ (OH,O)]\ [Si_2O_7]_4\}\ \{[F_3OH]\}$ (Rozenberg *et al*. 2003) to $Na\ Ba\ Ti_2\ Fe^{2+}_4\ (Si_2O_7)_2\ O_2\ (OH)\ F_2$.

(3) The end-member formula of lamprophyllite is $(Sr\ Na)\ Ti_2\ Na_3\ Ti\ (Si_2O_7)_2\ O_2\ (OH)_2$, and the crystal chemistry of Ba-rich lamprophyllite and barytolamprophyllite must be revised.

(4) The crystal structure and chemical composition of innelite must be re-investigated. Innelite belongs to Group III, but its chemical composition, based on structure refinement, does not match Group III. Moreover, the structural formula, $Na_2\ Ba_4\ Ca\ Ti_3\ O_4(Si_2O_7)_2\ (SO_4)_2$ (Chernov *et al*. 1971), contradicts the mineral formula $(Ba,K,Mn)_4\ (Na,Mg,Ca)_3\ Ti_3\ (Si_2O_7)_2\ (SO_4)_2\ O_3\ (OH,F)$ (Mandarino & Back 2004).

(5) The structure predicted for bornemanite is extremely improbable. It contradicts several findings characteristic of minerals with the TS block. In the predicted structure, (a) the TS block has two chemically different H sheets, (b) these H sheets are attached to the O sheet in different ways, (c) there are two types of linkage between TS blocks: they link directly (m = 0) or they link through the **I** block (m = 2). In bornemanite, Ti equals 3 *apfu*. Therefore, bornemanite belongs to Group III, and its TS block must exhibit linkage 1 and the stereochemistry of Group III: Ti occurs in H and O sheets, and two (Si_2O_7) groups link to *trans* edges of a Ti octahedron in the O sheet. The model of the crystal structure of bornemanite must be reconsidered.

(6) Although delindeite is not considered in this paper because of major vacancies in the O sheet, its crystal structure seems incorrect. It is closely related to the minerals with the TS block and should belong to Group III (to which it is identical in chemical composition), and yet the TS block in delindeite exhibits linkage 1 with stereochemistry of Group I. The present structure exhibits profound disorder at cation and anion sites and does not provide any explanation why stereochemistry of Group I occurs in the structure designed to have the stereochemistry of Group III. Thus the structure of delindeite does not obey the principles developed in the present work, and needs to be re-investigated.

My future work will include examination of several minerals that show inconsistencies with the general findings given here: surkhobite, innelite, bornemanite and delindeite.

ACKNOWLEDGEMENTS

I thank Dr. Frank C. Hawthorne for continued interest in my work. I am very grateful to referees Joel Grice and Fernando Cámara and Editor Robert F. Martin for their very useful comments on this manuscript.

This work was completed at the CNR – Instituto di Geoscienze e Georisorse, Unità di Pavia, Italy, in the fall of 2005.

REFERENCES

ANTHONY, J.W., BIDEAUX, R.A., BLADH, K.W. & NICHOLS, M.C. (1995): *Handbook of Mineralogy*. II. *Silica, Silicates*. Mineral Data Publishing, Tucson, Arizona.

APPLEMAN, D.E., EVANS, H.T., JR., NORD, G.L., DWORNIK, E.J. & MILTON, C. (1987): Delindeite and lourenswalsite, two new titanosilicates from the Magnet Cove region, Arkansas. *Mineral. Mag.* **51**, 417-425.

ATENCIO, F., COUTINHO, J.M.V., ULBRICH, M.N.C., VLACH, S.R.F., RASTSVETAEVA, R.K. & PUSHCHAROVSKY, D.YU. (1999): Hainite from Poços de Caldas, Minas Gerais, Brazil. *Can. Mineral.* **37**, 91-98.

BELLEZZA, M., FRANZINI, M., LARSEN, A.O., MERLINO, S. & PERCHIAZZI, N. (2004): Grenmarite, a new member of the götzenite – seidozerite – rosenbuschite group from the Langesundsfjord district, Norway: definition and crystal structure. *Eur. J. Mineral.* **16**, 971-978.

BELOV, N.V. (1976): *Essays on Structural Mineralogy*. Nedra, Moscow, USSR (in Russ.).

BELOV, N.V., GAVRILOVA, G.S., SOLOV'EVA, L.P. & KHALILOV, A.D. (1977): Refined structure of lomonosovite. *Sov. Phys. Dokl.* **22**, 422-424.

BLUMRICH, J. (1893): Die Phonolithe des Friedländer Bezirkes in Nordböhmen. *Tschermaks Mineral. Petrogr. Mitt.* **13**, 465-495.

BØGGILD, O.B. (1901): Epistolite, a new mineral. *Meddr. Grønland* **24**, 183-190.

BRÖGGER, W.C. (1887): Forelöbig meddelelse om mineralerne på de sydnorske augit-og nefelinsyeniters grovkornige gange. *Geol. Fören. Stockholm Förh.* **9**(4), 247-274.

BROWN, I.D. (1981): The bond-valence method: an empirical approach to chemical structure and bonding. *In* Structure and Bonding in Crystals II (M. O'Keeffe & A. Navrotsky, eds.). Academic Press, New York, N.Y. (1-30).

BUSSEN, I.V., DENISOV, A.P., ZABAVNIKOVA, N.I., KOZYREVA, L.V., MEN'SHIKOV, YU.P. & LIPATOVA, E.A. (1973): Vuonnemite, a new mineral. *Zap. Vses. Mineral. Obshchest.* **102**(4), 423-426 (in Russ.).

CANNILLO, E., MAZZI, F. & ROSSI, G. (1972): Crystal structure of götzenite. *Sov. Phys. Crystallogr.* **16**, 1026-1030.

CHAO, G.Y. (1991): Perraultite, a new hydrous Na–K–Ba–Mn–Ti–Nb silicate species from Mont Saint-Hilaire, Quebec. *Can. Mineral.* **29**, 355-358.

CHERNOV, A.N. ILYUKHIN, V.V., MAKSIMOV, B.A. & BELOV, N.V. (1971): Crystal structure of innelite, $Na_2Ba_3(Ba,K,Mn)(Ca,Ba)Ti(TiO_2)_2(Si_2O_7)_2(SO_4)_2$. *Sov. Phys. Crystallogr.* **16**, 65-69.

CHRISTIANSEN, C.C., GAULT, R.A., GRICE, J.D. & JOHNSEN, O. (2003b): Kochite, a new member of the rosenbuschite group from the Werner Bjerge alkaline complex, East Greenland. *Eur. J. Mineral.* **15**, 551-554.

CHRISTIANSEN, C.C., JOHNSEN, O. & MAKOVICKY, E. (2003a): Crystal chemistry of the rosenbuschite group. *Can. Mineral.* **41**, 1203-1224.

CHRISTIANSEN, C.C., MAKOVICKY, E. & JOHNSEN, O. (1999): Homology and typism in heterophyllosilicates. *Neues Jahrb. Mineral., Abh.* **175**, 153-189.

CHRISTIANSEN, C.C. & RØNSBO, J.G. (2000): On the structural relationship between götzenite and rinkite. *Neues Jahrb. Mineral., Monatsh.*, 496-506.

CHUKANOV, N.V., MOISEEV, M.M., PEKOV, I.V., LAZEBNIK, K.A., RASTSVETAEVA, R.K., ZAYAKINA, N.V., FERRARIS, G. & IVALDI, G. (2004): Nabalamprophyllite $Ba(Na,Ba)\{Na_3Ti[TiO_2O_2Si_4O_{14}](OH,F)_2\}$ – a new layer titanosilicate of the lamprophyllite group from Inagli and Kovdor alkaline-ultrabasic massifs, Russia. *Zap. Vser. Mineral. Obshchest.* **133**(1), 59-72 (in Russ.).

DROZDOV, YU.N., BATALIEVA, N.G., VORONKOV, A.A. & KUZ'MIN, E.A. (1974): Crystal structure of $Na_{11}Nb_2TiSi_4P_2O_{25}F$. *Sov. Phys. Dokl.* **19**, 258-259.

DUDKIN, A.B. (1959): Barium lamprophyllite. *Zap. Vses. Mineral. Obshchest.* **88**, 713-715 (in Russ.).

EGOROV-TISMENKO, YU.K. (1998): On the seidozerite–nacaphite polysomatic series of minerals: titanium silicate analogues of mica. *Crystallogr. Rep.* **43**, 271-277.

EGOROV-TISMENKO, YU.K. & SOKOLOVA, E.V. (1987): Comparative crystal chemistry of a group of titanium silicate analogues of mica. *In* Comparative Crystal Chemistry. Moscow State University, Moscow, USSR (96-106; in Russ.).

EGOROV-TISMENKO, YU.K. & SOKOLOVA, E.V. (1990): Homologous series seidozerite–nacaphite. *Mineral. Zh.* **12**(4), 40-49 (in Russ.).

ERCIT, T.S., COOPER, M.A. & HAWTHORNE, F.C. (1998): The crystal structure of vuonnemite, $Na_{11}Ti^{4+}Nb_2(Si_2O_7)_2(PO_4)_2O_3(F,OH)$, a phosphate-bearing sorosilicate of the lomonosovite group. *Can. Mineral.* **37**, 1311-1320.

ES'KOVA, E.M., DUSMATOV, V.D., RASTSVETAEVA, R.K., CHUKANOV, N.V. & VORONKOV, A.A. (2003): Surkhobite $(Ca,Na)(Ba,K)(Fe^{3+},Mn)_4Ti_2(Si_4O_{14})O_2(F,OH,O)_3$. The new mineral (the Alai Ridge, Tajikistan). *Zap. Vser. Mineral. Obshchest.* **132**(2), 60-67 (in Russ.).

FERRARIS, G. (1997): Polysomatism as a tool for correlating properties and structure. *In* Modular Aspects of Minerals (S. Merlino, ed.). *Eur. Mineral. Union, Notes in Mineralogy* **1**, 275-295.

FERRARIS, G., BELLUSO, E., GULA, A., SOBOLEVA, S.V., AGEEVA, O.A. & BORUTSKII, B.E. (2001a): A structural model of the layer titanosilicate bornemanite based on seidozerite and lomonosovite modules. *Can. Mineral.* **39**, 1665-1673.

FERRARIS, G., IVALDI, G., KHOMYAKOV, A.P., SOBOLEVA, S.V., BELLUSO, E. & PAVESE, A. (1996): Nafertisite, a layer titanosilicate member of a polysomatic series including mica. *Eur. J. Mineral.* **8**, 241-249.

FERRARIS, G., KHOMYAKOV, A.P., BELLUSO, E. & SOBOLEVA, S.V. (1997): Polysomatic relationships in some titanosilicates occurring in the hyperagpaitic alkaline rocks of the

Kola Peninsula, Russia. *Proc. 30th Int. Geol. Congress* **16**, 17-27.

FERRARIS, G., MAKOVICKY, E. & MERLINO, S. (2004): *Crystallography of Modular Materials*. Oxford University Press, Oxford, U.K.

FERRARIS, G., PUSHCHAROVSKY, D.YU., ZUBKOVA, N.V. & PEKOV, I.V. (2001b): The crystal structure of delindeite, $Ba_2\{(Na,K,\square)_3(Ti,Fe)[Ti_2(O,OH)_4Si_4O_{14}](H_2O,OH)_2\}$, a member of the mero-plesiotype bafertisite series. *Can. Mineral.* **39**, 1307-1316.

GALLI, E. & ALBERTI, A. (1971): The crystal structure of rinkite. *Acta Crystallogr.* **B27**, 1277-1284.

GERASIMOVSKY, V.I. (1950): Lomonosovite, a new mineral. *Dokl. Akad. Nauk SSSR* **70**, 83-86 (in Russ.).

GUAN, YA.S., SIMONOV, V.I. & BELOV, N.V. (1963): Crystal structure of bafertisite, $BaFe_2TiO[Si_2O_7](OH)_2$. *Dokl. Akad. Nauk SSSR* **149**, 123-126.

GUTKOVA, N.N. (1930): Sur un nouveau titanosilicate – la murmanite – de Lujawrurt (Kalbinsel Kola). *C.R. Acad. Sci. URSS*, 731.

HAWTHORNE, F.C. (1992): The role of OH and H_2O in oxide and oxysalt minerals. *Z. Kristallogr.* **201**, 183-206.

KHALILOV, A.D. (1989): Refinement of the crystal structure of murmanite and new data on its crystal chemistry. *Mineral. Zh.* **11**(5), 19-27 (in Russ.).

KHALILOV, A.D., MAKAROV, YE.S., MAMEDOV, KH.S. & P'YANSINA, L.YA. (1965b): Crystal structures of minerals of the murmanite–lomonosovite group. *Dokl. Akad. Nauk SSSR* **162**, 138-140 (in Russ.).

KHALILOV, A.D., MAMEDOV, KH.S., MAKAROV, YE.S. & P'YANSINA, L.YA. (1965a): Crystal structure of murmanite. *Dokl. Acad. Sci. USSR* **161**, 150-152.

KHOMYAKOV, A.P. (1995): *Mineralogy of Hyperagpaitic Alkaline Rocks*. Clarendon Press, Oxford, U.K.

KHOMYAKOV, A.P., KASAKOVA, M.E. & PUSHCHAROVSKII, D.YU. (1980): Nacaphite $Na_2Ca(PO_4)F$ – a new mineral. *Zap. Vses. Mineral. Obshchest.* **109**, 50-52 (in Russ.).

KHOMYAKOV, A.P., KUROVA, T.A. & CHISTYAKOVA, N.I. (1983): Sobolevite, $Na_{14}Ca_2MnTi_3P_4Si_4O_{34}$ – a new mineral. *Zap. Vses. Mineral. Obshchest.* **112**, 456-461 (in Russ.).

KHOMYAKOV, A.P., MEN'SHIKOV, YU.P., NECHELYUSTOV, G.N. & ZHOU, H. (2001): Bussenite, $Na_2Ba_2FeTiSi_2O_7(CO_3)(OH)_3F$, a new mica-like titanosilicate from the Khibina alkaline massif (Kola Peninsula). *Zap. Vser. Mineral. Obshchest.* **130**(3), 50-55 (in Russ.).

KHOMYAKOV, A.P., NECHELYUSTOV, G.N., SOKOLOVA, E.V. & DOROKHOVA, G.I. (1992): Quadruphite, $Na_{14}CaMgTi_4[Si_2O_7]_2[PO_4]_2O_4F_2$ and polyphite $Na_{17}Ca_3Mg(Ti,Mn)_4[Si_2O_7]_2[PO_4]_6O_2F_6$, two new minerals of the lomonovosite group. *Zap. Vser. Mineral. Obshchest.* **121**(1), 105-112 (in Russ.).

KRAVCHENKO, S.M., VLASOVA, E.V., KAZAKOVA, M.E., ILOKHIN, V.V. & ABRASHEV, K.K. (1961): Innelite, a new barium silicate. *Dokl. Akad. Nauk SSSR* **141**, 1198-1199 (in Russ.).

KRIVOVICHEV, S.V., ARMBRUSTER, T., YAKOVENCHUK, V.N., PAKHOMOVSKY, YA. A. & MEN'SHIKOV, YU. P. (2003): Crystal structures of lamprophyllite-2*M* and lamprophyllite-2*O* from the Lovozero alkaline massif, Kola peninsula, Russia. *Eur. J. Mineral.* **15**, 711-718.

LORENZEN, J. (1884): Untersuchung einiger Mineralien aus Kangerdluarsuk in Grönland. *Z. Kristallogr.* **9**, 243-254.

MAKOVICKY, E. (1997): Modularity – different type and approaches. *In* Modular Aspects of Minerals (S. Merlino, ed.). *Eur. Mineral. Union, Notes in Mineralogy* **1**, 315-343.

MANDARINO, J.A. & BACK, M.E. (2004): *Fleischer's Glossary of Mineral Species 2004*. The Mineralogical Record Inc., Tucson, Arizona.

MATSUBARA, S. (1980): The crystal structure of orthoericssonite. *Mineral. J.* **10**, 107-121.

MCDONALD, A.M., GRICE, J.D. & CHAO, G.Y. (2000): The crystal structure of yoshimuraite, a layered Ba–Mn–Ti silicophosphate, with comments of five-coordinated Ti^{4+}. *Can. Mineral.* **38**, 649-656.

MEN'SHIKOV, YU.P., BUSSEN, I.V., GOIKO, E.A., ZABAVNIKOVA, N.I., MER'KOV, A.N. & KHOMYAKOV, A.P. (1975): Bornemanite – a new silicophosphate of sodium, titanium, niobium and barium. *Zap. Vses. Mineral. Obshchest.* **104**, 322-326 (in Russ.).

MOORE, P.B. (1971): Ericssonite and orthoericssonite. Two new members of the lamprophyllite group, from Långban, Sweden. *Lithos* **4**, 137-145.

PAULING, L. (1929): The principles determining the structure of complex ionic crystals. *Am. Chem. Soc. J.* **51**, 1010-1026.

PEN, Z.Z. & SHENG, T.C. (1963): Crystal structure of bafertisite, a new mineral from China. *Scientia Sinica* **12**, 278-280 (in Russ.).

PENG, C. (1959): The discovery of several new minerals of rare elements. *Ti-chih K'o-hsueh* **10**, 289 (in Chinese).

PENG, Z., ZHANG, J. & SHU, J. (1984): The crystal structure of barytolamprophyllite and orthorhombic lamprophyllite. *Kexure Tongbao* **29**, 237-241.

PUSHCHAROVSKII, D.YU., PASERO, M., MERLINO, S., VLADYKIN, N.D., ZUBKOVA, N.V. & GOBECHIYA, E.R. (2002): Crystal structure of zirconium-rich seidozerite. *Crystallogr. Rep.* **47**, 196-200.

PYATENKO, YU.A., VORONKOV, A.A. & PUDOVKINA, Z.V. (1976): *Mineralogical Crystal Chemistry of Titanium*. Nauka, Moscow, USSR (in Russ.).

RAMSAY, W. & HACKMAN, V. (1894): Das Nephelinsyenitgebiet auf der Halbinsel Kola. *Bull. Soc. Géographie Finlande* **1**(2), 1-225.

RASTSVETAEVA, R.K. & ANDRIANOV, V.I. (1986): New data on the crystal structure of murmanite. *Kristallografiya* **31**, 82-87 (in Russ.).

RASTSVETAEVA, R.K., BORUTSKII, B.E. & SHLYUKOVA, Z.V. (1991a): Crystal structure of Hibbing (Khibinian) rinkite. *Sov. Phys. Crystallogr.* **36**, 349-351.

RASTSVETAEVA, R.K. & CHUKANOV, N.V. (1999): Crystal structure of a new high-barium analogue of lamprophyllite with a primitive unit cell. *Dokl. Chem.* **368**, 228-231.

RASTSVETAEVA, R.K. & DORFMAN, M.D. (1995): Crystal structure of Ba-lamprophyllite in the isomorphous lamprophyllite–barytolamprophyllite series. *Crystallogr. Rep.* **40**, 951-954.

RASTSVETAEVA, R.K., EVSYUNIN, V.G. & KONEV, A.A. (1995a): Crystal structure of K-barytolamprophyllite. C*rystallogr. Rep.* **40**, 472-474.

RASTSVETAEVA, R.K., PUSHCHAROVKSY, D.YU. & ATENCIO, D. (1995b): Crystal structure of giannetite (hainite). *Crystallogr. Rep.* **40**, 574-578.

RASTSVETAEVA, R.K., SIMONOV, V.I. & BELOV, N.V. (1971): Crystal structure of lomonosovite, $Na_5Ti_2[Si_2O_7][PO_4]O_2$. *Sov. Phys. Dokl.* **16**, 182-185.

RASTSVETAEVA, R.K., SOKOLOVA, M.N. & GUSEV, A.I. (1990): Refinement of the crystal structure of lamprophyllite. *Mineral. Zh.* **12**(5), 25-28 (in Russ.).

RASTSVETAEVA, R.K., TAMAZYAN, R.A., SOKOLOVA, E.V. & BELAKOVSKII, D.I. (1991b): Crystal structures of two modifications of natural Ba, Mn-titanosilicate. *Sov. Phys. Crystallogr.* **36**, 186-189.

ROZENBERG, K.A., RASTSVETAEVA, R.K. & VERIN, I.A. (2003): Crystal structure of surkhobite: new mineral from the family of titanosilicate micas. *Crystallogr. Rep.* **48**, 384-389.

SAF'YANOV, Y.N., VASIL'EVA, N.O., GOLOVACHEV, V.P., KUZ'MIN, E.A. & BELOV, N.V. (1983): Crystal structure of lamprophyllite. *Sov. Phys. Dokl.* **28**, 207-209.

SAHAMA, T.G. & HYTÖNEN, M.A. (1957): Götzenite and combeite, two new silicates from the Belgian Congo. *Mineral. Mag.* **238**, 503-510.

SEMENOV, E.I., KAZAKOVA, M.E. & SIMONOV, V.I. (1958): A new zirconium mineral, seidozerite, and other minerals of the wöhlerite group in alkaline pegmatites. *Zap. Vses. Mineral. Obshchest.* **87**, 590-597 (in Russian).

SHANNON, R.D. (1976): Revised effective ionic radii and systematic studies of interatomic distances in halides and chalcogenides. *Acta Crystallogr.* **A32**, 751-767.

SHIBAEVA, R.P., SIMONOV, V.I. & BELOV, N.V. (1964): Crystal structure of the Ca, Na, Zr, Ti silicate rosenbuschite, $Ca_{3.5}Na_{2.5}Zr(Ti,Mn,Nb)[Si_2O_7]_2F_2O(F,O)$. *Sov. Phys. Crystallogr.* **8**, 406-413.

SIMONOV, V.I. & BELOV, N.V. (1960): The determination of the crystal structure of seidozerite. *Sov. Phys. Crystallogr.* **4**, 146-157.

SKSZAT, S.M. & SIMONOV, V.I. (1966): The structure of calcium seidozerite. *Sov. Phys. Crystallogr.* **10**, 505-508.

SOKOLOVA, E.V. (1997): *Polysomatism, Polymorphism and Isomorphism in the Crystal Structures of New Silicate and Phosphate Minerals*. D.Sc. thesis, Moscow State University, Moscow, Russia (in Russ.).

SOKOLOVA, E.V. (1998): Polysomatic series seidozerite–nacaphite. *Zap. Vser. Mineral. Obshchest.* **127**(2), 111-114 (in Russ.).

SOKOLOVA, E.V., EGOROV-TISMENKO, YU.K. & KHOMYAKOV, A.P. (1987a): Special features of the crystal structure of Na_{14} Ca Mg Ti_4 $[Si_2O_7]_2$ $[PO_4]$ O_4 F_2 – homologue of sulphohalite and lomonosovite structure types. *Mineral. Zh.* **9**(3), 28-35 (in Russ.).

SOKOLOVA, E.V., EGOROV-TISMENKO, YU.K. & KHOMYAKOV, A.P. (1987b): Crystal structure of $Na_{17}Ca_3Mg(Ti,Mn)_4[Si_2O_7]_2[PO_4]_6O_2F_6$, a new representative of the family of layered titanium silicates. *Sov. Phys. Dokl.* **32**, 344-347.

SOKOLOVA, E.V., EGOROV-TISMENKO, YU.K. & KHOMYAKOV, A.P. (1988): Crystal structure of sobolevite. *Sov. Phys. Dokl.* **33**, 711-714.

SOKOLOVA, E.V., EGOROV-TISMENKO, YU.K. & KHOMYAKOV, A.P. (1989): Crystal structure of nacaphite. *Sov. Phys. Dokl.* **34**, 9-11.

SOKOLOVA, E.V. & HAWTHORNE, F.C. (2001): The crystal chemistry of the $[M_3O_{11-14}]$ trimeric structures: from hyperagpaitic complexes to saline lakes. *Can. Mineral.* **39**, 1275-1294.

SOKOLOVA, E.V. & HAWTHORNE, F.C. (2004): The crystal chemistry of epistolite. *Can. Mineral.* **42**, 797-806.

SOKOLOVA, E.V., HAWTHORNE, F.C. & KHOMYAKOV, A.P. (2005): Polyphite and sobolevite: revision of their crystal structures. *Can. Mineral.* **43**, 1527-1544.

TAKÉUCHI, Y., OHASHI, Y., SAWADA, H. & HAGA, N. (1997): Crystal structure of yoshimuraite $(Ba,Sr)_2(S,P)O_4Mn_2OH[Si_2O_7TiO]$, with discussion on its local symmetry. *In* Tropochemical Cell-Twinning (Y. Takéuchi, ed.). Terra Scientific Publishing Company, Tokyo, Japan (253-264).

VRÁNA, S., RIEDER, M. & GUNTER, M.E. (1992): Hejtmanite, a manganese-dominant analogue of bafertisite, a new mineral. *Eur. J. Mineral.* **4**, 35-43.

WATANABE, T., TAKÉUCHI, Y. & ITO, J. (1961): The minerals of the Noda–Tamagawa mine, Iwaté Prefecture, Japan. III. Yoshimuraite, a new barium–titanium–manganese silicate mineral. *Mineral J.* **3**, 156-167.

WOODROW, P.J. (1964): The crystal structure of lamprophyllite. *Nature* **204**, 375.

WOODROW, P.J. (1967): The crystal structure of astrophyllite. *Acta Crystallogr.* **B22**, 673-678.

YAMNOVA, N.A., EGOROV-TISMENKO, YU.K. & PEKOV, I.V. (1998): Crystal structure of perraultite from the coastal region of the Sea of Azov. *Crystallogr. Rep.* **43**, 401-410.

ZHOU, H, RASTSVETAEVA, R.K., KHOMYAKOV, A.P., MA, Z. & SHI, N. (2002): Crystal structure of new mica-like titanosilicate – bussenite, $Na_2Ba_2Fe^{2+}(TiSi_2O_7)(CO_3)O(OH)(H_2O)F$. *Crystallogr. Rep.* **47**, 43-46.

Received February 1, 2006, revised manuscript accepted July 15, 2006.

APPENDIX A. PREVIOUS WORK

Rosenbuschite, rinkite, hainite and lamprophyllite were described in the 19th century (Brögger 1887, Lorenzen 1884, Blumrich 1893, Ramsay & Hackman 1894). Epistolite (Bøggild 1901), murmanite (Gutkova 1930) and lomonosovite (Gerasimovsky 1950) were discovered in the first half of the 20th century, but there was still no information about crystal structures of these minerals. In the late 1950s and early 1960s, götzenite (Sahama & Hytönen 1957), barytolamprophyllite (Dudkin 1959), seidozerite (Semenov *et al*. 1958), bafertisite (Peng 1959), yoshimuraite (Watanabe *et al*. 1961) and innelite (Kravchenko *et al*. 1961) were found and described. At the same time, N.V. Belov and his coworkers began structure work on Ti-silicate minerals of this group: seidozerite (Simonov & Belov 1960), bafertisite (Guan *et al*. 1963, Pen & Sheng 1963), rosenbuschite (Shibaeva *et al*. 1964) and murmanite (Khalilov *et al*. 1965a) were the first structures to be done. The crystal structure of lamprophyllite was done by Woodrow (1964). In the 1970s, three new minerals were found: orthoericssonite (Moore 1971), bornemanite (Men'shikov *et al*. 1975) and vuonnemite (Bussen *et al*. 1973), and more structural work was done: rinkite (Galli & Alberti 1971), innelite (Chernov *et al*. 1971), lomonosovite (Rastsvetaeva *et al*. 1971), götzenite (Cannillo *et al*. 1972), vuonnemite (Drozdov *et al*. 1974). Khalilov *et al*. (1965b) used available structural information to compare the structures of murmanite, lomonosovite and epistolite (possible structure), and emphasized the stability of the main structural unit, a TS block. In two books, Belov (1976) and Pyatenko *et al*. (1976) considered the TS block as a stable fragment characteristic of several Ti-silicate structures. In the 1980s, delindeite (Appleman *et al*. 1987) and sobolevite (Khomyakov *et al*. 1983) were added to this group, and the crystal structure of barytolamprophyllite (Peng *et al*. 1984) was solved. Khomyakov *et al*. (1992) described two new minerals, quadruphite and polyphite, and Sokolova *et al*. (1987a, b, 1988) solved their crystal structures and that of sobolevite. Sokolova *et al*. (1989) solved the crystal structure of nacaphite, $Na(NaCa)(PO_4)F$, which was described as a new mineral by Khomyakov *et al*. (1980). Several potential mineral species with the TS block were described by Khomyakov (1995).

The crystal structure of nacaphite played a key role in understanding the crystal chemistry of minerals with the TS block. Egorov-Tismenko & Sokolova (1987, 1990) showed that (1) a fragment of the nacaphite structure occurs as an intermediate structural block between two TS blocks in the crystal structures of quadruphite, polyphite and sobolevite; (2) the TS block is the major structural unit in many structures, whereas the interlayer composition, *i.e.*, composition of the space between two TS blocks, differs; (3) the interlayer space is closely related to the crystal structure of nacaphite. Sokolova (1997, 1998) considered seidozerite, rinkite, götzenite, rosenbuschite, lamprophyllite, murmanite, epistolite, bafertisite, hejtmanite, innelite, lomonosovite, vuonnemite, quadruphite, polyphite, sobolevite and nacaphite as a polysomatic series *seidozerite – nacaphite* in which the seidozerite block (= TS block) is a stable structural unit, whereas the nacaphite block varies in size and chemical composition. Furthermore, Sokolova (1997) emphasized an important condition for formation of such a series: adjacent surfaces of two types of blocks must be similar and have practically identical unit-cell dimensions. Egorov-Tismenko (1998) considered a smaller number of minerals, seidozerite, lomonosovite, beta-lomonosovite, vuonnemite, quadruphite, sobolevite, polyphite and nacaphite as the polysomatic series *seidozerite – nacaphite* and emphasized the importance of similarity of adjacent surfaces of different blocks. Ferraris *et al*. (1997) added minerals of unknown structure but known cell-dimensions to the minerals studied by Egorov-Tismenko & Sokolova (1990), called them seidozerite derivatives and considered them as a merotype series in accord with Makovicky (1997). Ferraris *et al*. (1997) introduced a new name, the HOH block, in which O stands for the sheet of octahedra, and H, for heterogeneous silicate sheets. This name was applied not only to the TS block, with its (Si_2O_7) groups, but also to other types of silicate-containing sheets (Ferraris 1997). Christiansen *et al*. (1999) considered the crystal structures of minerals with HOH sheets as various polytypes and described three types of shifts of two H sheets relative to each other, *e.g*., in seidozerite, lamprophyllite and murmanite. In the last 15 years, several new minerals of this particular type have been described: perraultite (Chao 1991), hejtmanite (Vrána *et al*. 1992), bussenite (Khomyakov *et al*. 2001), surkhobite (Es'kova *et al*. 2003), kochite (Christiansen *et al*. 2003b) and grenmarite (Bellezza *et al*. 2004). In addition, crystal structures were solved for hejtmanite (Rastsvetaeva *et al*. 1991b), hainite (Rastsvetaeva *et al*. 1995b), yoshimuraite (Takéuchi *et al*. 1997), nabalamprophyllite (Rastsvetaeva & Chukanov 1999), delindeite (Ferraris *et al*. 2001b), bussenite (Zhou *et al*. 2002), surkhobite (Rozenberg *et al*. 2003), epistolite (Sokolova & Hawthorne 2004), and grenmarite (Bellezza *et al*. 2004), and a structure model was proposed for bornemanite (Ferraris *et al*. 2001a). However, nabalamprophyllite was not considered as a distinct mineral at that time; it was approved as a valid mineral species five years later (Chukanov *et al*. 2004).

Let me emphasize that here I am referencing the first determination of the structure. Later work is summarized in Table 1, and crystallographic data are taken from the latest refinement of the structure. For example, the crystal structure of hainite was solved by

Rastsvetaeva *et al*. (1995b), who called it *giannetite*. Atencio *et al*. (1999) published new data on hainite from Brazil and said that *giannetite* of Rastsvetaeva *et al*. (1995b) is equivalent to hainite. Thus the work by Rastsvetaeva *et al*. (1995b) is the first determination of the structure of hainite.

It is evident that a lot of work has been and is being done on this interesting group of minerals. To summarize, Egorov-Tismenko & Sokolova (1987, 1990) originally developed the crystal chemistry for minerals with the TS block characterized by (Si_2O_7) groups. Egorov-Tismenko (1998) redescribed in detail minerals with a TS block dealt with by Egorov-Tismenko & Sokolova (1990), and emphasized that those minerals are analogues of micas. Ferraris *et al*. (1997) and Ferraris (1997) considered minerals with various HOH blocks as different somatic series, and this work became part of the book on modular materials (Ferraris *et al*. 2004). Christiansen *et al*. (1999) considered minerals with HOH blocks that had different silicate radicals, *e.g*., astrophyllite (Woodrow 1967) and nafertisite (Ferraris *et al*. 1996). Christiansen *et al*. (1999) gave detailed descriptions of the structures with HOH blocks, and characterized different stacking sequences and cation distributions over mixed sites. Christiansen & Rønsbo (2000) reconsidered the structural relationship between götzenite and rinkite. Christiansen *et al*. (2003a) refined the structure and chemical formulae of seidozerite, götzenite, hainite and rosenbuschite, and considered the crystal chemistry of these minerals plus kochite as that of the rosenbuschite group.

Appendix B. Related Minerals

Orthoericssonite

Orthoericssonite, Ba ($Mn_{1.5}Fe^{2+}_{0.5}$) Fe^{3+} (Si_2O_7) O (OH), (orthorhombic, *a* 20.230, *b* 6.979, *c* 5.392 Å, space group *Pnmn*, *Z* = 4) (Moore 1971, Matsubara 1980), does not contain any Ti in its structure, and I do not consider it as a mineral with a TS block. However, the O sheet of the HOH block is identical to the O sheet in the structures of Group II: $M^O = M^{2+}$, but the topology of the HOH block is different from that in the structures of Group II. In orthoericssonite, $^{[5]}M^H = Fe^{3+}$. The substitution $Ti^{4+} \rightleftharpoons Fe^{3+}$ is quite common because of the similar size of the atoms: 0.58 Å for $^{[5]}Fe^{3+}$ and 0.51 Å for $^{[5]}Ti^{4+}$ (Shannon 1976). In orthoericssonite, linkage 1 (as in Groups I and III) occurs.

Delindeite

Delindeite, Ba_2 {(Na,K,□)$_3$ (Ti,Fe) [Ti_2(O,OH)$_4$ Si_4O_{14}] (H_2O,OH)$_2$}, has an HOH block in which about 40% of the cation sites of the O sheet are vacant (Ferraris *et al*. 2001b, Appleman *et al*. 1987): *a* 5.327, *b* 6.856, *c* 21.53 Å, β 93.80°, space group *A*2/*m*, *Z* = 2. In delindeite, 4 $M^O = (Na,K)_{1.36}$ □$_{1.64}$ + Ti, 2 M^H = 2 Ti, and the *P* sites are occupied by Ba. Thus the O sheet is not trioctahedral; hence the HOH block is not a TS block as defined here. Therefore delindeite does not contain the TS block in its crystal structure.

APPENDIX C. PROBLEMS

Bornemanite

Bornemanite, $BaNa_3\{(Na,Ti)_4[(Ti,Nb)_2O_2Si_4O_{14}](F,OH)_2\}PO_4$, $Z = 4$, occurs as very poor crystals, and though it was described thirty years ago (Men'shikov *et al*. 1975), there has been no possibility to determine its crystal structure. Ferraris *et al*. (2001a) used TEM, X-ray powder diffraction and a polysomatic approach to build a theoretical structure for bornemanite using lomonosovite and seidozerite blocks, *i.e*., two different structure-fragments. This is a very interesting approach, but many features are not in accord with the findings given here.

On the basis of the chemical composition of bornemanite reported in Ferraris *et al*. (2001a), I write its formula as $Na_3\,Ba\,Ti_{1.3}Nb_{0.7}\,Na_3Ti\,(Si_2O_7)_2\,(PO_4)\,O_2\,(OH,F)_2$, where $Ti_{1.3}Nb_{0.7}\,Na_3Ti\,(Si_2O_7)_2\,O_2\,(OH,F)_2$ describes the chemical composition of the TS block, *i.e*., $Ti_{1.3}Nb_{0.7}$ corresponds to $2M^H$, Na_3Ti corresponds to $4M^O$, $O_2\,(OH,F)_2$ corresponds to $4\,X^O$, and Na_3Ba and (PO_4) describe the chemical composition of the **I** block. In the TS block, ideally $Ti_2\,Na_3Ti\,(Si_2O_7)_2\,O_2\,(OH,F)_2$, Ti amounts to 3 *apfu*. Hence, bornemanite belongs to Group III, and the TS block has to exhibit linkage 1 and the stereochemistry of Group III: Ti occurs in the H and O sheets, two (Si_2O_7) groups link to *trans* edges of a Ti octahedron in the O sheet. Thus the structure model of bornemanite (Ferraris *et al*. 2001a) is extremely improbable, and is not considered in this paper.

Surkhobite

It is not possible to get reasonable bond-distances or to write a chemical formula for surkhobite in accord with the structure data presented by Rozenberg *et al*. (2003). However, one can try to get a correct formula for surkhobite. I know that (1) the unit cells and structure topology of surkhobite and perraultite are identical, (2) the TS block in perraultite, $Ti_2\,(Mn^{2+}{}_4)\,(Si_2O_7)_2\,O_7\,(OH)_2\,F$, and in surkhobite, $Ti_2\,(Fe^{2+}{}_4)\,(Si_2O_7)_2\,O_7\,(OH)\,F_2$, each has a negative charge of –3, and (3) to compensate for the negative charge of the TS block, the charge of the **I** layer has to be +3. In perraultite, the **I** layer contains Ba Na with a total charge of +3. In surkhobite, a total charge of the **I** layer = Ba Ca is +4, and this results in a positively charged formula. The chemical formula of surkhobite presented by Es'kova *et al*. (2003) was derived from a wet-chemical analysis done in 1977, with no new electron-microprobe data. I suspect that an excess of Ca arises from an admixture of fluorite, which commonly occurs with surkhobite and perraultite. Surkhobite should be re-analyzed, in order to correct its chemical formula. The probable formula of surkhobite is $Na\,Ba\,Ti_2\,Fe^{2+}{}_4\,(Si_2O_7)_2\,O_2\,(OH)\,F_2$.

APPENDIX D. REVISION OF CHEMICAL FORMULAE

In this paper, I have dealt with minerals for which the chemical formulae are written imprecisely or inaccurately, *i.e*., where the structure-refinement results contradict the chemical composition obtained by electron-microprobe analysis. I will consider the chemical formulae of some minerals of Group I, and will pay special attention to the content of F, emphasizing that the correct content of anions is as important as the correct content of cations in a formula of a mineral.

Group I: kochite, rosenbuschite, hainite, götzenite

On the basis of electron-microprobe data and structure-refinement results, Christiansen *et al*. (2003a), Bellezza *et al*. (2004) and Rastsvetaeva *et al*. (1991a) gave the formulae for rosenbuschite-group minerals, grenmarite and rinkite as shown below:

götzenite, Z = 1,
$Ca_2\,(Na,Ca)_2\,Ca_2\,Na\,Ti\,(Si_2O_7)_2\,F_2\,F_2$,;

hainite, Z = 1,
$(Ca,Zr,Y)_2\,(Na,Ca)_2\,Ca_2\,Na\,Ti\,(Si_2O_7)_2\,F_2\,F_2$,;

seidozerite, Z = 1,
$Zr_4\,Na_2\,Mn_2\,Na_4\,Na_2\,Ti_2\,(Si_2O_7)_4\,F_4\,O_4$,;

grenmarite, Z = 1,
$(Zr,Mn)_2\,(Zr,Ti)\,(Mn,Na)\,(Na,Ca)_4\,(Si_2O_7)_2\,(O,F)_4$,;

rinkite*, Z = 2,
$\{TiF(O,F)(Si_2O_7)_2\}\{Na(Na,Ca)_2F(O,F)\}\{(Ca,REE)_4\}$;

kochite, Z = 1,
$Zr_2\,(Mn,Zr)_2\,(Na,Ca)_4\,Ca_4\,Na_2\,Ti_2\,(Si_2O_7)_4\,F_4\,O_4$,;

rosenbuschite, Z = 1,
$Zr_2\,Ca_2\,(Na,Ca)_4\,Ca_4\,Na_2\,Zr\,Ti\,(Si_2O_7)_4\,F_4\,O_4$;

* in the rinkite formula, three sets of curly brackets (1–3) show: a "ribbon-type mixed *radical*" (1), "the chemical composition of the middle layer" (2), "and outer layers" (3) "of the three-layered package" (Rastsvetaeva *et al*. 1991a); in a more compact form, $Na\,(Na,Ca)_2\,Ti\,(Ca,REE)_4\,(Si_2O_7)_2\,F_2\,(O,F)_2$, $Z = 2$.

Christiansen *et al*. (2003a) calculated the formula units for götzenite, hainite, seidozerite, kochite and

rosenbuschite (Table A1). Note that almost all chemical datasets presented in Table A1 have low totals. Christiansen *et al*. (2003a) gave the following content of F: 3.53 (4.00), 3.24 (4.00), 3.78 (4.00), 5.43 (4.00) and 6.04 (4.00) *apfu* for the corresponding minerals, where the numbers in brackets show the contents of F in the formulae written above. There is a reasonable agreement for seidozerite, 3.78 (4.00) *apfu*, less so for götzenite, 3.53 (4.00) *apfu*, and the numbers are significantly different for kochite, hainite and rosenbuschite: 5.43 (4.00), 3.24 (4.00) and 6.04 (4.00) *apfu*, respectively. Note that in Christiansen *et al*. (2003a), the numbers of F (*apfu*) from EMPA are always odd (except for seidozerite, where it is 4 *apfu*), whereas the contents of F given in the structural formulae are invariably 4 *apfu*. There are two anion sites that can host F, F(9) and *X*(8) (Table A2). The *F*(9) site involves an X^{O}_{A} anion in my terminology, the incident bond-valence sum is about 1.00 *vu*, and hence it is fully occupied by F in all structures of Table A2 (there is no OH present). For a formula unit with 4 Si *apfu*, this site gives 2 F *apfu* for götzenite, hainite, seidozerite, kochite and rosenbuschite. The *X*(8) site involves an X^{O}_{M} anion in my terminology. In seidozerite, the bond-valence sum at this anion is 1.70 *vu* (Table A2), and O is dominant at this site. Therefore *X*(8) + F(9) sites give O_2F_2 for the formula unit of seidozerite with 4 Si *apfu*. There are two sites, *X*(8a) and *X*(8b), in the crystal structures of kochite and rosenbuschite. The mean bond-valence sums at the X(8) anion are 1.60 and 1.38 *vu* for kochite and 1.66 and 1.36 *vu* for rosenbuschite (Table A2). Certainly, these values indicate local order of anions locally associated with order of cations.

In kochite and rosenbuschite, the *X*(8a) site ideally receives bond valence from Ti^{O} + $\mathbf{Zr^{H}}$ + $2^{[6]}Na^{O}$, and the X(8b) anion ideally receives bond valence from Ti^{O} + $\mathbf{(Mn^{2+})^{H}}$ + $2^{[6]}Na^{O}$. Therefore, O should be dominant at the *X*(8a) site, and F should be dominant at the *X*(8b) site. The *X*(8a) and *X*(8b) sites in kochite give O_2 F_2 for the formula unit with 8 Si *apfu*. The total number of anions is F_4 O_2 F_2 (= F_6O_2), and this value is in reasonable agreement with the observed F contents of 5.43 and 6.04 *apfu*, respectively, for kochite and rosenbuschite, much closer than F_4 in the formula unit reported at the

TABLE A1. CHEMICAL COMPOSITION AND FORMULA UNIT OF MEMBERS OF THE ROSENBUSCHITE GROUP

Mineral	götzenite		hainite		seidozerite		kochite		rosenbuschite	
Sample	WBC-13		LF-A2		1993.158		WBC-12		LF-A5	
	wt.%	*apfu**	wt.%	*apfu**	wt.%	*apfu**	wt.%	*apfu**	wt.%	*apfu**
SiO_2	30.85	8.00	30.50	8.00	30.73	8.00	31.19	8.00	29.94	8.00
Al_2O_3	0.05	0.02	0.05	0.02	0.08	0.02	0.05	0.02	n.d.	
TiO_2	9.24	1.80	8.16	1.61	13.88	2.72	8.42	1.62	4.56	0.92
SnO_2	n.d.**		n.d.		n.d.		n.d.		0.19	0.02
ZrO_2	1.41	0.18	3.96	0.51	21.83	2.77	11.90	1.49	19.66	2.56
HfO_2	n.d.		0.08	0.01	0.38	0.03	0.09	0.01	0.46	0.04
Nb_2O_3	1.12	0.13	1.23	0.15	0.77	0.09	1.85	0.21	1.35	0.16
Ta_2O	n.d.		0.03	0.00	0.01	0.00	0.02	0.00	0.11	0.01
MgO	n.d.		n.d.		1.53	0.59	0.01	0.00	0.06	0.02
MnO	1.04	0.23	0.73	0.16	3.86	0.85	4.92	1.07	0.91	0.21
FeO	0.44	0.10	0.69	0.15	2.93	0.64	1.08	0.23	0.50	0.11
CaO	36.70	10.20	29.64	8.33	1.86	0.52	21.39	5.88	23.40	6.70
SrO	0.18	0.03	0.08	0.01	0.19	0.03	0.12	0.02	0.14	0.02
Na_2O	6.31	3.17	7.45	3.79	14.69	7.41	9.85	4.90	9.16	4.75
Y_2O_3	0.90	0.12	4.35	0.61	0.19	0.03	0.38	0.05	1.00	0.14
La_2O_3	1.66	0.16	0.63	0.06	n.d.		0.24	0.02	n.d.	
Ce_2O_3	2.71	0.26	1.67	0.16	n.d.		0.57	0.05	0.13	0.01
Nd_2O_3	0.44	0.04	0.71	0.07	n.d.		n.d.		n.d.	
Gd_2O_3	0.39	0.03	0.20	0.02	n.d.		n.d.		n.d.	
Dy_2O_3	n.d.		0.98	0.08	n.d.		n.d.		n.d.	
Er_2O_3	n.d.		0.59	0.05	n.d.		n.d.		n.d.	
Yb_2O_3	n.d.		0.74	0.06	n.d.		n.d.		n.d.	
F	8.60	7.05	7.81	6.48	4.59	3.78	6.70	5.43	7.15	6.04
O = F	–3.62		–3.29		–1.93		–2.82		–3.01	
O		29.84		29.67		31.80		29.92		30.23
Total	98.43		97.08		95.58		95.95		95.84	
Σanions†		36.90		36.15		35.58		35.36		36.27
Σcations††		16.45		15.88		15.67		15.55		15.67

* calculated on the basis of 8 Si apfu; ** not detected, † ideal sum is 36, †† ideal sum is 16. Data after Christiansen *et al.* (2003a).

beginning of this section. Thus, both in kochite and rosenbuschite, Zr–Mn^{2+} order in the H sheet couples to O–F order at the X^{O}_{M} sites.

In hainite, the *X*(8) site receives a bond valence of 0.67 (Ti^{O}) + 0.42 {½ [Ca (Y, REE)]^{H}} + 0.34 ($2^{[6]}Na^{O}$) = 1.43 *vu*. If O and F occupy the *X*(8) site in the ratio 1:1, then the *X*(8) + *F*(9) sites give F_2 + (OF) = F_3O per formula unit, which correlates well with total content of F (= 3.24 *apfu*) reported in Table A1.

In götzenite, the *X*(8) anion receives a bond valence of 0.67 (Ti^{O}) + 0.33 ($^{[6]}Ca^{H}$) + 0.67 ($2\ ^{[6]}Ca^{O}$) = 1.67 *vu*. Table A2 gives *X*(8) = 1.25 *vu*. Disorder of Ca and Na over M^{O} and M^{H} sites gives a reason for disorder of O and F atoms at the *X*(8) site, and the *X*(8) + *F*(9) sites in götzenite give F_2 + (OF) = F_3O per formula unit.

Thus my inspection of bond-valence sums for anions (= possible F sites) (Table A2) reveals significant inconsistencies between the final chemical formulae and the EMPA data for götzenite, hainite, kochite and rosenbuschite. These inconsistencies must be corrected.

Here is a summary of the changes to the anion content of these formulae:

götzenite $F_2\ F_2 \rightarrow F_2\ (FO) = F_3O$;

hainite $F_2\ F_2 \rightarrow F_2\ (FO) = F_3O$;

kochite $F_4\ O_4 \rightarrow F_4\ F_2\ O_2$;

rosenbuschite $F_4\ O_4 \rightarrow F_4\ F_2\ O_2$.

Calculation of formula units on an anion basis with O + F = 18 *apfu* is shown in Table A3. There are no chemical data for rinkite from Kola (Anthony *et al*. 1995), but Rastsvetaeva *et al*. (1991a) gave the chemical formula as $(Ti_{0.92}\ Nb_{0.06}\ Zr_{0.03})\ (Ca_{3.7}\ Na_{2.4}\ REE_{0.8}\ Sr_{0.15})\ (Si_{3.85}\ O_{14})\ O_{1.3}\ F_{2.55}$, where REE = $Ce_{0.315}\ Nd_{0.19}\ La_{0.10}\ Y_{0.09}\ Pr_{0.05}\ Sm_{0.03}$. This formula has a negative charge of –1.15. Inspection of the structural information from Rastsvetaeva *et al*. (1991a) shows that (1) the REE are statistically distributed over 2 $^{[7]}M^{H}$ and 2 $^{[8]}A^{P}$ sites, which give (Ca_3REE); (2) the anion at the X^{O}_{A} site receives bond valence from $^{[8]}Na^{O}$ + $^{[6]}(Na\ Ca)^{O}$ + ¼ $^{[8]}(Ca_3REE)^{P}$: 0.125 + 0.5 + 0.28 = 0.91 *vu,* and hence this site is occupied solely by F; (3) the X^{O}_{M} anion receives bond-valence from $^{[6]}Ti^{O}$ + $^{[6]}(Na\ Ca)^{O}$ + ¼ $^{[7]}(Ca_3REE)^{P}$: 0.67 + 0.5 + 0.32 = 1.49 *vu*, and hence this site is occupied by F and O in a 1:1 ratio. The anions can be written as F_2 (OF) with a total charge of –5 instead of $O_{1.3}\ F_{2.55}$ with a total charge of –5.15. It is impossible to get any charge information from the formula given by Rastsvetaeva *et al*. (1991a), as it does not contain any fixed stoichiometric coefficients.

In accord with the ideal proportions of constituents at the cation and anion sites (Table 3), I use the general formula (11) of the type $A^{P}_{2}\ M^{H}_{2}\ M^{O}_{4}\ (Si_2O_7)_2\ X^{O}_{4}$, and write the revised chemical formulae of the Group I in Table A4.

TABLE A2. BOND-VALENCE SUMS (*vu*) FOR SELECTED ANION SITES IN ROSENBUSCHITE-GROUP CRYSTALS

	götzenite WBC-13	hainite LF-A2	seidozerite 1993.158	kochite WBC-12		rosenbuschite LF-A5	
				a	*b*	*a*	*b*
X(8) *	1.25	1.31	1.70	1.60	1.38	1.66	1.36
F(9)	0.96	0.96	0.98	1.02	0.99	1.01	0.98

* Mixed site occupied by both oxygen and fluorine; *a* and *b* denote *X*(8)*a* and *X*(8)*b* sites. The information is extracted from Table 5 of Christiansen *et al.* (2003a).

TABLE A3. UNIT FORMULAE* OF MEMBERS OF THE ROSENBUSCHITE GROUP

	götzenite NBC-13	hainite LF-A2	seidozerite 1993.158	kochite WBC-12	rosenbuschite LF-A5
Si *apfu*	3.90	3.98	4.05	4.07	4.00
Al	0.01	0.01	0.01	0.01	0
Ti	0.88	0.80	1.38	0.83	0.46
Zr	0.09	0.25	1.40	0.76	1.28
Sn^{4+}	0	0	0	0	0.01
Nb	0.06	0.07	0.05	0.11	0.08
Hf	0	0	0.01	0	0.02
Ta	0	0	0	0	0
Mn^{2+}	0.11	0.08	0.43	0.54	0.10
Mg	0	0	0.30	0	0.01
Fe^{2+}	0.05	0	0.32	0.12	0
Fe^{3+}	0	0.08	0	0	0.06
Ca	4.98	4.15	0.26	2.99	3.35
Sr	0.01	0.01	0.02	0.01	0.01
Na	1.55	1.89	3.75	2.49	2.37
Y	0.06	0.30	0.01	0.03	0
La	0.08	0.03	0	0.01	0
Ce	0.13	0.08	0	0.03	0
Nd	0.02	0.03	0	0	0
Gd	0.02	0.01	0	0	0
Dy	0	0.04	0	0	0
Er	0	0.02	0	0	0
Yb	0	0.03	0	0	0
Σcations	11.95	11.86	11.99	12.00	11.75
F	3.44	3.22	1.91	2.77	3.02
O	14.56	14.78	16.09	15.23	14.98

* Chemical composition is taken from Table A1. The formulae are calculated on the basis of O + F = 18 *apfu*.

TABLE A4. REVISED CHEMICAL FORMULAE OF THE GROUP I

Mineral		$A^{P}_{2}\ M^{H}_{2}$	M^{O}_{4}	$(Si_2O_7)_2$	X^{O}_{4}
götzenite	1	$Ca_2\ Ca_2$	$Na\ Ca_2\ Ti$	$(Si_2O_7)_2$	F_2 (OF)
hainite	1	Ca_3 (Y,REE)	Na (Na Ca) Ti	$(Si_2O_7)_2$	F_2 (OF)
seidozerite	2	$Na_2\ Zr_2$	$Na_2\ Mn\ Ti$	$(Si_2O_7)_2$	$F_2\ O_2$
grenmarite*	2	$Na_2\ Zr_2$	$Na_2\ Mn\ Zr$	$(Si_2O_7)_2$	$F_2\ O_2$
rinkite	2	Ca_3 REE	Na {Na,Ca} Ti	$(Si_2O_7)_2$	F_2 (OF)
kochite	2	Ca_2 Mn Zr	$Na_3\ Ti$	$(Si_2O_7)_2$	$F_3\ O$
rosenbuschite**	1	$Ca_4\ Ca_2\ Zr_2$	Na_6 Ti Zr	$(Si_2O_7)_4$	$F_8\ O_2$

* The chemical formula of grenmarite is written by analogy with that of seidozerite, *i.e.*, $X^{O}_{4} = F_2\ O_2$.
** The chemical formula of rosenbuschite is given for a doubled minimal cell.

APPENDIX E: TABLE A5. MINERAL FORMULAE

	Fleischer's Glossary of Mineral Species 2004	This work
Group I		
götzenite	$Na_2\ Ca_5\ Ti\ (Si_2O_7)_2\ (F,OH)_4$	$Na\ Ca_6\ Ti\ (Si_2O_7)_2\ O\ F_3$
hainite	$(Na_2\ Ca_5\ )\ (Ti,Zr)_2\ (Si_2O_7)_2\ (F,OH)_4$	$Na_2\ Ca_4\ (Y,REE)\ Ti\ (Si_2O_7)_2\ O\ F_3$
seidozerite	$(Na,Ca)_4\ (Zr,Ti,Mn)_4\ (Si_2O_7)_2\ (O,F)_4$	$Na_4\ Mn\ Zr_2\ Ti\ (Si_2O_7)_2\ O_2\ F_2$
grenmarite	$(Zr,Mn)_2\ (Zr,Ti)\ (Mn,Na)\ (Na,Ca)_4\ (Si_2O_7)_2\ (O,F)_4$	$Na_4\ Mn\ Zr_3\ (Si_2O_7)_2\ O_2\ F_2$
rinkite	$(Ca,Ce)_4\ Na\ (Na,Ca)_2\ Ti\ (Si_2O_7)_2\ F_2\ (O,F)_2$	$Na_2\ Ca_4\ REE\ Ti\ (Si_2O_7)_2\ O\ F_3$
kochite	$Na_2\ (Na,Ca)_4\ Ca_4\ (Mn,Ca)_2\ Zr_2\ (Si_2O_7)_4\ (O,F)_4\ F_4$	$Na_3\ Ca_2\ Mn\ Zr\ Ti\ (Si_2O_7)_2\ O\ F_3$
rosenbuschite	$(Ca,Na)_6\ (Zr,Ti)_2\ (Si_2O_7)_2\ (F,O)_4$	$Na_6\ Ca_6\ Zr_3\ Ti\ (Si_2O_7)_4\ O_2\ F_6$
Group II		
perraultite	$K\ Ba\ Na_2\ (Mn^{2+},Fe^{2+})_8\ (Ti,Nb)_4\ Si_8\ O_{32}\ (OH,F,H_2O)_7$	$(Na\ Ba)\ Mn_4\ Ti_2\ (Si_2O_7)_2\ O_2\ (OH)_2\ F$
surkhobite	$(Ca,Na)\ (Ba,K)\ (Fe^{2+},Mn)_4\ Ti_2\ (Si_4O_{14})\ O_2\ (F,OH)$	$(Na\ Ba)\ Fe_4\ Ti_2\ (Si_2O_7)_2\ O_2\ (OH)\ F_2$
bafertisite	$Ba\ (Fe^{2+},Mn^{2+})_2\ Ti\ O\ (Si_2O_7)\ (OH,F)_2$	$Ba_2\ Fe^{2+}_4\ Ti_2\ (Si_2O_7)_2\ O_2\ (OH)_4$
hejtmanite	$Ba\ (Mn^{2+},Fe^{2+})_2\ Ti\ O\ (Si_2O_7)\ (OH,F)_2$	$Ba_2\ Mn^{2+}_4\ Ti_2\ (Si_2O_7)_2\ O_2\ (OH)_4$
yoshimuraite	$Ba_2\ Ba_2\ Ti_2\ Mn_4\ (Si_2O_7)_2\ (PO_4)_2\ O_2\ (OH)_2$	$Ba_4\ Mn^{2+}_4\ Ti_2\ (Si_2O_7)_2\ (PO_4)_2\ O_2\ (OH)_2$
bussenite	$Na_2\ Ba_2\ Fe^{2+}\ Ti\ Si_2\ O_7\ (CO_3)\ (OH)_3\ F$	$Na_4\ Ba_4\ Fe^{2+}_2\ Ti_2\ (Si_2O_7)_2\ (CO_3)_2\ O_2\ (OH)_2\ (H_2O)_2\ F_2$
Group III		
lamprophyllite	$(Na,Mn,Ca,Fe)_3\ (Sr,Ba,K)_2\ (Ti,Fe)_3\ O_2\ (Si_2O_7)_2\ (O,OH,F)_2$	$Na_3\ (Sr\ Na)\ Ti_3\ (Si_2O_7)_2\ O_2\ (OH)_2$
barytolamprophyllite	$(Na,K)_2\ (Ba,Ca,Sr)_2\ (Ti,Fe)_3\ (SiO_4)_4\ (O,OH)_2$	$Na_3\ (Ba\ K)\ Ti_3\ (Si_2O_7)_2\ O_2\ (OH)_2$
nabalamprophyllite	$Ba\ (Na,Ba)\ \{Na_3Ti[Ti_2O_2Si_4O_{14}]\ (OH,F)_2\}$	$Na_4\ Ba\ Ti_3\ (Si_2O_7)_2\ O_2\ (OH)_2$
innelite	$(Ba,K,Mn)_4\ (Na,Mg,Ca)_3\ Ti_3\ (Si_2O_7)_2\ (SO_4)_2\ O_3\ (OH,F)$	$Na_2\ Ca\ Ba_4\ Ti_3\ (Si_2O_7)_2\ (SO_4)_2\ O_4$
epistolite	$Na_2\ (Nb,Ti)_2\ Si_2O_9\ \bullet\ n(H_2O)$	$Na_4\ Ti\ Nb_2\ (Si_2O_7)_2\ O_2\ (OH)_2\ (H_2O)_4$
vuonnemite	$Na_{11}\ Ti\ Nb_2\ (Si_2O_7)_2\ (PO_4)_2\ O_3\ (F,OH)$	$Na_{11}\ Ti\ Nb_2\ (Si_2O_7)_2\ (PO_4)_2\ O_3\ F$
Group IV		
murmanite	$(Na,\square)_2\ (Na,Ca)_2\ (Ti,Fe,Mn)_2\ (Ti,Nb)_2\ (Si_2O_7)_2\ O_2\ (O,OH)2\bullet\ 4(H_2O)$	$Na_4\ Ti_4\ (Si_2O_7)_2\ O_4\ (H_2O)_4$
lomonosovite	$Na_5\ Ti_2\ O_2\ Ti_2\ (Si_2O_7)\ (PO_4)\ O_4$	$Na_{10}\ Ti_4\ (Si_2O_7)_2\ (PO_4)_2\ O_4$
quadruphite	$Na_{14}\ Ca\ Mg\ Ti_4\ (Si_2O_7)_2\ (PO_4)_4\ O_4\ F_2$	$Na_{14}\ Ca_2\ Ti_4\ (Si_2O_7)_2\ (PO_4)_4\ O_4\ F_2$
sobolevite	$Na_{14}\ Ca\ (Mg,Mn)\ Ti_4\ [Si_2O_7]_2\ [PO_4]_4\ O_4\ F_2$	$Na_{13}\ Ca_2\ Mn_2\ Ti_3\ (Si_2O_7)_2\ (PO_4)_4\ O_3\ F_3$
polyphite	$Na_{17}\ Ca_3\ Mg\ (Ti,Mn)_4\ (Si_2O_7)_2\ (PO_4)_6\ O_3\ F_5$	$Na_{18}\ Ca_4\ Ti_4\ (Si_2O_7)_2\ (PO_4)_6\ O_4\ F_4$

The formulae of grenmarite is from Bellezza *et al.* (2004) and that of nabalamprophyllite, from Chukanov *et al.* (2004)